University of Pretoria

Faculty of Health Sciences

School of Medicine

Department of Physiology

The effects of neuroinflammation induced by systemic lipopolysaccharides on the hippocampi of aged Sprague-Dawley rats

By Nonkululeko Dhlamini

14131120

Submitted in fulfilment of the requirements for the degree

Master of Science (MSc Human Physiology)

Supervisor: Dr Janette Bester

University of Pretoria

Department of Physiology

Co-supervisor: Prof Peet du Toit

University of Pretoria

Department of Physiology

2022

Abstract

Dementia affects a significant number of South Africans. In 2015, an estimated 186, 000 South Africans were recorded as being patients of this irreversible condition. Alzheimer's disease (AD) accounts for 60% to 80% of reported dementia cases. It is estimated that more than 46.8 million people are affected by AD, worldwide. According to the 2015 World Alzheimer's Report, an estimated 186,000 South Africans struggled with dementia in 2015, and this number is anticipated to increase to 275 000 by 2030. In the past decades, two hallmarks termed amyloidosis and taupathy have received major acknowledgement in neurodegenerative studies. Although this knowledge has tremendously contributed towards the understanding of the molecular mechanisms underlying AD, therapeutic treatments that reverse the disease are yet to be discovered. Therefore, exploring the aetiology of the disease using a popular rodent-model of inflammation can help provide some missing links required for long-term therapeutic strategies. Previous research has validated the use of lipopolysaccharide (LPS) in rodent models to replicate characteristics of AD and examine the inflammatory pathways and molecules involved. Therefore, in this study, the hippocampal region of male Sprague-Dawley rats was examined for AD-like (cognitive and histological) pathologies in response to repeated exposure to LPS. Subjects were assorted into one control group and three experimental groups, and the results of the experimental group were compared against the control group. LPS sourced from *Escherichia coli* 055:B5 was administered through repeated subcutaneous (SC) injection to induce a chronic systemic inflammatory response. Cognitive assesssments were conducted using a series of three behavioural experiments commonly used by researchers. This included the Y-maze, novel object recognition (NOR), and open-field tests. To quantitatively determine the effects of LPS-induced neuroinflammation on hippocampal neuroglia-astrocytes and microglia, biochemical assays involving ELISA and confocal microscopy were performed. To identify astrocytes and microglia, anti-glial fibrillary protein (GFAP) and anti-ionized calcium-binding adaptor molecule 1 (Iba1) fluorescent markers were used to stain hippocampal sections and view by microscopy. Previous findings have conveyed the benefits of honey as an anti-inflammatory agent against infectious pathogens. Therefore, during the experimental period of this study, Manuka honey was introduced to the subjects by oral gavage. The effects of honey as a "mopping agent" were identified by

comparison of the experimental groups against the control group. Therefore the aim of this study was to investigate the effects of neuroinflammation induced by systemic lipopolysaccharide from *Escherichia coli* 055:B5 on the hippocampi of Sprague-Dawley rats. Cognitive assessments revealed that LPS exposure, over a 10-day period, did not significantly impair short-term spatial working memory, learning capacity and spontaneous memory, and anxiety, and locomotor activity. Confocal microscopy showed that LPS significantly increased the quantity of microglia detected by Iba1 antibody. This suggests that LPS exposure induced neuroinflammation in the hippocampal region, however, the nature of the inflammatory response, physiological or pathological, was unclear.

Keywords: Alzheimer's disease (AD), lipopolysaccharide (LPS), inflammation, *Escherichia coli*, hippocampus, microglia, astrocytes, honey, novel object recognition (NOR) test, open-field test, y-maze test, subcutaneous

Declaration of Originality and Authorship

I, the undersigned, hereby declare that the thesis titled

"**The effects of neuroinflammation induced by systemic lipopolysaccharides on the hippocampi of aged Sprague-Dawley rats**"

Is my original work and has not ever been presented for academic award to this or any other tertiary institution for another degree. I have read and understand the University of Pretoria's policy on plagiarism.

Herewith, I submit this thesis to the University of Pretoria for the degree Master of Science in Human Physiology.

Candidate Name: Nonkululeko Dhlamini

Student Number: 14131120

	05 April 2022
Signature	Date

Acknowledgements

Throughout the course of this research project I have received immense support and assistance, for which I am grateful.

Firstly, I wish to thank my supervisor, Dr Janette Bester, whose expertise was invaluable in framing the research question and methodology. Your perceptive feedback and unwavering support motivated me to develop my thinking and brought my work to a higher level. From beginning to end, you provided support, understanding and wisdom, which has greatly contributed to my growth as a researcher and an individual. To my co-supervisor, Prof Peet du Toit, thank you for your motivation that has fostered my passion for scientific research.

To my colleagues during this research project, Karabo Rathebe, Glory Tambwe and Victoria Verrall, thank you all for your efforts, advice and relief from the challenges associated with this project.

Further, I wish to thank the staff at the University of Witwatersrand Central animal services unit. Your guidance, patience and kindness contributed to the success of the experimental period of this study. To Prof Willie Daniels, thank you for your collaboration on this study. You provided me with the expertise, support and assistance that I needed to triumphantly complete my dissertation.

To the staff from the University of Pretoria Microscopy and microanalysis unit, thank you for your tremendous support and guidance. Your expertise were helpful regarding confocal microscopy and sample preparation.

I would like to thank my family. To my parents, Bhekithemba and Makhosazana Dhlamini, words cannot describe my gratitude. Thank you for your unconditional love and support. Without you, I would not be the ambitious, independent person I am today. To my sibling, Mpendulo Dhlamini, thank you for your constant motivation and challenging questions. I hope to make you proud and inspire you to pursue all of your dreams.

Finally, to my best friend, Pieter Cronje, thank you all for your support in this project. Your contributions did not go unnoticed. I am truly blessed to have you by my side.

The funding of the National Research Fund (NRF) towards this study is hereby acknowledged. The views and deductions expressed in this study are those of the principal investigator and are not credited to the NRF.

Table of Contents

Table of Figures

List of Tables

List of Abbreviations

Aβ	Amyloid beta
AD	Alzheimer's disease
ANS	Autonomic nervous system
APP	Amyloid precursor protein
ApoE	Apolipoprotein E
BBB	Blood brain barrier
BSA	Bovine serum albumin
CA	Cornu Ammonis
CAS	Central animal services
C1q	Complement component 1q
CD	Cluster of differentiation
CNS	Central nervous system
CSF	Cebrospinal fluid
CSFs	Colony-stimulating factors
CT	Computerized tomography
Cdk5	Cyclin-dependent protein kinase 5
COX-2	Cyclooxygenase-2
CVO	Circumventricular organs
DAMPs	Damage-associated molecular pattern
DG	Dentate gyrus
ELISA	Enzyme-linked immunosorbent assay
GALT	Gastrointestinal-associated lymphoid tissue
GFAP	Glial fibrillary acidic protein
GIT	Gastrointestinal tract
GSK3β	Glycogen synthase kinase 3β

H&E	Hematoxylin and eosin
Iba-1	Ionized calcium-binding adapter molecule
IF	Immunofluorescence
IHC	Immunohistochemistry
IL	Interleukin
iNOS	Inducible nitric oxide synthase
IFN	Interferon
LBP	LPS-binding protein
LPS	Lipopolysaccharide
MAC	Membrane attack complex
MAPs	Microtubule-associated proteins
MTL	Medial temporal lobe
MRI	Magnetic resonance imaging
NFT	Neurofibrillary tangle
NO	Nitric oxide
NORT	Novel object recognition test
NVU	Neurovascular unit
PAMPs	Pathogen-assosciated molecular patterns
PBS	Phosphate buffered saline
PET	Positron emission tomography
PNS	Peripheral nervous system
PRR	Pattern recognition receptor
ROS	Reactive oxygen species
TBS	Tris buffered saline

TIR	Translocated intimin receptor
TLR	Toll-liike receptor
TNF-α	Tumor necrosis factor α
OM	Outer membrane

Site Map

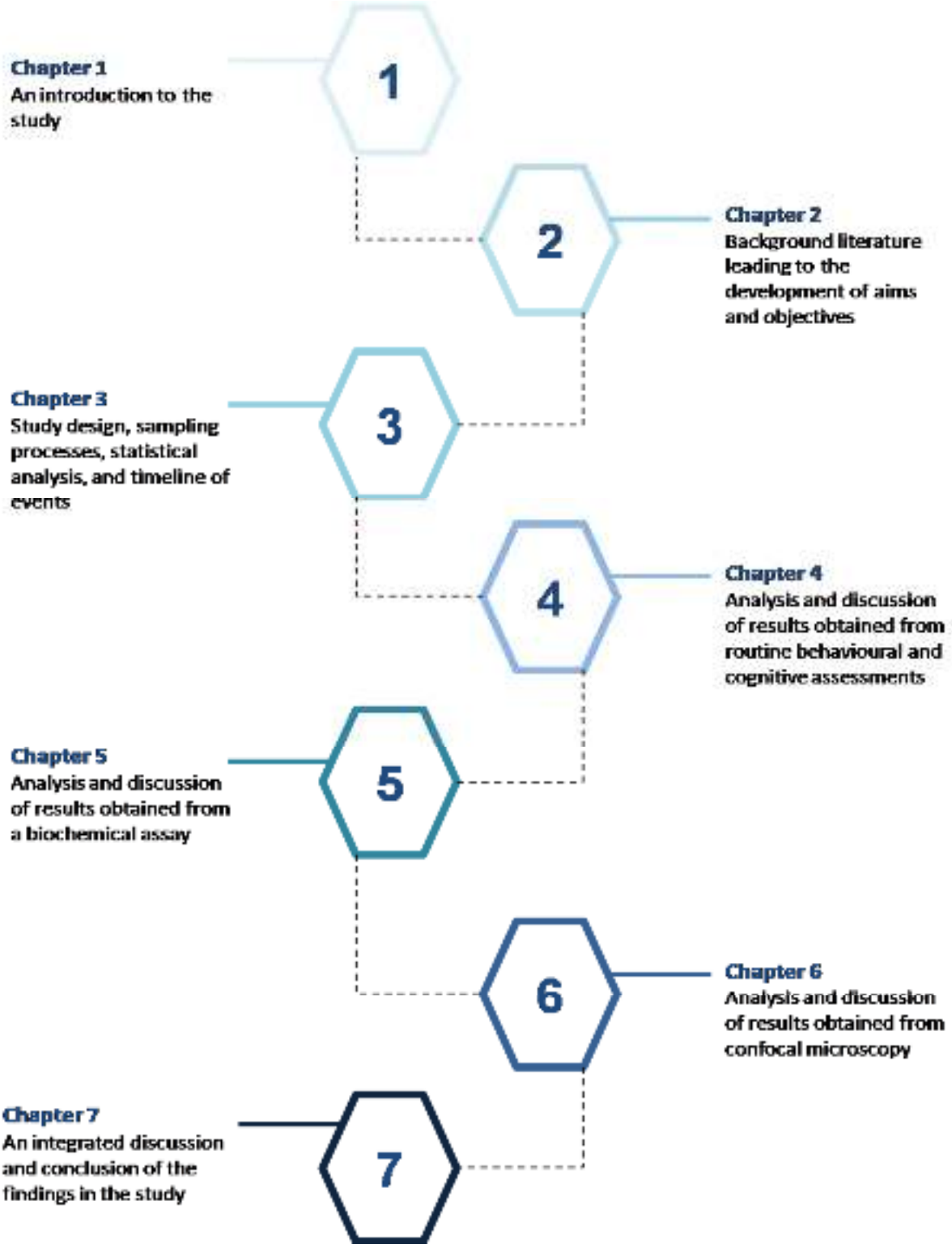

1

Chapter 1: Introduction

1.1 Background

Dementia is characterized as a steady and sequential decline in cognitive ability with far-reaching effects that restrict independent occupational and social functioning.[1] It is best described as a syndrome rather than a distinct illness, which has been recognized as the main cause of disability and dependency amongst older individuals.[2] It is caused by a multitude of conditions or injuries that interfere with the brain's activity and performance, leaving patients with impaired memory, communication, and self-care skills.[1]

Depending on the disease subtype, symptoms can manifest in various forms among different individuals.[3] However, clinically, these symptoms are broadly categorized into four impairment groups, namely memory, cognitive, behavioural, and physical impairments.[3] Individuals with mild dementia often display impaired episodic memory, spatial navigation, performance in social and work environments, and difficulties remembering recently learned information such as peoples' names and specific details of personal objects (agnosia).[3,4] This is partially due to cortical damage that occurs along pathways that descend in the hippocampus and defects in the anterior-temporal system.[4] In the moderate stage of dementia, individuals tend to display erratic changes in mood and sleeping patterns, difficulties in language and communication (dysphasia), and problems performing manual tasks like dressing themselves (apraxia).[3] As the disease progresses to the severe stage; individuals become physically impaired and more dependent on caregivers for assistance with personal care as they become frail and confused.[1]

The prevention and treatment of dementia is a global health issue. A cost of illness comparison study showed that in 2015 the global cost of dementia was 818 billion USD.[5] According to a census conducted in 2011, approximately 2.2 million South Africans are suffering from some form of dementia, wherein a large proportion of this number is a result of the dementia-HIV/AIDS complex.[6,7]

2

Chapter 2: Literature Review

2.1 Introduction to Alzheimer's Disease-type dementia

Serving as the most common cause of dementia, Alzheimer's disease (AD) is an irreversible and steadily advancing neurodegenerative condition characterized by cognitive and behavioural deterioration.[8] The term "Alzheimer's disease" was authored by Emil Kraepelin in 1910.[2] This was in honour of his colleague Alois Alzheimer, a German psychiatrist and neuroscientist who was the first to note the most distinctive neuropathological brain change; neurofibrillary tangles (NFTs) in the brain of a female patient following her hospitalization for psychiatric related symptoms.[2]

Alzheimer's disease is known to only affect humans, with a disposition that exists across all racial groups.[5] Due to a higher life expectancy and decreasing oestrogen levels with age-as a result of menopause- women are more vulnerable to developing AD than males.[6] While the disease is often paralleled with aging, researchers have realized that it can arise at any age.[7] The detail for this occurrence is however still unknown. Currently, there is no cure for AD; therefore, comprehensive understanding of the disease and the development of therapeutic targets are of particular interest to researchers.

2.2 Pathological hallmarks of Alzheimer's disease

The molecular premise underlying the pathology of AD is controversial.[7] Nonetheless, two prominent pathological hallmarks have been widely recognized and accepted. First, AD is characterized by the extracellular deposition and aggregation of amyloid-β (Aβ) proteins, in the form of senileclumps known as plaques and second, the intracellular expression of aggregated tau proteins, in the form of hyperphosphorylated filaments known as NFTs.[8]

2.2.1) Amyloid hypothesis

Aβ peptides are derived from a type-1 transmembrane glycoprotein known as amyloid precursor protein (APP).[9] APP is predominantly found in the synapses of neurons and various tissue structures including the brain, heart, thymus.[9] APP processing is explicitly controlled by neuronal activity.[10] Neurons that express high levels of APP favour the amyloidogenic pathway, in that they facilitate the process of neurotoxic Aβ

peptides formation.[10] Therefore, Aβ accumulation in brain regions with high neuronal activity gives rise to AD vulnerability.[10] In the amyloidogenic pathway, APP is enzymatically cleaved by β-secretase and γ-secretase to yield a Aβ peptides of 37 to 49 amino acids in length into the extracellular space, cerebrospinal fluid, and plasma.[11] These newly formed Aβ peptides exist in various forms; monomers, oligomers, fibrils, and plaques.[12] Essentially, Aβ monomers aggregate to form soluble oligomers that may spread across the brain and deposit as fibrils and plaques.[12] Aβ fibrils are insoluble, degradation resistant fibres made from aggregated oligomers and Aβ plaques are formed by large, unbranched and insoluble aggregated fibrils.[12] Aβ peptides with 40 and 42 amino acids are the most prevalent, where un-mutated $A\beta_{42}$ is the most pathogenic isoform.[13] Because of their additional hydrophobic residues, $A\beta_{42}$ monomers have rapid aggregation kinetics which makes them more prone to aggregation- hence they are closely linked to AD.[14] However, earlier studies indicate that both $A\beta_{40}$ and $A\beta_{42}$ ($A\beta_{42}$:$A\beta_{40}$ ratio) peptides influence each other's aggregation and toxic properties, such that the aggregation of $A\beta_{42}$ is restricted by the presence of $A\beta_{40}$, whilst the presence of $A\beta_{42}$ monomers promotes $A\beta_{40}$ aggregation.[15,16,17,18,19,20,21] Also, it has been reported that the accumulation of insoluble $A\beta_{42}$ is a major contributor to AD pathogenesis.[12]

In AD, the amount of Aβ peptides produced remains constant but the clearance rate is significantly lowered.[22] This is because excess native Aβ monomers are subject to abnormal and highly specific conformational changes that result in fibrillar structures represented as plaques.[11] Amyloid plaques can induce cellular damage and death via apoptosis or necrosis using receptor-ligand interactions or the disturbance of plasma membranes if the fibril is large enough.[23,24] Examples of this cellular damage is observed when Aβ plaques interact with microglial receptors and through Aβ-driven lipid peroxidation, they cause inflammation and increases the output of reactive oxygen species (ROS).[25,26] These pathways give value to the effects of amyloid deposition (amyloidosis) and its association with AD. To summarize, the amyloid hypothesis suggests that plaque formation prompts a series of events including the formation of histopathological lesions, NFTs, synaptic dysfunction and toxicity, neuronal death, microglial and astrocyte activation and mitochondrial dysfunction; all of which trigger neuroinflammation within the cerebral cortex, hippocampus and amygdala.[27]

2.2.2) Tau hypothesis

Tau protein, a member of the microtubule-associated proteins (MAPs), is a heat-stable hydrophilic protein found in the axon of a neuron.[28] Tau protein is encoded by the MAPT gene and due to alternative splicing of its different mRNAs species; six notable tau isoforms are produced in the human brain.[29] The role of tau protein is to promote microtubule polymerization and stabilization.[30] Most importantly, tau serves to maintain neuronal morphology and regulate axonal transport.[31] It has also been associated with defective oxidative phosphorylation and apoptotic activity that results in mitochondrial fragmentation.[31] Unregulated mitochondrial dynamics promote an over-production of ROS that are capable of inducing post-translational modifications in proteins across a cell, thereby implicating tau protein in neurodegenerative diseases.[31]

In tauopathies like AD, changes in the structure, function, and quantity of tau protein occur.[31] Patients with AD display a higher quantity of tau protein in all forms; normal, phosphorylated or aggregated.[32] Aggregates appear as NFTs and their degree of phosphorylation is almost four folds greater than in the normal human brain.[32,33,34] Aging is also an important risk factor for tauopathies because it coincides with a reduced tau protein turnover that results in its accumulation.[35] Similarly to Aβ peptides, excess tau proteins are subject to post-translational alterations such as phosphorylation, aggregation, glycosylation and glycation, all of which raise proteotoxicity.[35] Due to its phosphoprotein nature, the biological activity of tau protein is largely controlled by its degree of phosphorylation.[31] In AD, tau is hyperphosphorylated by several proteins such as glycogen synthase kinase 3β (GSK3β) and cyclin-dependent protein kinase 5 (Cdk5).[36] This abnormal and irreversible hyperphosphorylation causes an involuntary delay in neuronal activity and resultant progression in neurodegeneration.[37] Hyperphosphorylation, which precedes the formation of NFTs, decreases tau's affinity for microtubules thus increasing the quantity of unbound protein to abnormal levels.[36] Unbound tau proteins create non-fibrillary deposits which undergo further structural modifications where they transform from an unfolded pre-tangle to a more defined β-pleated sheet that self-assembles into NFTs typically found in the stoma of neurons.[36]

NFTs are described as cytotoxic intraneuronal masses of insoluble cytoskeletal components comprised mainly of phosphorylated tau proteins capable of inducing neuronal death, thereby contributing to AD.[37] In the brain, a substantial amount of NFTs are localized in the transentorhinal and entorhinal layer.[37] They spread across the brain and facilitate the appearance of Aβ plaques in the hippocampus as AD progresses.[37] Findings by Binder, L and colleagues suggest that NFTs play a crucial role in the progression of AD by promoting a synergistic relationship between Aβ and tau proteins that intensifies neuronal loss.[22]

In short, Aβ peptides and NFTs are deposited mainly into the hippocampus, amygdala and entorhinal cortex where they impair learning, memory, and behavioral circuits.[12] Jointly, Aβ plaques connect to their binding receptors and drive downstream pathways that trigger tau hyperphosphorylation, and ROS production.[12] This results in inflammatory reactions which induce excessive calcium influx, synaptic and mitochondrial dysfunction and neuronal death, ultimately giving rise to AD.[12]

2.3 Brain regions affected in Alzheimer's disease

Neuropathological lesions associated with AD occur decades before the onset of clinical symptoms.[38] Difficulties in detecting AD during its primary stages are common. This often results in intensified symptoms such as the complete loss of intellectual ability, and great financial responsibility, not excluding the emotional and physical distress experienced by the caregiver.[39] Currently, clinicians are limited to providing a provisional diagnosis which often occurs at the last stage of the disease, because even though the preclinical stage is accompanied by clinical signs and symptoms, these are often obscured or misinterpreted as symptoms of other cognitive illnesses or old age.[40] Nonetheless, an accurate diagnosis requires posthumous assessment.[41]

As a result, considerable efforts have been made to establish neuro-imaging techniques for early detection andslowing disease progression such as computed tomography (CT), magnetic resonance imaging (MRI) and positron emission tomography (PET).

Neuropathological lesions associated with AD are coupled with structural irregularities in the brain, particularly the medial temporal lobe (MTL) and hippocampus.[42] Initial Aβ aggregates appear on most parts of the cortex even during typical aging, whereas tau

pathology begins in the transentorhinal region and progresses in an activity-dependent fashion across sensitive functional pathways.[43,44,45]

The MTL is a network of anatomically similar structures consisting of the: parahippocampal gyrus [dentate gyrus (DG), subicular complex and Cornu Ammonis (CA) subfields] as well as the neighboring entorhinal cortex, perirhinal cortex,and parahippocampal cortex.[46,47] The MTL is the first brain region to display neurodegeneration (atrophy).[48] Atrophy of the MTL is frequently observed on MRI scans of AD patients and is correlated to neural damage and disease severity.[49,50] Reports by Morrison, JH[51] indicate that the entorhinal-hippocampal circuit is impaired during the early stages of AD, followed by a steady dissociation of the MTL regions, resulting in an ultimate loss of communication between the surrounding neocortex. This may possibly highlight the pathway of cognitive decline during aging in the onset of AD. Also, MTL atrophy is linked to reduced performance in memory-related tasks.[52]

Histopathological examinations have revealed that the hippocampus is influenced by Aβ plaques and NFTs in the primary stages of the disease, thus confirming its significance in diagnosis.[53] The hippocampus is a highly vulnerable continuation of the cerebral cortex distinguished as an S-shaped layer of tightly packed neurons embedded deep within the MTL to form part of the limbic lobe.[54] It is a highly complex structure with ductile properties that make it easily modifiable by neuropathological disorders.[55] The hippocampus plays a role in neurogenesis, spatial memory, and orientation, emotional behavior, modulation of hypothalamic functions and the major functions of learning, memory formation, and retention.[56,57,58] In rats, learning and memory are inherently associated with the dorsal hippocampus, whilst emotional behavior is associated with the ventral hippocampus.[59]

As outlined above, the hippocampus is a major target for amyloid and tau pathology. By use of functional connections, NFTs first invade the transentorhinal and anterolateral entorhinal cortex followed by the CA subfields and the neocortex.[60,61] The spatiotemporal sequence of NFT spreading matches the progression of brain atrophy.[62] Unlike Aβ, the degree of NFT expression strongly correlates with disease severity.[63] Aβ deposition occurs mainly in the hippocampus, neocortex, and cerebrovasculature (also known as cerebral amyloid angiopathy).[64]

That said, over the past decade, a third characteristic has been implicated in the pathogenesis of AD that may possibly present a link between the aforementioned hallmarks.[65] The brain tissue of AD patients indicates the occurrence of a persistent inflammatory response, neuroinflammation, which arises as a consequence of disrupted equilibrium between pro-inflammatory and anti-inflammatory signals.[66] Neuroinflammation is progressively being acknowledged as a core feature of neurodegenerative diseases such as AD not merely because it is linked to neurodegeneration but it also promotes and intensifies both Aβ and tau protein abnormalities.[65,67]

2.4 Dementia-associated inflammation

2.4.1) Overview of systemic inflammation

Generally, a regulated systemic inflammatory response is a localized and beneficial defense mechanism facilitated by the host immune system to remove harmful agents such as an infection, cellular or tissue damage, irritation or trauma through various molecular and cellular events which act to minimize and clear the harmful agent, followed by restoration and repair processes.[68]

Within the context of microbial infection; systemic inflammation is triggered when cells of the innate immune system alongside various epithelial cells use their surface-exposed pattern recognition receptors (PRRs) to detect either; a) pathogen-associated molecular patterns (PAMPs), which are microorganism-derived and evolutionarily preserved exogenous structures found on pathogens, or b) damage-associated molecular patterns (DAMPs), which are endogenous stress cues produced by cells to prompt spontaneous cell death.[69,70] Together, PAMPs and DAMPs form biomolecules that bind to specific receptors of the PRR family (i.e. Toll-like receptors) to enhance autophagy- thereby preventing genome instability and necrosis.[71] Autophagy is an essential lysosome-mediated process, aimed at maintaining homeostasis.[71] It involves the removal of toxic protein aggregates and degradation of macromolecules,(i.e. carbohydrates, proteins) intracellular pathogens and organelles (i.e. mitochondria, endoplasmic reticulum).[71,72]

At the circulatory level, inflammation is marked by changes in vascular permeability that function to increase blood flow to the site of injury, and stimulate leukocyte

chemotaxis that is driven by the release of pro-inflammatory cytokines and chemokines.[68] Whilst at the tissue level, inflammation is marked by: redness and heat (caused by the increase in blood flow), swelling (caused by fluid accumulation), pain (caused by the release of inflammatory mediators which excite neuronal endings), and tissue immobility.[73] Despite the fact that the resultant inflammatory response is dependent on many factors of the initial stimulus, the processes share a common mechanism consisting of i) recognition of the harmful stimuli using cell surface PRRs; ii) stimulation of inflammatory pathways; iii) release of inflammatory mediators and the iv) mobilization of inflammatory cells.[74] Ultimately, inflammation that runs unregulated in time, space or intensity is a hallmark of several pathologies.[75]

2.5 Neuroinflammation

Neuroinflammation is a chronic and complex inflammatory reaction across the central nervous system (CNS); the brain or spinal cord.[76] It is mediated by biochemical and cellular reactions comprising the formation and release of pro-inflammatory cytokines such as; interleukins (IL)-1β,IL-6, IL-18, tumor necrosis factor α (TNF-α), interferons (IFNs), colony-stimulating factors (CSF), chemokines; CCL2, CCL5, CXCL1, ROS, nuclear factor kappa-light-chain-enhancer of activated B cells (NF-κB), enzymes cyclooxygenase-2 (COX-2), inducible nitric oxide synthase (iNOS), coagulation factors like platelet-activating factor and secondary messengers; nitric oxide (NO) and prostaglandins.[76] Neurodegenerative conditions such as AD is linked and frequently preceded by neuroinflammation which plays an essential dual role.[77] This is partly due to the fact that Aβ accumulation induces a chronic neuroinflammatory state which participates in AD progression.[78,79]

The degree and complexity of neuroinflammation are influenced by the setting, time span and course of the primary insult, given that each tissue displays diverse features of inflammation due to biochemical, immunological and physiological differences.[76,80] Acute neuroinflammation, however, has advantages such as immune conditioning, neuro-immune communication, injury reduction and axonal and myelin restoration.[77,76]

2.5.1) The complex foundation of neuroinflammation

Neuroinflammation participates in disease resolution and provides neuroprotection during an acute-trial reaction by restricting activation of the pathogenetic cascade but

on the other hand, it may become deleterious under a chronic response, as seen in clinical conditions.[81,82] Vicious or pathological neuroinflammation is linked to a disruption of the blood-brain barrier (BBB), microglial activation and proliferation, stimulated release of inflammatory mediators, astrocyte mobilization and abnormal neuronal signaling all of which may contribute to the degradation of the CNS microenvironment, consequently resulting in clinical implications.[83,84] This phenomenon is depicted in **Figure 1**.[85] The CNS microenvironment possesses unique characteristics. It has a distinct chemical composition and neurotransmitter pool which promotes neural function, in addition to its poor protein content which reduces cell proliferation and oxidative stress.[86] This microenvironment is rarely subjected to systemic toxins that minimize neural impairment.[86] Moreover, it has the capablilty to restrict the movement of inflammatory mediators, thereby preventing local inflammation.[86]

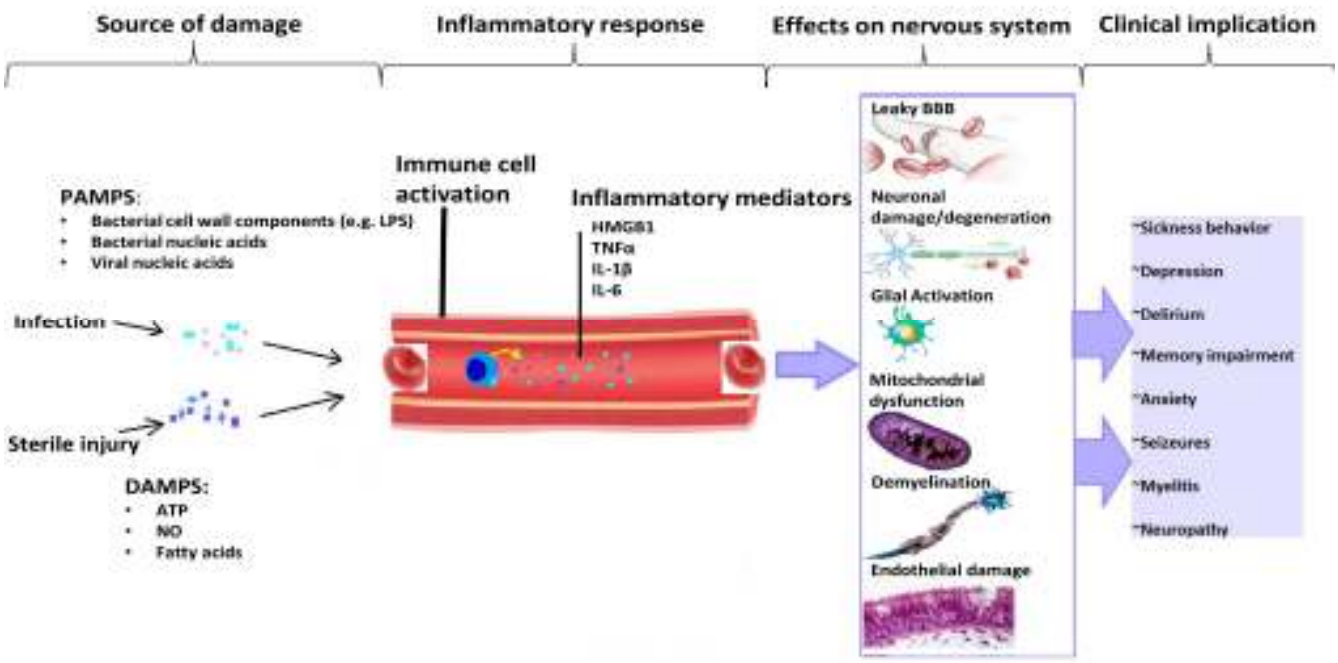

Figure 1: The complex inteaction between infection or injury, the induced inflammatory response, and subsequent clinical implications.

2.5.2) Blood-brain barrier

The BBB is a highly differentiated and stratified membrane made from non-fenestrated endothelial cells connected to each other by tight junctions and pericytes, which surrounds two continuous basement membranes and astroglial end-feet to collectively form the neurovascular unit (NVU).[86] At the molecular level, the BBB is embedded with receptors, transporter proteins, and exoenzymes which direct and regulate interactions along the barrier.[86] Taken as a whole, these components play a key role in the provision and maintenance of a homeostatic and immuno-protected CNS microenvironment by conserving the integrity of the BBB and limiting interactivity between the innate immune system and acquired immune system.[87,83] In AD, systemic inflammation driven by microglia, macrophages, and immune cells is linked to CNS dysfunction, disrupted BBB, reduced bulk flow of cerebrospinal fluid (CSF) over the BBB and accelerated Aβ deposition in the hippocampus.[88,89,90] At the same time, cerebrovascular deposition of Aβ plaques in the CNS initiates pro-inflammatory and cytotoxic events whilst potentially playing a role in the degeneration of pericytes, endothelial cells, and smooth muscle cells, all of which promote extensive BBB permeability.[91,92] BBB dysfunction also corresponds with higher levels of

hyperphosphorylated perivascular tau protein close to vital hippocampal blood vessels.[93] Thus, both Aβ and tau pathology may advance BBB disruption to exacerbate neuroinflammation and neurodegeneration.[94] Reversibly so, neurodegeneration coexists with microgliosis and astrogliosis. [95,96]

2.5.3) Glial cells of the CNS

Neuroglia (glia) are non-neuronal tissue cells of the nervous system isolated from the rest of the body by the BBB.[97] They serve as support structures for neurons whilst providing nourishment, maintaining homeostasis and form the myelin sheath.[97] Glia is broadly categorized into two classes; macroglia and microglia. Macroglia are further split into 7 different cell types, each playing a unique role (**Figure 2**).[97,98,99,100,101]

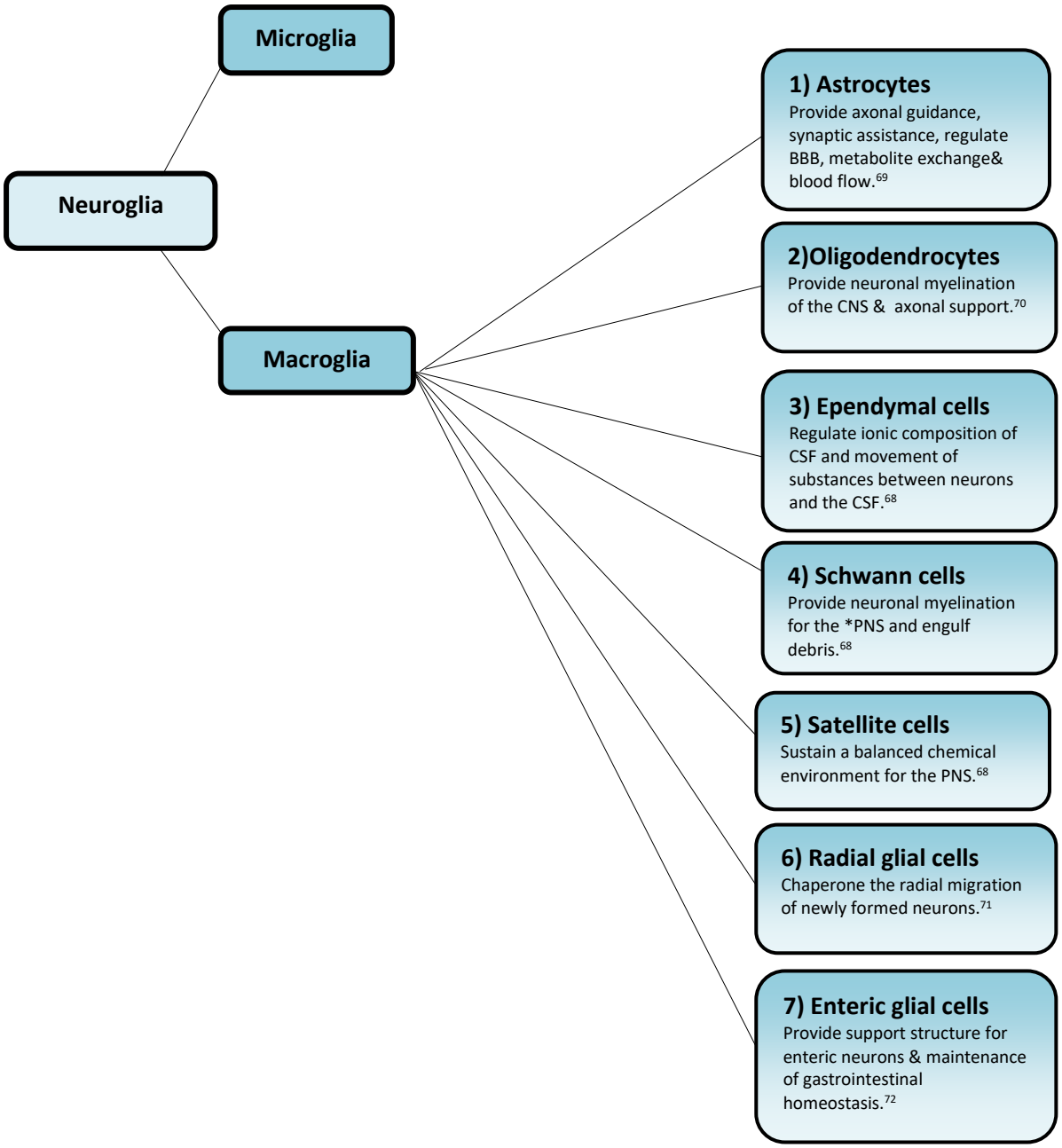

Figure 2: Classification of neuroglial cells, with their main roles in the CNS and *peripheral nervous system (PNS).

Evidence that supports neuroinflammation as the link between Aβ deposition, tau abnormality and neurodegeneration arises from human and rodent studies where activated microglia, which is associated with disease progression, were observed near amyloid aggregates within the AD brain.[102,103]

2.5.3.1) Microglia

Microglia are tissue-resident phagocytic cells of the innate immune system ubiquitously dispersed within the gray and white matter of the CNS.[104] They account for ±10%-15% of all glial cells and their amount generally stays constant from late postnatal development to old age due to concurrent proliferation and apoptosis.[105,106] Microglia are involved in CNS function, evolution, homeostasis and disturbances.[105] They also participate in phagocytosis, synaptic maturation, pruning and protection, neurogenesis and the regulation of cognitive functions.[105,107] From an immunological perspective of infected or injured tissue; microglia detect inflammatory signals, produce and release inflammatory mediators and participate in both the inflammatory response and resolution processes.[107] This primary function of immune surveillance is facilitated by a diverse range of receptors for neurotransmitters, cytokines, chemokines and toll-like receptors (TLRs).[108,109]

2.5.3.2) Reactive microglia and its implications

In their inactivated resting state, as is the case in healthy adult brains, they are structurally referred to as ramified units with small stationary cell bodies and cell processes that constantly expand and contract; continuously scanning their assigned environment and relaying information straight to other microglia, nerve fibers, astrocytes, T-cells, myeloid progenitor cells and blood vessels.[105] Upon detection of a pathological stimuli (i.e. infection,neuronal degeneration or protein presence or aggregation) within the CNS, their impressive plasticity and regular state of motion enables them to rapidly respond by transitioning into an activated state (microglial activation) of altered structure and molecular composition characterized by contracted cell processes, enlarged cell bodies and migration towards the site of injury where they eradicate pathologens or damaged cells and execute inflammatory functions via innate immunity.[105] On a molecular scale, microglial activation involves cytoskeletal rearrangements that change the sequence of receptors displayed on their surfaces in addition to the amplified expression of potentially cytotoxic molecules such as cytokines, chemokines, prostaglandins and ROS.[107]

In the event of an exaggerated immune response and consequent overproduction of immune molecules: microglia lead to a significantly modified neural microenvironment,

consequently characterizing them as a hallmark of neuroinflammation and brain pathology.[110,111] In AD, it is speculated that the force driving microglial activation and the resultant overproduction of inflammatory mediators is the expression of Aβ plaques; for the reason that some studies have indicated that activated microglia can engulf these plaques but because the microglia become so inflated and inefficient at binding Aβ that after a certain period they become incapable of processing the plaques.[65,112] Microglia also have the ability to respond to APP and NFTs.[113] During preclinical AD, the initial inflammatory reaction provides beneficial effects as it contributes towards the clearance of Aβ plaques, however, sustained inflammation and microglia-associated neurotoxins worsen AD pathology as they sustain reactive microgliosis which results in accumulated Aβ proteins and persistent cytokine signalling that recruits more microglia to the plaques, ultimately causing neuronal damage or death.[112,114,115]

2.5.3.3) Astrocytes

Similarly to microglia, astrocytes are CNS-resident signal conductors of the innante immune system.[116] They possess a variety of functional and structural features involved in several physiological activities.[116] Astrocytes are the most abundant neuroglial cell.[117] Their pathological reaction is known as reactive astrogliosis, a complex, multistep and disease-specific response marked by cellular, morphological and functional changes directed towards neuroprotection and the restoration of damaged neural tissue in response to CNS injuries.[118] Astrogliosis is associated with important positive functions, however, under certain conditions it may lead to deleterious outcomes.[119] Apart from supplying structural support to neurons, astrocytes are essential for the sustainability, homeostasis, and functioning of a healthy CNS.[120] Other functions include synaptogenesis, synaptic plasticity, neurotransmitter uptake and reuptake, receptor trafficking, gliotransmission, regulation of extracellular space composition and volume, maintenance of the BBB, inflammation and higher cognitive functions.[120,121,122,123,124]

2.5.3.4) Astrogliosis and its implications

In light of their key role of facilitating CNS functions, it is unsurprising that any disruptions thereof promote the onset and progression of cerebral pathologies like

dementia.[125] Reactive astrocytes receive directive information from surrounding cells and deliver different messages to effecter cells that influence or initiate an appropriate response.[119] Such astrocytes are marked by functional impairments, accumulation of hypertrophic astrocytes surrounding Aβ plaques and amplified expression of glial fibrillary acidic protein (GFAP) in all four lobes of the brain and the CSF.[126] GFAP is a protein involved in cell communication, BBB function, mitosis, and repair processes, and its increased expression is associated with AD progression.[126,127] Similarly to microglia when exposed to Aβ plaques, astrocytes can initiate inflammation and the release of cytokines, chemokines and ROS, which exacerbates the progression of dementia.[128] Moreover, astrocytes produce and release gliotransmitters which facilitate synaptic plasticity and regulate learning and memory in distinct brain regions like the cerebral cortex and hippocampus.[129,130] Any disturbances in gliotransmission (such as the presence of Aβ plaques) causes an increase in calcium (Ca^{2+}) signaling, altered neural homeostasis, and synaptic transmission which also advances disease pathology.[131,132] Not only do reactive astrocytes produce a variety of chemokines that permeate the BBB and attract inflammatory cells, they also produce molecules that dampen the effects of inflammatory cells.[133,134]

In regions such as the cortex, hippocampus, and cerebellum, hypertrophic astrocytes bind and sheathe amyloid plaques while penetrating any unbound plaques resulting in their fragmentation, diffusion and varied morphology.[135] Extracellular molecules such as purines, growth factors, plasma proteins, Aβ or steroid hormones invoked by endotoxins such as lipopolysaccharides (LPS) have the ability to initiate or regulate astrogliosis.[119] When peripheral infections arise from immune system invaders like LPS, they produce PAMPs which infiltrate the BBB, and upon exposure to astrocytes, will induce and exaggerate their pro-inflammatory potential thereby steering astrogliosis towards cytotoxicity.[136,137]

LPS is implicated in (neuro) inflammation, given that its systemic release is characterized by the activation of a strong inflammatory response and the infiltration of leukocytes from the periphery to the CNS resulting in neuroinflammation, mitochondrial dysfunction, and neurodegeneration.[138]

2.6 Lipopolysaccharide

2.6.1) Structure of lipopolysaccharide

The membrane of Gram-negative bacteria (**figure 3**[139]) such as *Escherichia coli*, is comprised of a cell envelope made from two membranes parted by peptidoglycan containing, hydrophilic cavity called the periplasm.[140] The outer membrane (OM) is the foremost layer of the envelope, composed of an asymmetric phospholipid bilayerinterlaced with proteins - serving as the inner leaflet, while LPS, serves as the outer leaflet.[141]

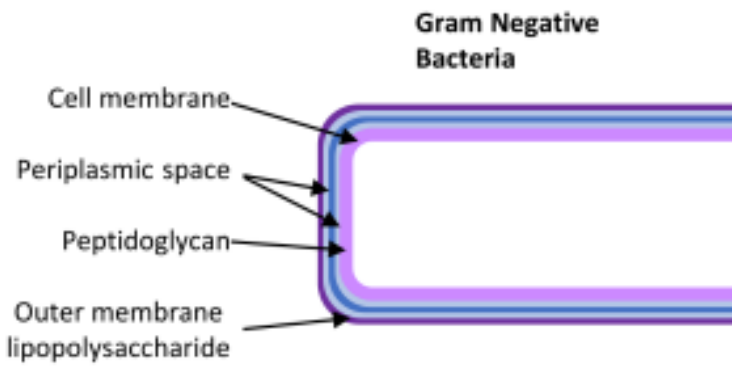

Figure 3: The membrane structure of gram-negative bacteria.

This bacterial endotoxin is a negatively charged, amphiphilic and heat-stable glycoconjugate that readily clusters into micelles or vesicles in aqueous solutions.[142] It accounts for 10% - 15% of the overall quantity of molecules present in the OM and makes up 75% of the entire bacterial surface.[143] LPS is characterized by three distinct structural components: (i) Lipid A -the innermost hydrophobic component that is responsible for the toxicity of LPS- made from a disaccharide acylated with fatty acids; (ii) the core domain which joins lipid A to the O-antigen, which is made from a non-repetitive short-chain oligosaccharide of approximately 9 sugars; and the (iii) O-antigen, an unevenly distributed hydrophilic oligosaccharide of repetitive glycan units that extends toward the bacterial surface.[144] The formation and assembly of LPS components occurs in the cytoplasm, followed by translocation to the external

membrane.[143] The O-antigen exhibits a high level of inter- and intra-species variation, making it the key component governing strain specificity.[145]

2.6.2) Function of lipopolysaccharide

LPS carries out two significant functions: firstly, it facilitates a defense reaction against adverse environmental conditions by providing a protective barrier to Gram-negative bacteria; consequently making it essential for bacterial resistance and viability.[146] Secondly, because of its quick recognition and sensing, LPS can initiate an immunological reaction within the host immune system leading to the removal of a bacterial infection.[147] In essence, it activates the complement system to enhance inflammation and inhibit the development of the membrane attack complex (MAC) on the pathogen cell surface.[143] However, this immunological reaction needs to be balanced or it may become detrimental to the host.[148] Rampant bacterial overgrowth causes an abundant release of unbound/free LPS into the circulatory system which activates monocytes and endothelial cells, inducing an exaggerated systemic immune response that involves an excess production of inflammatory mediators that cause tissue damage, septic shock or death.[148] In contrast, low amounts of LPS benefit the host by granting protection against local infections through the immediate activation of immune reactions such as the production and activation of dendritic cells, natural killer cells, B- and T-cell functions, initiation of fever and the complement cascade.[138]

2.6.3) Proteins involved in liopolysaccharide induced toll-like receptor 4 signalling cascade

LPS is easily identified by the innate immune system.[140] Contact with the immune system is initiated through recognition of the lipid A receptor, which prompts the involvement of the adaptive immune response through the O-antigen.[140] The innate immune system uses PRRs such as Toll-like receptor 4 (TLR4) and glycoprotein MD-2, as the first line of defense that forms a complex functioning to identify PAMPs (i.e. LPS) for the purpose of stimulating intracellular signaling pathways that activate the cellular expression of inflammatory mediators. [147,149] Cluster of differentiation 14 (CD14) is a glycoprotein anchored on the membrane of monocytes and macrophages (mCD14) or soluble in plasma (sCD14) which increases the potency of the immune response to LPS via stimulation of the TLR4 signal pathway. [150]

2.6.4) Mechanism of action of liopolysaccharide induced toll-like receptor 4 signalling cascade

LPS-binding protein (LBP), a lipid transferase present in the liver and released into plasma, will first detect the presence of endotoxin bacterial components and proceed to bind to the lipid A domain of LPS, dislodging it from the bacterial membrane.[150] LBP then shuttles LPS monomers to CD14 proteins and these CD14 proteins will finally deliver the LPS monomers to a TLR4/MD2 complex.[150] The receptor binding of LPS to the TLR4/MD2 complex activates the fusion of cytosolic translocated intimin receptor (TIR) domains of TLR4 causing the mobilization of downstream accessory proteins.[151] This TLR4 signaling transduction pathway activates the expression of pro-inflammatory cytokines and IFNs via NF-κB nuclear translocation and IFN regulatory factors, respectively.[148,152] Importantly, TLR4 can be stimulated by LPS at a concentration as low as 0.1 ng/mL.[153] The signaling cascade is also characterized by the release of ROS, anti-inflammatory cytokines i.e. IL-1 receptor antagonist (IL-1Ra), IL-4, IL-10, IL-13, anti-microbial peptides, TNF-α, prostaglandin E2, IFN-γ, C-reactive protein, hydroxyl radicals, NO and O_2^-.[150,154] **Figure 4** represents the LPS induced TLR4 signalling cascade.

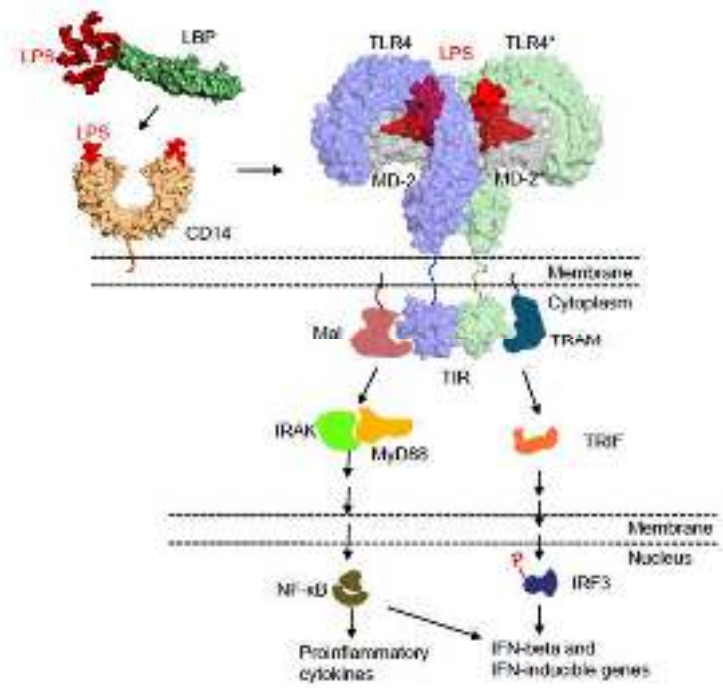

Figure 4: The LPS induced TLR4 signaling cascade that activates an innate immune response. Source: Supplementary Figure 1, Park, BS *et al* (2012).[155]

LBP-deficient mice show a hypo-responsive effect to LPS- as demonstrated by reduced amounts of serum inflammatory mediators and increased mortality rates after infection with *Escherichia coli*.[156] In the gut, LBP is secreted into the lumen not only to detect bacterial invasion but to also regulate symbiont-derived LPS, making it fundamental for intestinal homeostasis.[157]

2.7 Probable sites of lipopolysaccharide entry

2.7.1) Gut microbiome and its development

All mammals are colonized by plentiful and heterogeneous populations of microbial species that are central to the organization and function of the host; in that, they play a role in energy regulation, metabolism, intestinal epithelial health, immunological processes, and neurodevelopment.[158,159,160] The human gastrointestinal tract (GIT) houses 10^{13} -10^{14} different species of symbiotic, commensal and pathogenic microorganisms consisting of bacteria, archaea, viruses, fungi, phages and protozoa that collectively form an ecological community known as the microbiome.[161,158] The microbiome is an adaptive community susceptible to extensive changes in composition and efficacy in response to numerous factors such as diet, external environmental signals (i.e. geography and culture), pathological conditions and medical therapies (i.e. antibiotics).[162] However, microbiome inhabitation is not limited to the gut, other body areas of microbial colonization include the skin and oral cavity.[163] Microbial flora in the neonatal GIT is inherited maternally during childbirth where the species of the flora is largely influenced by the mode of delivery.[163] In toddlers, the composition, heterogeneity, and efficacy parallel the healthy adult gut microbiome and is related to usual developmental milestones, up until late adulthood (~65 years) where there is a shift that favors Bacteroidetes and Clostridium cluster IV.[164,165] Considering that almost 70%-80% of the immune system inhabits the mucosal lymphoid tissue of the GIT, it is unsurprising that growing evidence proposes that microbiota participate in the physiology, development, and pathology of their host organisms, thus implicating them in both health and disease states, where they develop and maintain host immunity.[166,167]

2.7.1.1) Limitations of the gastrointestinal tract

The intestinal lumen is sheathed by a continuous layer of epithelial cells that form a protective barrier and interaction surface for internal organs against microbial pathogens and antigens and the relay of information between the host and gut microbiota, respectively.[168] However, intestinal bacteria are capable of synthesizing and releasing a variety of substances that disrupt the integrity of the epithelial barrier by increasing its permeability and enabling the uncontrolled movement of gut microbiota into the lamina propria, where a majority of intestinal immune cells are localized within the gut-associated lymphoid tissues (GALT).[169,170] Consequently, systemic inflammatory responses that compromise the integrity and functionality of the BBB are triggered.[169] When the BBB is compromised, microbes from the gut infiltrate the CNS environment to induce neuroinflammation which ultimately leads to neurodegeneration.[171]

2.7.1.2) Brain-Gut-Microbiome Axis

The gut-brain axis describes a neural, immune, endocrine and metabolic mechanism of communication between the microbiota, GIT and the brain in a bidirectional pathway by virtue of the autonomic nervous system (ANS) and circumventricular organs (CVOs).[169,172] The ANS is at the epicenter of this interaction through its signaling divisions: the sympathetic (via the prevertebral ganglia) and parasympathetic (via the vagus nerve) nervous systems. Jointly, each division functions to detect gut microbiota and transmit information to the CNS where it is integrated, modified and a suitable reaction is implemented.[173,174] Afferent fibers of the vagus nerve express TLR4s that are capable of detecting gut pathogens like LPS and sending signals to the brain to activate inflammatory pathways.[161]

Elderly individuals are faced with the possible development of a hyper-stimulated immune state that is characterized by chronic, low-grade inflammation called inflammaging.[175] Inflammaging is associated with a sustained inflammatory reaction of the GIT mucosa that is induced by an age-related shift in the microbiome composition, heterogeneity, and efficacy resulting in increased: permeability of the epithelial barrier, bacterial translocation into the bloodstream, pro-inflammatory

cytokines, BBB permeability, and neuroinflammation.[176] **Figure 5**[177] illustrates the gut-brain communication and the presumed involvement of gut microbiota in AD.

In conjunction with the complex interaction between the microbiome, gut, and brain, it is meaningful to note that the gut microbiome is interrelated to the oral cavity microbiome by composition and heterogeneity.[163] Recent evidence suggests that there is an association between oral pathogens and changes in gut microbial composition in addition to inflammatory changes in brain tissue.[163,178]

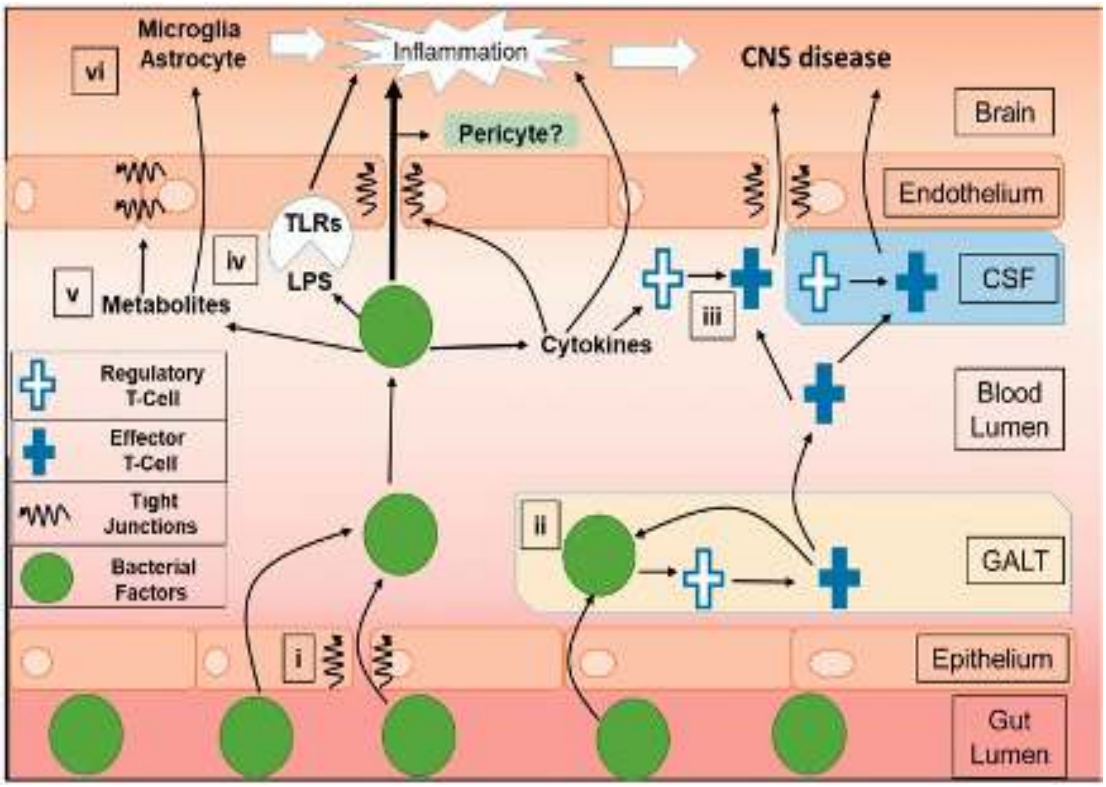

Figure 5:[177] Intestinal microbiota from the gut lumen is the source of a great number of bacterial factors such as bacterial amyloids (produced by *Escherichia coli*), LPS and other toxins, that are detected by TLRs of enteroendocrine cells (EECs) which are found on the epithelial membrane.[179,180] (i)These factors are capable of disrupting the permeability of the epithelium to promote their movement into the bloodstream. (ii) In the blood lumen, these factors can penetrate the GALT where they activate immune cells to proliferate e.g. T-cells resulting in direct communication with the innate immune system.[171,181] (iii) Regulatory T-cells circulating in the bloodstream survey the blood, lymphoid tissue, and CSF, this altered cellular environment stimulates T-cell brain permeation.[182](iv) Bacterial factors such as LPS activate inflammatory pathways that trigger increased cytokine levels and BBB permeability; they may also be detected by endothelial TLR4s of the brain thereby stimulating neuroinflammation and CNS pathologies.[183] (v) Microbial metabolites are capable of activating tight junction proteins, subsequently restoring BBB integrity, though, they are also capable of infiltrating the BBB, priming microglia and astrocytes, stimulating neuroinflammation, disrupting Aβ clearance and increasing neurotoxicity.[184,185]

2.7.1.3) Oral cavity pathogens

The periodontium is a set of tissue structures composed of the gingival, periodontal ligaments, cementum and alveolar bone,that surround and support the teeth.[186] Periodontal disease (periodontitis) is a persistent inflammatory condition of the periodontium.[187] In its progressed state, periodontitis is presented by damage to the periodontal ligament and decay of the alveolar bone.[187] Risk factors for this disease include smoking, poor oral hygiene, hormonal changes in females, medications, stress and advancing age.[188]

2.7.1.4) The interrelation between oral cavity flora and the gut microbiome

Growing evidence suggests an association between periodontitis and systemic diseases including AD.[189] It is unclear whether periodontal pathogens initiate the onset of systemic diseases or if systemic diseases trigger the accumulation of periodontal pathogens.[188] However, it is noted that the swallowed salivary bacterial content of patients with periodontitis is ~10^{12} bacteria/day.[190] A study by Tiisanoja, A *et al* (2019).[191] found a stronger association between tooth decay and AD in comparison to other oral diseases such as periodontitis and stomatitis. Nonetheless, research suggests that toxic bacterial molecules like LPS or peptidoglycan may originate from the ingestion of periodontal pathogens (i.e.*P.gingivalis* and *T.denticola*) causing either a change in the composition of the gut microbiome or the activation of an inflammatory response.[192] Mice that are orally infected with *P.gingivalis* exhibit impaired learning and memory skills in addition to depression-associated behavior.[193,194] Migrating periopathogens and pathogenic gut microbes in the bloodstream are detected by systemic and CNS immune cells.[195] If pathogens are abundant, inflammatory mediators are produced in surplus and released.[195] These mediators disrupt the integrity of the BBB ultimately leading to neuroinflammation and contributing towards AD development.[195,163] The pathways resulting in pathological outcomes are illustrated in **figure 6**.

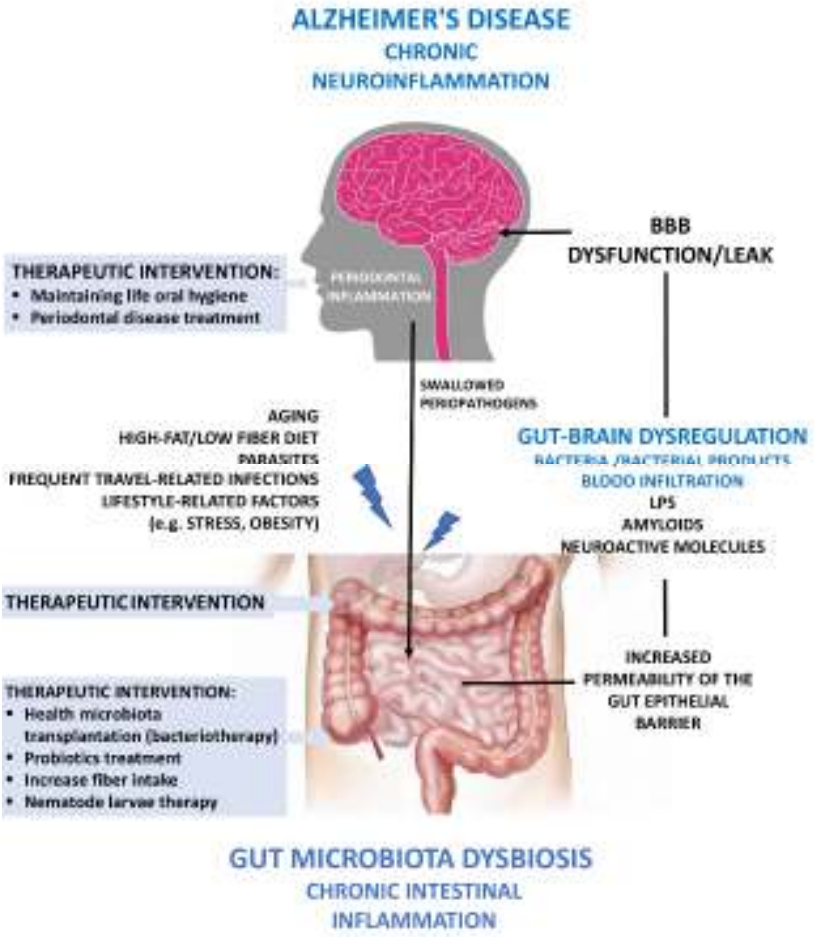

Figure 6:[163] The pathways linking gut microbiota, oral flora, and AD.

Pathogens from oral diseases cause periodontal inflammation which releases toxic molecules into the intestinal lumen causing infiltration of microbes into the bloodstream and signal transmission to the CNS that destabilizes the BBB, leading to chronic neuroinflammation and possibly AD.

2.8 Using the hippocampus to measure the degree of induced neuroinflammation

Though the pathophysiology of AD has been central to dementia research, the basic processes that facilitate disease pathogenesis and progression are yet to be understood.

Due to a close link between the vulnerability to amyloid and tau pathology, high astrocyte and microglial activity and its role in learning and memory decline, the hippocampus is a classic and valuable model for investigating the effects of dementia-related neuroinflammation.[196] For this study, three important components have been selected which may shed light on the effects of LPS induced neuroinflammation as well as the protective and therapeutic benefits of honey in a dementia-type animal model.

2.8.1) Neuroglial activation in neuroinflammation

Neuroinflammation is prevalent in neurodegenerative conditions. Characterized by three features; glial cell activation, the release of inflammatory mediators and permeation of peripheral immune cells into the brain tissue, its chronic state plays a major role in disease pathogenesis.[197] The neuron-astrocyte-microglia triad is essential for the normal functioning of the brain, any inefficiency in this interaction may trigger neurodegeneration.[198,199] The surface membranes of astrocytes and microglia contain receptors that bind molecules secreted by neurons.[200,201] This activates downstream intracellular pathways that induce the degradtion of apoptotic neurons and abnormal cells.[202] Also, because Aβ production occurs in several cells including neurons, its presence leads to an innate immune reaction that activates astrocytes and microglia to facilitate its own clearance from the brain.[203,204] Characterized by hypertrophic cells and increased hippocampal GFAP expression, the degree of astrogliosis is linked to cognitive deterioration.[205] Along with this, microglia is the predominant cell type to engulf fibrillary Aβ proteins irrespective of the conditions but because this phagocytic process is dysfunctional in AD, pro-inflammatory mediators escalate and Aβ deposition rises to overwhelming and pathogenic levels.[206,207] Marked by an upregulated state at the site of injury following neuronal damage-mediated inflammation, calcium-binding adapter molecule Iba1, is used as a marker for microglial activation and migration during the clearance of tau deposits.[208,209,210]

Promisingly, new studies exploring alternative dementia treatments suggest that honey may provide prophylactic effects against Aβ deposition and LPS-induced neuroinflammation on the hippocampus.[211]

2.8.2) Honey as a protective agent

Honey is a natural functional food produced by worker bees that has been used as a nutrient and traditional medicine since ancient times.[212] It is a hypersaturated liquid composed mainly of fructose and glucose in addition to various bioactive compounds and antioxidants including; polyphenols, flavonoids, amino acids, minerals, vitamins B,C,E, enzymes and organic acids.[212] In favor of its biological, pharmacological and physiological properties, many people resort to honey as an alternative to chemical treatments, also because it has fewer side effects.[213] Amongst a myriad of health benefits, shown in **figure 7**, honey is becoming more popular in neural disease research.

Figure 7: A summary of the documented therapeutic effects of honey.[214]

Numerous studies have attempted to elucidate the exact biological pathways that render honey as a neuroprotective agent in dementia. An inquiry by Tonks *et al.* (2003) showed that exposing monocytes to Manuka honey increased the production of TNF-α and interleukins

IL-1β, IL-6 via a TLR4 dependent pathway.[215] Another study revealed that Manuka honey improves cellular viability while reducing apoptosis and neuroinflammation by lowering caspase 3, p-p38 and p-Erk1/2 protein levels in LPS-exposed macrophages.[216] The benefits of honey extend to the GIT as well as brain tissue and its respective functions.The high carbohydrate content in honey facilitates *bifidobacterium* proliferation in the GIT whilst the polyphenol content suppresses the growth of intestinal pathogens that incite gut leakiness and allow LPS entry into circulation.[217] Furthermore, Al-Rahbi *et al*.(2014) found that oral ingestion of honey increases the expression of neurons in the hippocampus in addition to brain-derived neurotrophic factor, which is related to enhanced spatial memory.[218]

Considering the inefficiency and harsh side effects of synthetic remedies of dementia, it is valuable to explore the protective effects of functional foods such as honey.

2.8.3) Behavioural tests in dementia-type models

Animal models are used in a wide range of biomedical studies to investigate and gain insight into specific theories concerned with the physiological, cellular and molecular mechanisms underlying AD dementia etiology. Behavioral assays are also used to quantify cognitive impairments such as learning and memory in animal species. The main goal of these tests is to advance knowledge on already existing treatments while developing new and better effective strategies against diseases affecting humans.[254]

2.9 Aim and Objectives

With a comprehensive understanding of the implications of neuroinflammation on dementia and the mechanisms underlying its manifestation in the hippocampus, the following questions emerge;

i. Doesa chronic systemic LPS exposure cause AD-like brain damage and symptoms? If so, how does it present itself?
ii. If chronic systemic LPS does indeed cause AD-like brain damage and symptoms, are these effects evident in the behavioral pattern of Sprague Dawley rats?
iii. Does oral ingestion of honey mop-up the deleterious effects of chronic LPS exposure, both histologically and behaviorally?

These questions give rise to the following aim and objectives:

Aim

The aim of this study is to investigate the effect of neuroinflammation induced by systemic lipopolysaccharide on the hippocampus of 10 weeks old male Sprague-Dawley rats.

In order to achieve the aim the objectives are to

Quantitative biochemical assays

- Assess the progression of amyloid β (Aβ) pathology by measuring the concentration of soluble $A\beta_{42}$ levels in the hippocampal tissue of male Sprague-Dawley rats using sandwich ELISA assay.

- Determine the number of astrocytes present in the hippocampal tissue of Sprague-Dawley rats by immunofluorescence staining with glial fibrillary acidic protein (GFAP) antibody using confocal microscopy and ImageJ.

- Identify astrocyte activity (astrogliosis) in the hippocampal tissue of Sprague-Dawley rats by measuring fluorescent intensity using a GFAP antibody using confocal microscopy and ImageJ.

- Identify microglial activity (microgliosis) in the hippocampal tissue of aged Sprague-Dawley rats by co-labeling tissue sections with Iba1 and CD68 antibodies and counting the number of Iba1 positive cells using confocal microscopy and ImageJ and measuring the fluorescent intensity of co-localized Iba1 and CD68 positive cells using ImageJ.

- Identify the protective effects of honey on the astrocyte and microglial expression/quantity in the hippocampal tissue of aged Sprague-Dawley rats using ImageJ.

- Identity the amyloidosis in the hippocampal tissue of aged Sprague-Dawley rats by measuring fluorescent intensity using Thioflavin-T (ThT) dye using confocal microscopy and ImageJ.

Behavioral analysis

- Assess the effects of systemically induced neuroinflammation on the short-term spatial working memory of Sprague-Dawley rats using the spatial recognition Y-maze test.

- Assess the effects of systemically induced neuroinflammation on the learning capacity and spontaneous memory of Sprague-Dawley rats using the novel object recognition test.

- Assess the effects of systemically induced neuroinflammation on the exploratory behavior, anxiety and locomotor activity of Sprague-Dawley rats using the open field test.

3

Chapter 3: Study Design, Sampling, and Statistics

3.1 Study Design

This study adopted a randomized intervention approach using an animal model. A total of forty Sprague-Dawley rats, housed at the University of the Witwatersrand Central Animal Services (CAS) unit was used. The subjects were randomly assigned into four sample groups, with each group containing ten subjects (n=10). The four groups and their treatment were assigned as indicated in **table 1**.

Table 1: Categorization of the experimental groups and the treatment received per group. SC=subcutaneous

Sample group name	Treatment type	Treatment received	Category
PBS	PBS only	Daily SC injection of 0.1M PBS at a volume of 0.1ml/kg for 10 days.	Control group
PBS + H	PBS and Honey	Daily SC injection of 0.1M PBS at a volume of 0.1ml/kg for 10 days + 0.5 ml honey* per kg of rat via oral gavage from day 4 until day 10.	Experimental group 1
LPS	LPS	Daily SC injection of 0.1M LPS dissolved in 0.1M PBS at a volume of 0.1ml/kg for 10 days.	Experimental group 2
LPS + H	LPS and Honey	Daily SC injection of 0.1M LPS dissolved in 0.1M PBS at a volume of 0.1ml/kg for 10 days. + 0.5 ml honey* per kg of rat via oral gavage from day 4 until day 10.	Experimental group 3

*The Manuka honey was mixed 50% v/v with distilled water to enable a comfortable consistency for the rats.

Prior to termination, behavioural tests using the spatial recognition Y-maze, novel object recognition (NOR) test and open field test were performed on all the animals. This was followed by quantitative sample analysis on the dorsal hippocampal region using ELISA and Immunostaining assays.

3.2 Ethical Considerations

Ethical approval was obtained from the University of Pretoria Health Sciences Research Ethics Committee as well as University of Pretoria Animal Ethics Committee under protocol number 181-2020 (addendum 1). Ethical approval was also obtained from the University of the Witwatersrand Animal Research Ethics Committee, Faculty of Health Sciences under protocol number 2019/07/44/C (addendum 2). Approval from the University of Pretoria, MSc Committee was granted (addendum 3).

The following animal ethical concerns were adhered to:

- All animal subjects were treated with sensitivity and respect;
- No animal subjects were subjected to intentions which were not directly concerned with the research project objectives and methodology;
- Professional standards were upheld in accordance with research training given prior;
- Responsibility for the proper care and use of the animal subjects;
- Integrity towards the animal subjects were promoted through honesty and fairness;

3.3 Sampling Population and Procedures

Sampling Population:

Ten-week-old Sprague Dawley rats, with an average weight of 250-300 grams were maintained at the University of the Witwatersrand, CAS housing facility, as shown in **figure 8 (A-D)**. In this study, the Sprague Dawley rat strain was favoured because of its clam temperament and ease of handling[219], which is significant for behavioural analyses. A male-only population was used in this study to limit the number of probable confounding variables caused by hormonal fluctuations in female populations. The subjects were housed conventionally with sizes laid down per the South African National Standards (SANS) 10386:2008 recommendations. Subjects were provided with standard irradiated “Epol” rat pellets and municipal water ad libitum. The subjects were housed in pairs per cage and

autoclaved pinewood shavings were used as a bedding material, along with white facial tissue paper for enrichment as photographically indicated in **figure 8 (E-F)**. The room temperature was maintained at 23°C (± 2°C) with a relative humidity of 50% (± 20%) and a 12-hour night/dark cycle throughout the study.

Figure 8: Facilities of the CAS unit that were used during this project.

(A-D). The subjects were housed in pairs inside cages containing pinewood shavings and an object for the subjects to play with (E-F).

The subjects were given a seven-day habituation period prior to the start of the experimental period where the first dose of LPS and/or PBS was administered. The experimental period

extended for 10 days. Thus, the total housing period of the subjects was 19 days. Trials to assess rodent behavioural patterns were carried out at the University of the Witwatersrand-health sciences campus, CAS laboratory. Histological analyses were conducted at the University of Pretoria (Lynnwood Rd, Hatfield, Pretoria, 0002), Haematology and bone analysis laboratory-Natural Sciences 2 building. The experimental procedures followed during this study are indicated in **figure 9.**

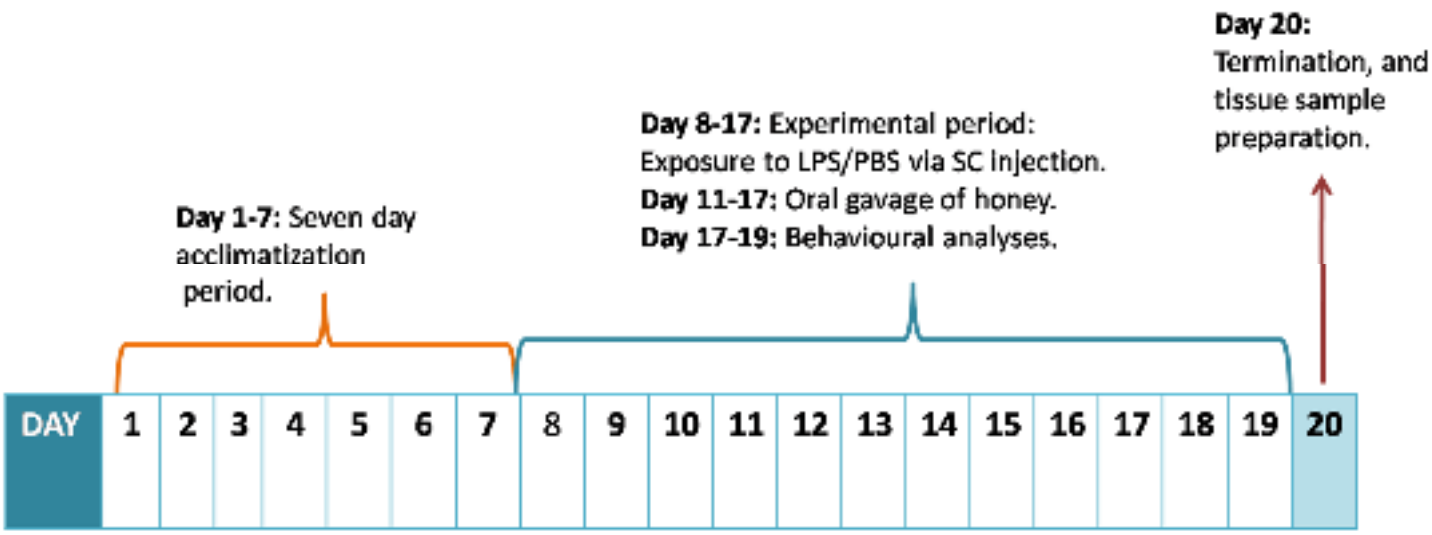

Figure 9: An overview of the procedures that were conducted throughout this study. During the seven-day acclimatization period, subjects were acclimatized to handling and the environment. Next, subjects were administered 0.1M LPS and/or 0.1M PBS via subcutaneous injection for ten days (experimental period). During this 10-day experimental period, Manuka honey was introduced in the intervention groups (PBS+H group and LPS+H group) on day 11 via oral gavage at a volume of 0.5 ml/kg, diluted at 50% v/v with distilled water to enable comfortable consistency. Behavioural analyses were performed between day 17-19. Day 20 was reserved for termination and sample preparation.

The Manuka honey, acquired from Advancis Medical, has no additives and is both filtered and sterilized thus limiting the cofounding effects of possible contaminants. Manuka honey is a medical grade honey sourced from New Zealand that shows potent anti-inflammatory and antioxidant effects as well as enhances immunity by stimulating white blood cells and promotes a good intestinal flora balance. As a result of the filtration process of the medical grade honey there is no variability between samples and thus pooling is not necessary.

Day 20 was reserved for termination and sample preparation. Before termination, each animal was weighed, and the core body temperature was measured using a digital thermometer. Isofor® was used as an inhalation anaesthetic inside the gas chamber which each animal was placed in for 30 seconds. Next, cardiac puncture was performed to euthanize the animals as well as to enable blood collection into applicable Vacutainer blood collection tubes. Blood samples were used for a separate study that took place in conjunction with this study. Ethical approval was obtained for the use of blood samples- Protocol number: 171/2020.This was followed by perfusion with cold sterile saline solution and decapitation by guillotine. Lastly, the brain was carefully extracted from the skull. Each brain was separated into the left and right hemispheres. The right hemisphere was used for biochemical analyses, while the left hemisphere was used for confocal microscopy. **Figure 10** summarizes the process of sample collection.

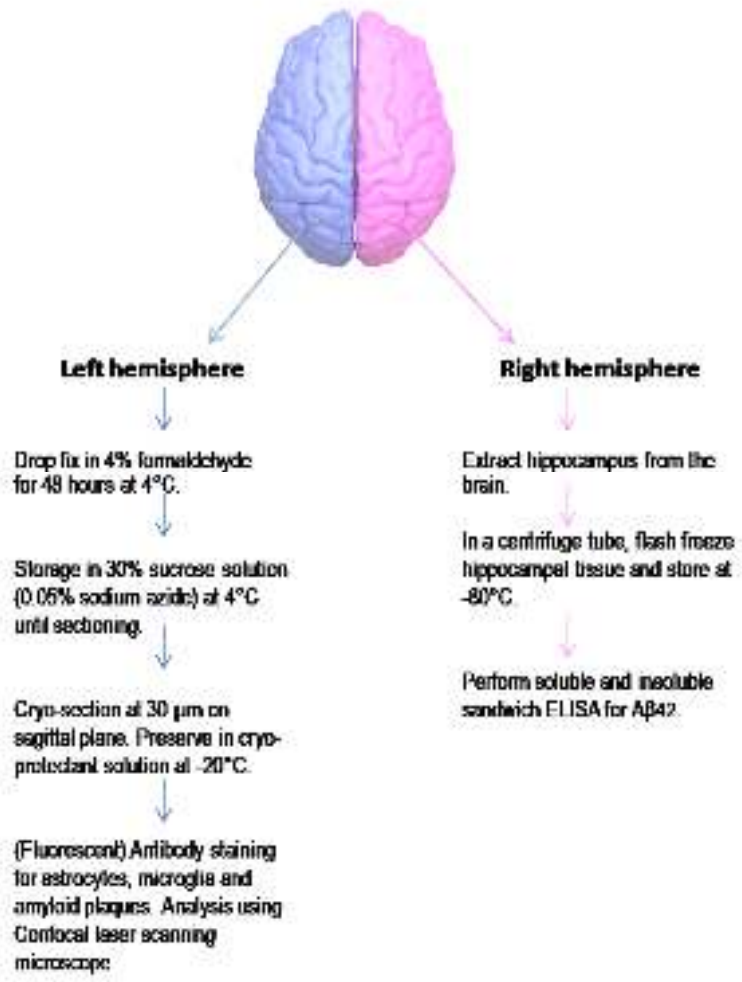

Figure 10: A summary showing the sequence of events followed to prepare hippocampal tissue samples for biochemical and histological assays after the subjects were terminated.

3.4 Statistics

This study and all experimental procedural details were discussed with a statistician from the South African Medical Research Council Biostatistics Unit and a letter granting statistical support was been provided (addendum 5). The specific statistical tests and analyses employed per experiment can be found in the method and materials section of their respective following chapters.

4

Chapter 4: Behavioural analyses

4.1 Chapter Objectives

This chapter will address the methods and results pertinent to the following objectives:

- The effects of systemically induced neuroinflammation on the short-term spatial working memory of Sprague-Dawley rats using the spatial recognition two-trial Y-maze test.

- The effects of systemically induced neuroinflammation on learning capacity and spontaneous memory of Sprague-Dawley rats using the novel object recognition test.

- The effects of systemically induced neuroinflammation on exploratory behaviour, anxiety, and locomotor activity of Sprague-Dawley rats using the open field test.

4.2 Introduction

Due to the slow-paced progression of dementia and the prolonged pre-clinical period before a provisional diagnosis, researchers are often forced to look at alternative ways to understand the aetiology of the disease while developing new treatment strategies.[218]
Animal models are instrumental resources to better understand the biological mechanisms underlying dementia.[218] Behavioural assessments that reflect aspects of cognitive, social, and locomotor ability pave the way for advances in novel therapies, such as the possible effects of honey in the alleviation of neuroinflammation.[218] **Table 2** lists various behavioural tests used to assess specific features of dementia-like pathology in rodent models *in vivo*.

Table 2: A summary of various behavioural tests conducted on dementia-type rodent populations.[255,256]

TEST	FUNCTION TESTED
Open field test	Locomotor activity, anxiety, and habituation
Morris water maze test	Spatial learning and memory
Fear conditioning	Emotional and contextual memory
Radial arm water maze test	Spatial learning (episodic-like) and working memory
Forced alternation Y maze	Working memory and exploratory behaviour
T maze	Spatial and working memory
Novel object recognition test	Recognition memory
Spontaneous alternation Y maze	Spatial working memory, reference working memory, and habituation

Given that neurological damage is coupled with memory impairment, spatial or working memory is often affected.[220] The Y-maze paradigm provides means to examine cognition and navigational schemes, something that is of significance in identifying brain mechanisms and possible remedial treatments.[220] In addition, studies have shown that the NOR task is a robust and sensitive assay for assessing the cognitive-dysfunction activity of compounds such as LPS.[221] As this task allows to assess non-spatial memory that is devoid of emotional and learning factors in rodents.[222] Lastly, the open field test has been recognized as a straight-forward assay to evaluate anxiety-like behaviour and locomotor impairments in rodents.[220] It's basic protocol does not require subjects to undergo prior training or pre-conditioning. Reports by Fields, C indicate that a rise in enteric load of LPS amplifies anxiety-like behaviour across both sexes.[223] Altogether, these assays were chosen as most appropriate to meet the objectives of this chapter.

4.2.1) Spatial recognition two-trial Y-maze test

The spatial recognition two-trial Y-maze test is a behavioural test that examines learning ability, spatial working memory, and reference working memory in rodents.[218,219] This test is based on the notion that rodents are naturally explorative animals that show a willingness to explore new or strange environments.[219] Active engagement between multiple areas of the brain such as the hippocampus, prefrontal cortex, and basal forebrain is essential to execute

such activities.[220] Therefore, it is presumed that rodents without impaired prefrontal functions will recall previously explored arms and show more interest in the unvisited arms by entering more often.[219] Findings by Deacon, R.M *et al.*[221] (2006) showed that animals with hippocampal lesions tend to display a side preference and poorer performance during this task. Y-maze paradigms are also used in disease and transgenic rodent models to assess the effects of novel chemical agents and treatments on cognitive performance and degree of cognitive impairment.[220]

4.2.2) Novel Object Recognition (NOR) Test

The NOR test is an exploratory test based on simple visual recall behaviour. It is used to evaluate different stages of learning (i.e., encoding, retention, or retrieval), object recognition, and memory (i.e., short-term memory or long-term memory) in murine models.[222] It has been successfully applied to transgenic rodent models, lesion studies as well as neurodegenerative models.[223]

4.2.3) Open Field Test

The open-field is an exploratory task used to assess anxiety-like behaviour and locomotor activity in murine models.[224,225] This assay is centered around a parameter called "thigmotaxis", whereby, animals experiencing high levels of anxiety show a tendency to stay within close proximity to the walls of the arena.[220]

4.3 Methods and Materials

Behavioural analyses were conducted over a three-day period at the CAS unit, University of the Witswatersrand. The conditions of testing in the laboratory such as temperature, noise level, light intensity, and humidity were monitored and maintained throughout. With each assessment conducted, the apparatus was cleaned with 70% ethanol and allowed to dry completely between each trial run, to remove any olfactory cues.

For each assay conducted, an overhead camera was placed directly above the apparatus to video track the trials for each assessment. ANY-maze Video Tracking System (Version 4.2; Stoelting Co., Wood Dale, Il) was used to obtain and collate the results from the behavioural assessments for subsequent analysis.

The weight of each rat was measured and recorded daily throughout the experimental period. The welfare of each rat was also monitored and recorded daily on a welfare monitoring sheet (addendum 4) . Characteristics evaluated include movement, nourishment, breathing, and changes in behaviour during handling and facial expressions. The Rat Grimace scale, illustrated in **figure 11**, uses changes in facial expressions to quantify the degree of pain and discomfort in rats.[224] During the experimental period, pain and discomfort were monitored daily using this grading scale. The four parameters of interest were orbital tightening, nose/cheek flattening, ear changes, and whisker changes. If an “Obviously present” score was observed for any of the parameters, the subject would have been excluded from the study.

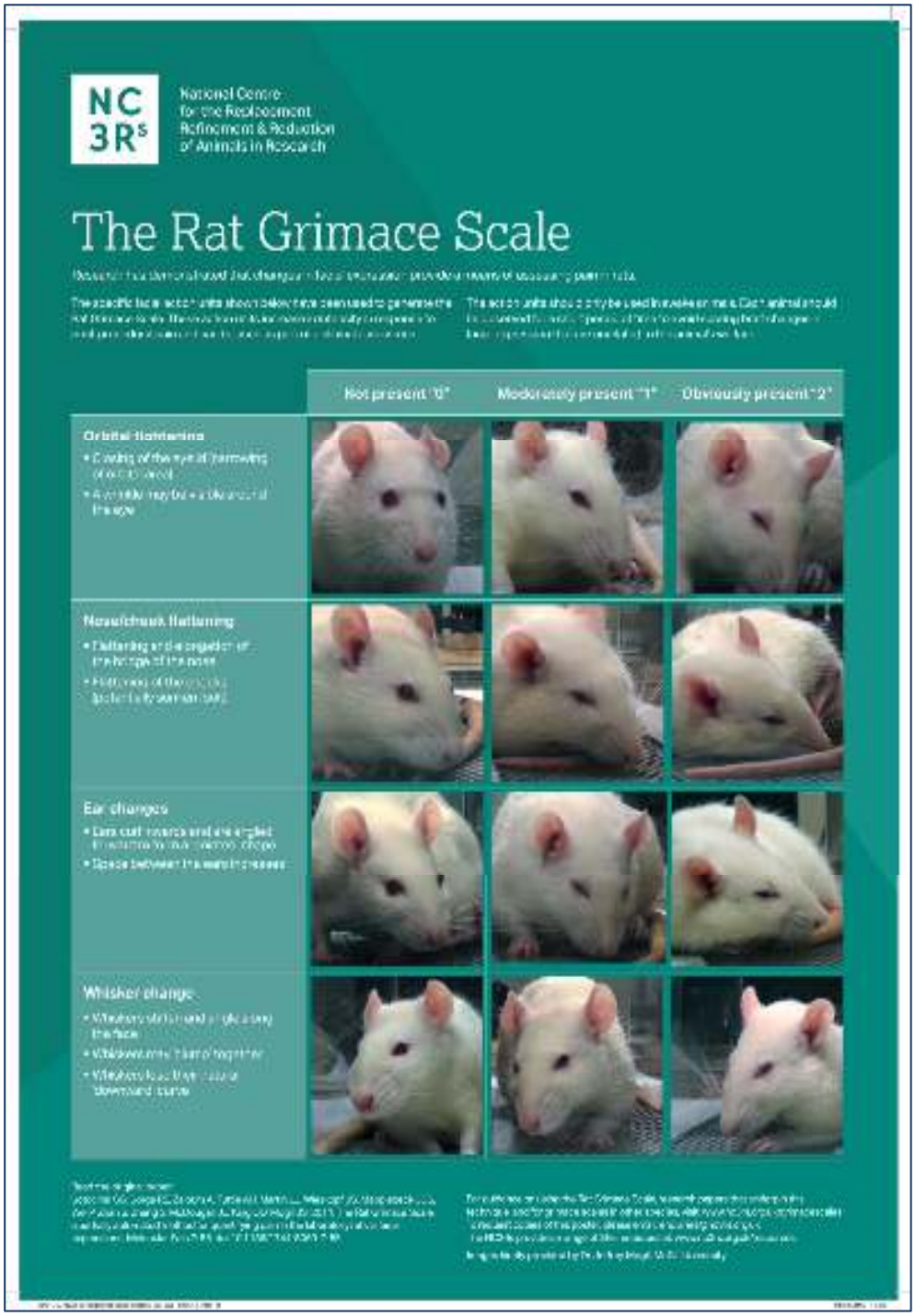

Figure 11: The Rat Grimace Scale uses various facial expressions to quantify signs of discomfort in rats during laboratory experiments.[224]

Figure 12 gives an overview of the behavioural assays conducted during the experimental period. It was recommended to conduct testing over three days to ensure that the subjects did not experience too much stress or get too tired.

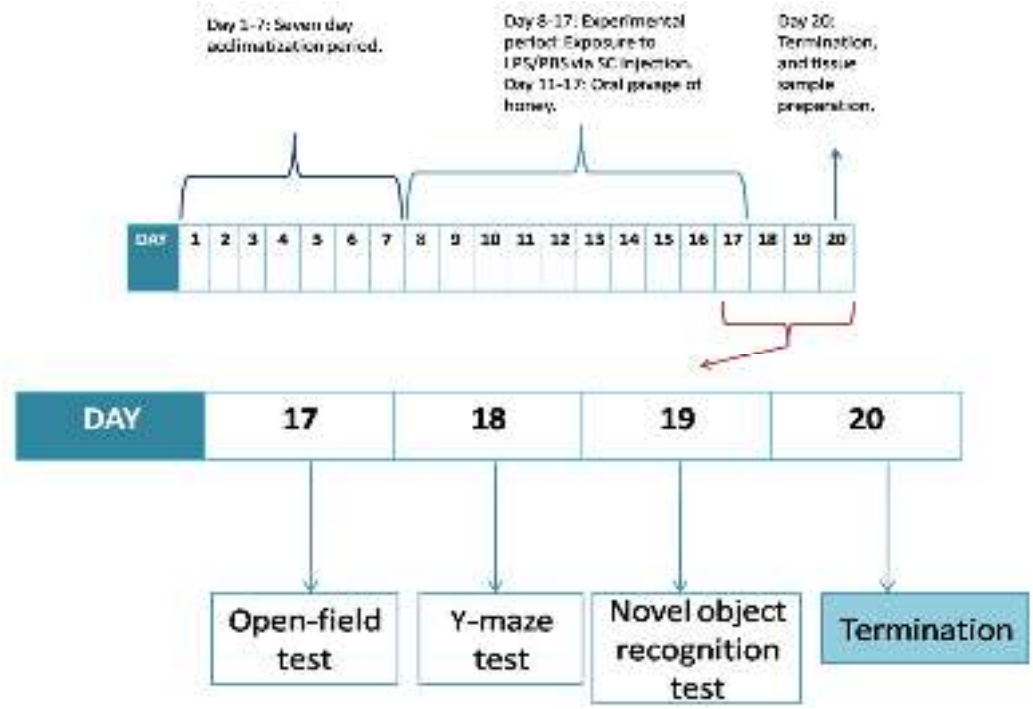

Figure 12: An overview of the study, highlighting the behavioural assays conducted before termination. Open-field analysis was performed on day 17, whilst the two-trial Y-maze test was completed on day 18, and the NOR test was conducted on day 19.

4.3.1) Behavioural analyses

4.3.1.1) Spatial recognition two-trial Y-maze assay

Testing occurred in two trials inside a Y-shaped chamber of three arms distanced at an angle of 120° relative to each other. The subject was placed at the central mid-zone area where all three arms meet, and it is allowed to explore the maze freely. Entry into an arm was characterized by the placement of all four paws within the boundaries of an arm. The time spent in each arm was also noteworthy. The laboratory temperature, noise level, light intensity, and humidity were controlled and maintained for all subjects during all experimental procedures. Light intensity in the testing room was dimmed to stimulate exploratory behaviour.

Apparatus: A Y-shaped maze made from Plexiglas, with three arms equally distributed at an angle of 120°. The arms were classified as follows; long (L), familiar (F), and novel (N). Each arm had a length of 63 cm, 54.9 cm, and 59.4 cm, respectively. All three arms had a width of 10 cm and a height of 15 cm to prevent escape from the maze. In **figure 13 (C)**, an overhead camera was prepared above the maze to video track and record memory and learning behaviour for subsequent analyses.

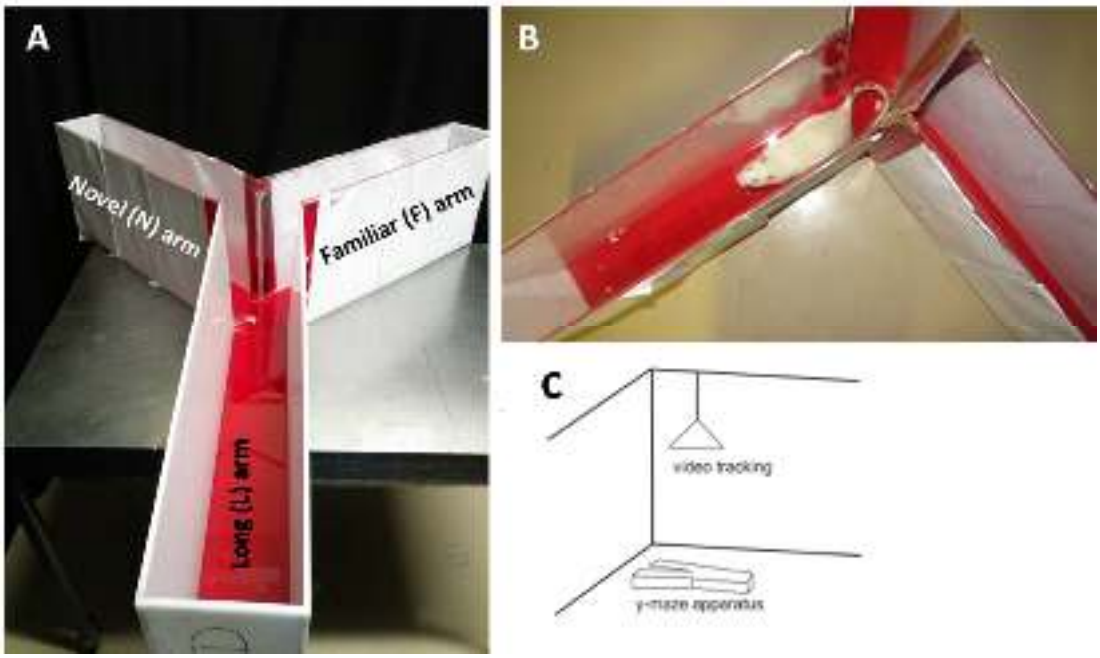

Figure 13: A graphic representation of the Y-maze apparatus (A) and the test subject inside the arena (B). An overhead camera with a video recording system was used to track behavioural activity (C). Image adapted from Prieur, E *et al*. (2019).[225]

Exploration trial: Plexiglas intercepted the novel arm of the maze, leaving only two arms available to explore. Subjects were brought in their housing cage into the laboratory testing room and allowed to acclimatize for one and a half hours in the absence of individuals and the testing apparatus. The rat was then placed in the central mid-zone of the Y-maze and allowed to freely explore the two available arms for two minutes and 30 seconds. The subjects were given a four-hour inter-trial interval before the testing trial of the procedure was conducted.

Testing (recognition) trial: The Plexiglas intercepting the novel arm was removed, leaving all three arms available for exploration. Each rat was brought into the laboratory testing room and allowed to acclimatize for ten minutes. The rat was placed in the mid-zone of the Y-maze and allowed to freely explore all arms of the maze for two minutes and 30 seconds.
Given that this test relies on novelty seeking and the innate tendency of rodents to explore their surroundings, it is anticipated that they will spend more time in the previously inaccessible (novel) arm than the two familiar arms. Therefore, the ability to differentiate the novel arm from familiar ones is used as a marker of spatial recognition memory.[226]

For consistency and analysis, the arms of the y-maze were classified as shown in **figure 14**.

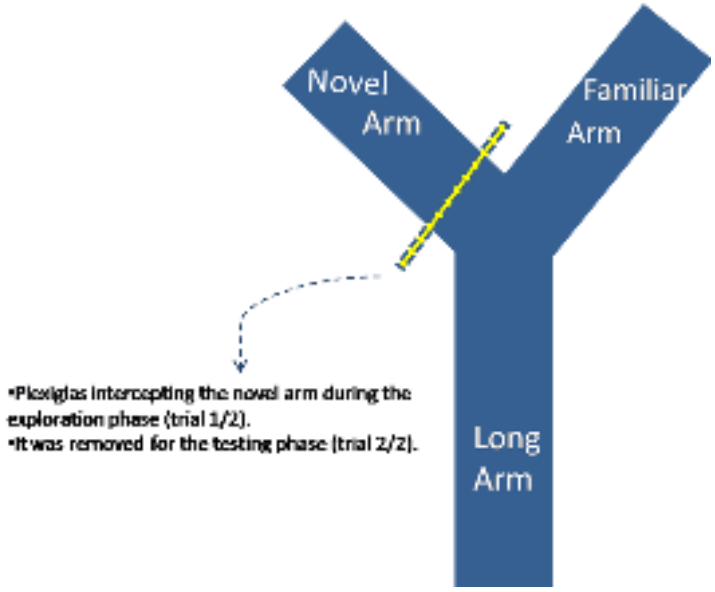

Figure 14: A diagram showing the classification of the arms of the y-maze apparatus.

Once the exploration and testing (recognition) trial were completed, the following parameters were considered for each arm of the maze:

i. Number of head entries
ii. Time spent within the arm
iii. The average speed
iv. The average number of visits
v. Time mobile
vi. Time immobile

4.3.2) Novel Object Recognition Test (NORT)

The assessment involved two trials; the training trial and the test trial.[227]

Apparatus: An open arena made from non-porous plastic with the following dimensions: a 65 cm (length) 60 cm (breadth) x 20 cm (height).

Training trial: This was conducted on day 17 of the experimental period. Each subject was brought in its housing cage into the laboratory testing room and allowed to acclimatize for ten minutes. The subject was placed at the centre of the arena and allowed to acclimatize for 30 seconds. Next, it was briefly removed from the arena while two identical objects (X + X), were placed inside the arena at opposite ends of each other (i.e., West and East). The subject was placed in between the two objects with its head facing the interior wall of the arena and

allowed to explore the identical objects for two minutes. Exploratory activity was assessed and used to evaluate memory retention and recall. Exploration was defined as the sweeping or sniffing of an object, with the subjects' nose pointed up towards the object, within a distance of 3 cm or less from the object. Finally, the subject was removed from the arena and returned to its housing cage.

Object selection: The objects were smaller than the subjects. They were made from soft foam and bright contrasting colours. They differed slightly in shape to stimulate exploratory behaviour.

Testing trial: This was performed on day 18 of the experimental period. One of the familiar objects (X) used during the training trial together with a novel object (Y) was placed inside the open arena, at opposite ends of one other. The subject was brought in its holding cage into the laboratory testing room and immediately placed at the centre of the objects (X + Y) inside the arena with its head facing the interior wall of the arena. The rat was allowed to freely explore the environment and the familiar object (X) vs. novel object (Y) for two minutes, as seen in **figure 15**. Exploratory activity was assessed and used to determine memory recall. Exploration was defined as the sweeping or sniffing of the object with the rats' nose pointed up towards the object, within 3 cm or less from the object. It was expected that rats with well-trained memory will discriminate between the familiar object (X) and the novel object (Y) and will spend more time exploring the novel object using induced preference and memory recall functions.

Figure 15: Testing trial of the novel object recognition test. The familiar object (A) and novel object (B) were placed at opposite ends. The test subject was allowed to explore each object for 2 minutes freely.

4.3.3) Open Field Analysis

Day 19 was reserved for the open-field assessment.

Apparatus: A wall-enclosed Plexiglas chamber with the dimensions: 1 m (length) x 1 m (breadth) and a height of 0.5 m to prevent the rat from escaping the enclosure. Using ANY-maze Video Tracking System, the base was divided into 25 smaller squares of 20 cm x 20 cm, which comprised the outermost area. The outmost area was further divided into an innermost area of 85 cm x 85 cm. **Figure 16 (A)** illustrates the open-field arena during the assessment, whereas **Figure 16 (B)** is a visual representation of the apparatus as displayed on the video tracking software.

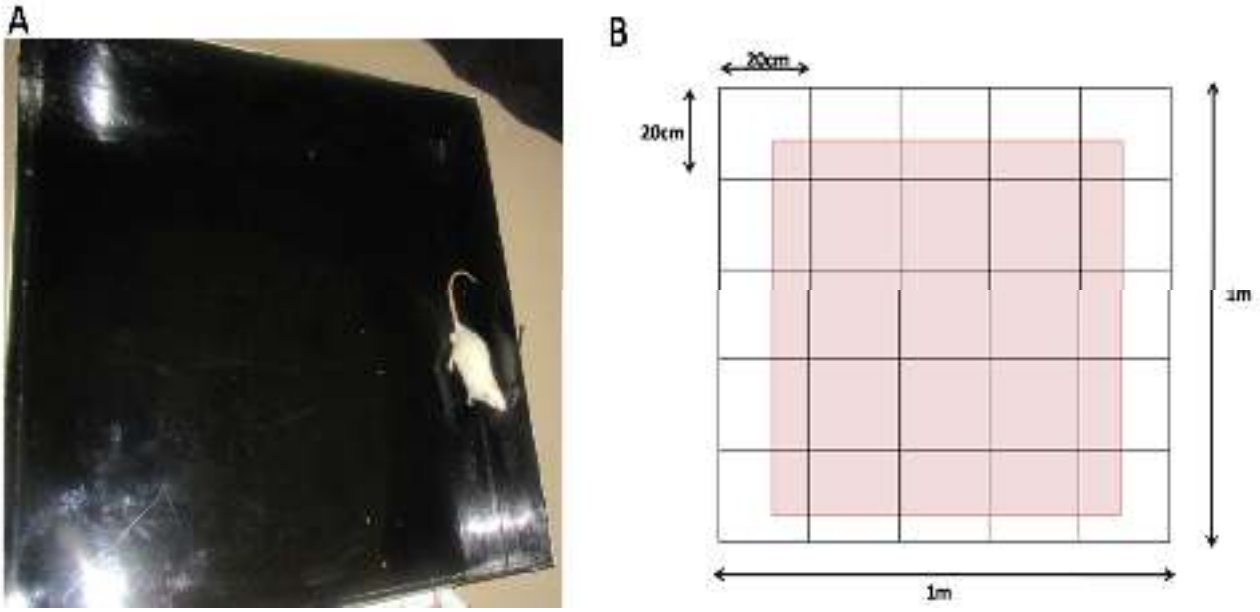

Figure 16: An illustration of the open-field arena with the subject inside (A). The surface of the open-field arena as depicted on Any-maze software (B). The outermost area comprises the entire 1 m x 1 m perimeter, and the innermost area includes the shaded region.

On the floor, it was positioned so that an overhead luminous light was the brightest on the innermost region and dim in the outermost area. This was built on the notion that rodents are fearful of large, bright spaces and are likely to seek shelter at the peripheral walls of the open field until they are comfortable and begins to explore, moving towards more brilliant light at the centre of the open field.

Testing trial: Habituation was not required for this assay. The subject was brought into the laboratory testing room and allowed to acclimatize for ten minutes without any individuals. The subject was gently placed inside the open-field, at the outermost area of dim light. A five-minute period was given for exploration. Exploratory activity was recorded as the number of lines crossed by the subject in five minutes. A line crossing was defined as all four paws crossing a boundary line that separates adjacent quadrants. It was expected that rats with less anxiety or unimpaired mobility would show more exploratory behaviour, thereby crossing more lines than those who were more anxious or with mobility issues. Behaviour was recorded from the time of subject placement into the field until the end of the trial.

4.4 Results

All statistical tests were completed using GraphPad™ Prism (version 9.2.0) for Windows (GraphPad™ Software, San Diego, California USA). The D'Agostino-Pearson normality test was used to establish that the dataset was normally distributed. Data was analysed using one-way analysis of variance (ANOVA). Post-hoc checks with Dunnett's multiple comparisons test were used to compare the three experimental groups to the control group. The results were represented as mean ± standard error of mean (SEM). Error bars indicate SEM. The p-value was set at $p < 0.05$, with a 95% confidence interval.

To characterize the effects of LPS-induced neuroinflammation on spatial working memory, learning capacity, and exploratory behaviour, the control group (PBS only) was compared to the three experimental groups (LPS only vs. LPS + H vs. PBS + H) using the Y-maze test, NORT and open-field test, respectively. Close examination of the mean scores per group reveal non-significant differences between them, although notable differences in performance between the groups were observed and thus discussed.

4.4.1) Spatial recognition Y-maze Analysis

Memory and learning impairments in the long arm of the y-maze were evaluated by analyzing the number of head entries into the arm during the exploration and testing/recognition trial as shown in **table 3** and **figure 17**. The number of head entries were not significantly different across the groups. Data from the testing trials were compared to exploration trial. To determine the performance of subjects, the control group was compared against the experimental groups.

Table 3: A summary of the mean scores and p-values obtained when evaluating the average number of entries into the long arm of the Y-maze chamber during the exploration trial (Trial 1/2), testing trial (Trial 2/2), in comparison to the novel arm (Trial 2/2-Novel arm).

Summary of the descriptive statistics of the number of head entries-long arm				
Group	Trial	Mean	Adjusted P-value	Significant?
PBS	Trial 1/2	5.1	-	-
PBS vs. LPS		4.5	0.6086	No
PBS vs. LPS+H		4.8	0.9184	No
PBS vs. PBS+H		4.7	0.8329	No
PBS	Trial 2/2	4.2	-	-
PBS vs. LPS		2.8	0.2009	No
PBS vs. LPS+H		3.5	0.7064	No
PBS vs. PBS+H		3.5	0.7064	No
PBS	Trial 2/2 (Novel arm)	7.5	-	-
PBS vs. LPS		8	08794	No
PBS vs. LPS+H		7.4	0.9987	No
PBS vs. PBS+H		7	0.8794	No

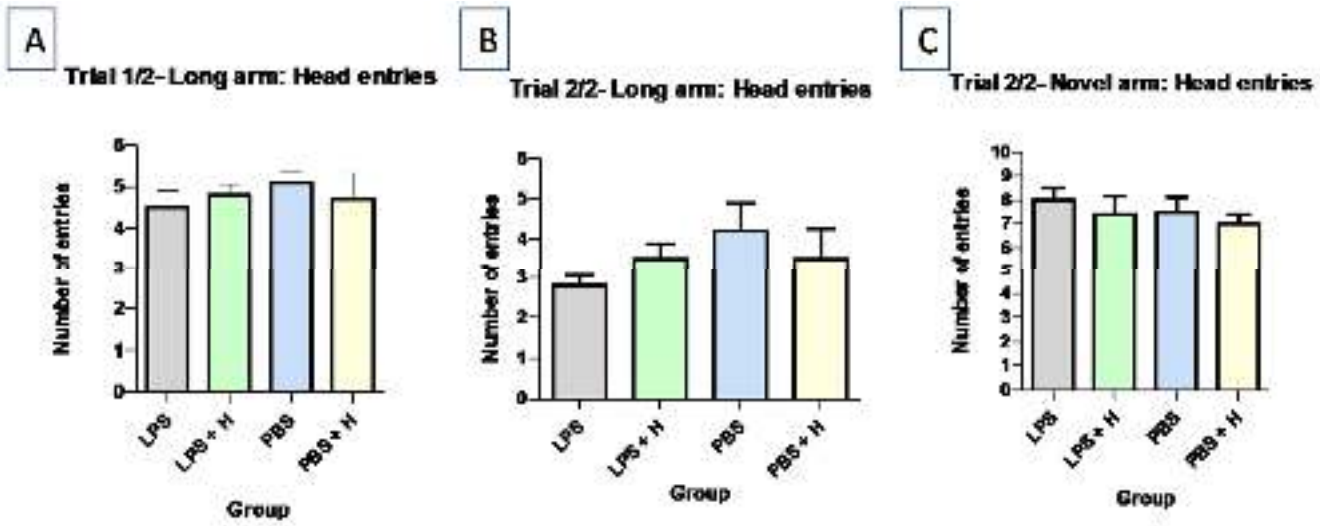

Figure 17 (A-C): Bar graph plot with mean and standard error of mean (SEM) for the number of head entries into the long and novel arm of the Y-maze chamber. Trial 1/2-Long arm shows the average number head entries into the long arm during the exploration trial (A). Trial 2/2-Long arm shows the average number head entries into the long arm during the testing/recognition trial (B). Trial 2/2-Novel arm shows the average head entries into the novel arm during the testing/recognition trial (C).

Next, the time spent in the long arm was analyzed and presented in **table 4** and **figure 18**. Results show that the time spent in the long arm during trial 2/2 was not significantly different than trial 1/2. And the time spent in trial 2/2 in the novel arm was not significantly different than trial 2/2 in the long arm.

Table 4: A summary of the mean scores and p-values obtained when evaluating the average time spent in the long arm of the Y-maze chamber during the exploration trial (Trial 1/2), testing/recognition trial (Trial 2/2), in comparison to the novel arm (Trial 2/2-Novel arm).

Summary of the descriptive statistics of the time spent-long arm				
Group	Trial	Mean	Adjusted P-value	Significant?
PBS	Trial 1/2	45.23	-	-
PBS vs. LPS		40.81	0.5729	No
PBS vs. LPS+H		43.12	0.9177	No
PBS vs. PBS+H		42.56	0.8512	No
PBS	Trial 2/2	28.17	-	-
PBS vs. LPS PBS vs. LPS+H		24.56 31.25	0.7458 0.8217	No No
PBS vs. PBS+H		21.35	0.2889	No
PBS	Trial 2/2 (Novel arm)	50.28	-	-
PBS vs. LPS		50.34	>0.9999	No
PBS vs. LPS+H		42.31	0.1664	No
PBS vs. PBS+H		44.69	0.4227	No

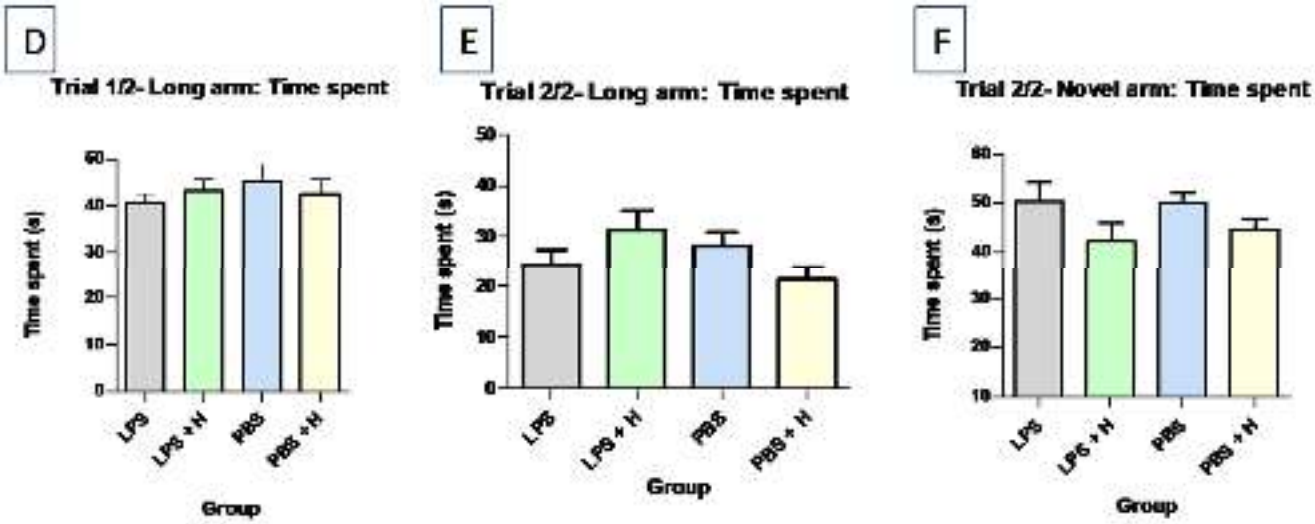

Figure 18 (D-F): Bar graph plot with mean ± SEM for the average time spent in the long and novel arm of the Y-maze chamber. Trial 1/2-Long arm shows the average time spent in the long arm during the exploration trial (D). Trial 2/2-Long arm shows the average time spent in the long arm during the testing/recognition trial (E). Trial 2/2-Novel arm shows the average time spent in the novel arm during the testing/recognition trial (F).

Then, the average speed scored within the long arm was assessed and presented in **figure 19** and **table 5**. In trial 2/2 of the novel arm, a significant difference ($p<0.0347$) was noted

when the control group was compared to the PBS + H group . This suggests that the PBS + H treated group may have navigated the novel arm of the maze at higher speeds as a result of honey intake.

Table 5: A summary of the mean scores and p-values obtained when evaluating the average speed of the subject in the long arm of the Y-maze chamber during the exploration trial (Trial 1/2), testing/recognition trial (Trial 2/2), in comparison to the novel arm (Trial 2/2-Novel arm).

Summary of the descriptive statistics of the average speed-long arm				
Group	**Trial**	**Mean**	**Adjusted P-value**	**Significant ?**
PBS	Trial 1/2	0.07220	-	-
PBS vs. LPS		0.07110	0.9973	No
PBS vs. LPS+H		0.07000	0.9797	No
PBS vs. PBS+H		0.06610	0.7237	No
PBS	Trial 2/2	0.08440	-	-
PBS vs. LPS		0.07520	0.7589	No
PBS vs. LPS+H		0.06510	0.2314	No
PBS vs. PBS+H		0.07320	0.6408	No
PBS	Trial 2/2 (Novel arm)	0.06290	-	-
PBS vs. LPS		0.07030	0.3504	No
PBS vs. LPS+H		0.07520	0.0567	No
PBS vs. PBS+H		0.07630	0.0347	Yes *

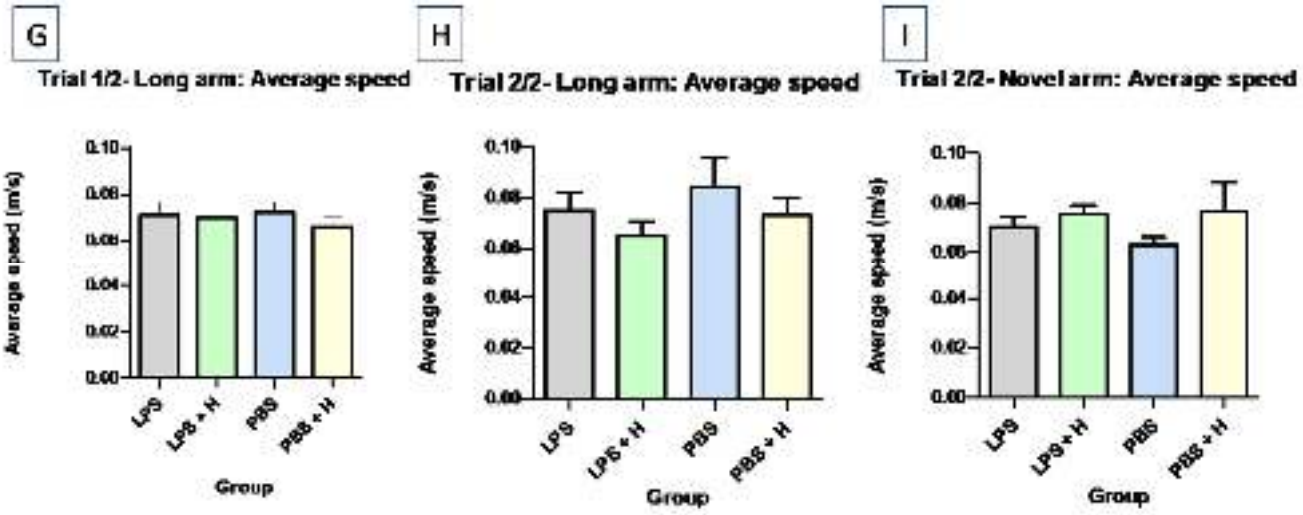

Figure 19 (G-I): Bar graph plot with mean ± SEM for the average speed of the subject in the long and novel arm of the Y-maze chamber. Trial 1/2-Long arm shows the average speed of the subject in the long arm during the exploration trial (G). Trial 2/2-Long arm shows the average speed of the subject

in the long arm during the testing/recognition trial (H). Trial 2/2-Novel arm shows the average speed of the subject in the novel arm during the testing/recognition trial (I).

Next, the average number of visits into the long arm, as shown in **table 6** and **figure 20**, was recorded and analysis revealed that the number of visits did not significantly differ during the three trials, or between the sample groups.

Table 6: A summary of the mean scores and p-values obtained when evaluating the average number of visits into the long arm of the Y-maze chamber during the exploration trial (Trial 1/2), testing/recognition trial (Trial 2/2) , in comparison to the novel arm (Trial 2/2-Novel arm).

Summary of the descriptive statistics of the average number of visits-long arm				
Group	**Trial**	**Mean**	**Adjusted P-value**	**Significant?**
PBS	Trial 1/2	9.7	-	-
PBS vs. LPS		10.06	0.9814	No
PBS vs. LPS+H		10.30	0.9238	No
PBS vs. PBS+H		10.37	0.8987	No
PBS	Trial 2/2	8.650	-	-
PBS vs. LPS		9.730	0.7573	No
PBS vs. LPS+H		11.03	0.1967	No
PBS vs. PBS+H		9.090	0.9759	No
PBS	Trial 2/2 (Novel arm)	11.81	-	-
PBS vs. LPS		11.35	0.9753	No
PBS vs. LPS+H		9.650	0.2893	No
PBS vs. PBS+H		9.390	0.2095	No

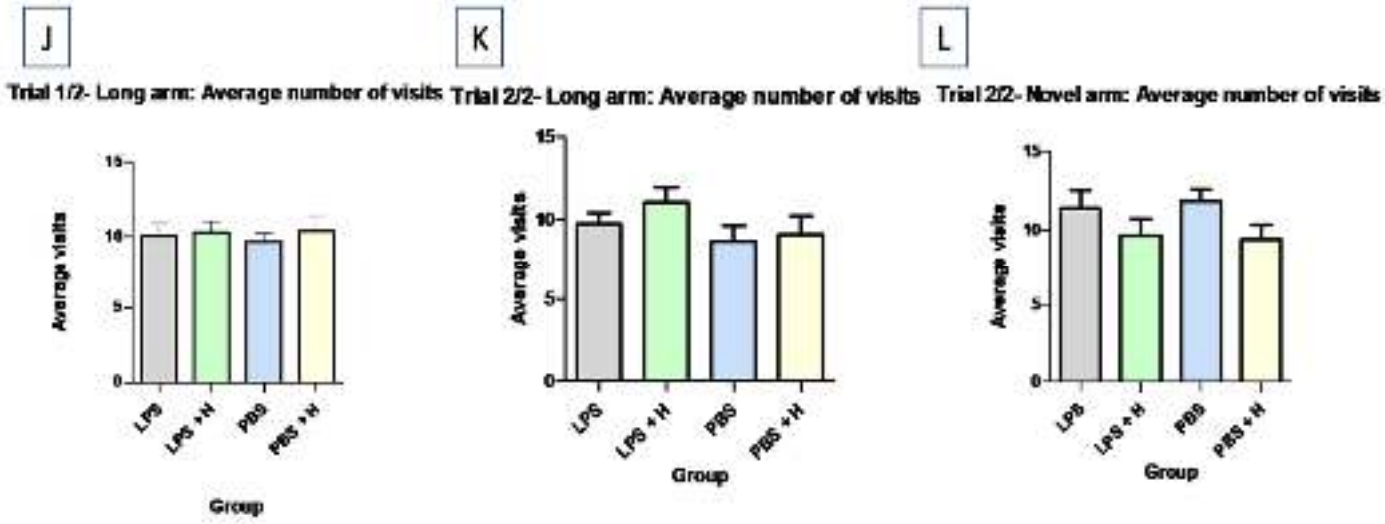

Figure 20 (J-L): Bar graph plot with mean ± SEM for the average number of visits into the long and novel arm of the Y-maze chamber. Trial 1/2-Long arm shows the average speed of the subject in the long arm during the exploration trial (J). Trial 2/2-Long arm shows the average speed of the subject in the long arm during the testing/recognition trial (K). Trial 2/2-Novel arm shows the average speed of the subject in the novel arm during the testing/recognition trial (L).

Lastly, the time spent in a state of motion and the time spent immobile in the long and novel arm was evaluated for inter-trial and inter-group comparison. This is shown in **table 7** and **table 8,** and graphically presented in **figure 21** and **figure 22. Table 7** shows significant differences ($p<0.0440$) and ($p<0.0237$) in the long arm during trial 2/2 was noted when the control group was compared to the LPS group and PBS + H group, respectively.

Table 7: A summary of the mean scores and p-values obtained when evaluating the time lapsed while the subject was mobile in the long arm of the Y-maze chamber during the exploration trial (Trial 1/2), testing/recognition trial (Trial 2/2) , in comparison to the novel arm (Trial 2/2-Novel arm).

Summary of the descriptive statistics of the time mobile-long arm				
Group	**Trial**	**Mean**	**Adjusted P-value**	**Significant?**
PBS	Trial 1/2	19.12	-	-
PBS vs. LPS		20.13	0.9403	No
PBS vs. LPS+H		21.05	0.7144	No
PBS vs. PBS+H		18.79	0.9976	No
PBS	Trial 2/2	13.18	-	-
PBS vs. LPS		8.780	0.0440	Yes *
PBS vs. LPS+H		10.88	0.4251	No
PBS vs. PBS+H		8.320	0.0237	Yes *
PBS	Trial 2/2 (Novel arm)	30.02	-	-
PBS vs. LPS		33.37	0.7187	No
PBS vs. LPS+H		29.81	>0.9999	No
PBS vs. PBS+H		31.19	0.9810	No

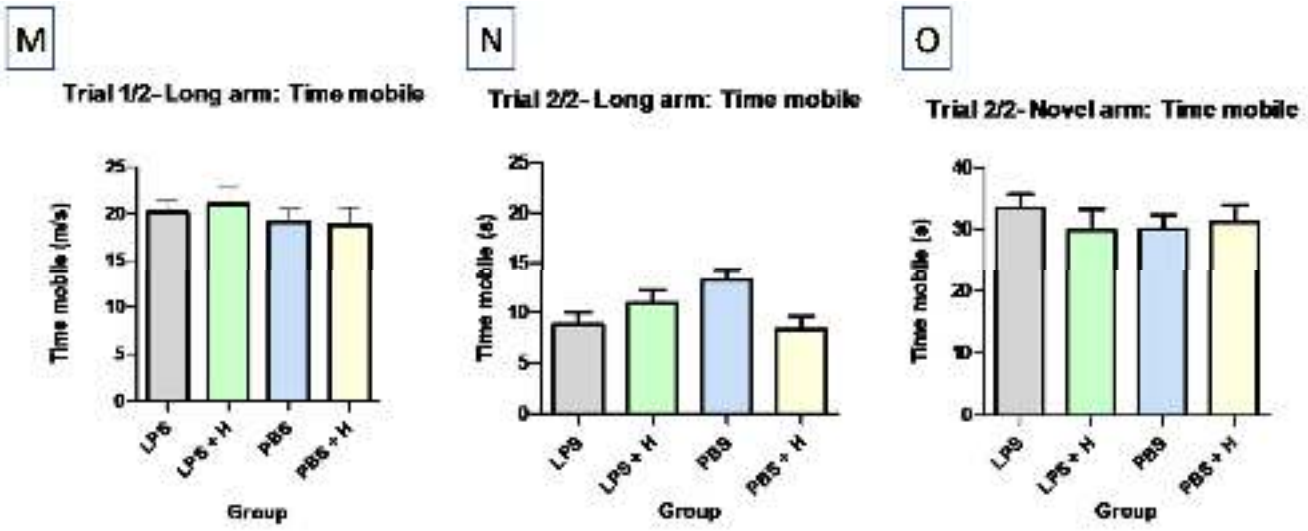

Figure 21 (M-O): Bar graph plot with mean ± SEM for time lapsed while the subject was mobile in the long and novel arm of the Y-maze chamber. Trial 1/2-Long arm shows the time mobile in the long arm during the exploration trial (M). Trial 2/2-Long arm shows the time mobile in the long arm during the testing/recognition trial (N). Trial 2/2-Novel arm shows the time mobile in the novel arm during the testing/recognition trial (O).

Table 8 shows that significant differences ($p<0.0183$) and ($p<0.0449$) in the novel arm during the testing trial were present when the control group was compared to the LPS + H group and PBS + H group, respectively. This is supported by findings in **table 4.**

Table 8: A summary of the mean scores and p-values obtained when evaluating the time lapsed while the subject was immobile in the long arm of the Y-maze chamber during the exploration trial (Trial 1/2), testing/recognition trial (Trial 2/2) , in comparison to the novel arm (Trial 2/2-Novel arm).

Summary of the descriptive statistics of the time immobile-long arm				
Group	**Trial**	**Mean**	**Adjusted P-value**	**Significant ?**
PBS	Trial 1/2	26.10	-	-
PBS vs. LPS		20.66	0.3107	No
PBS vs. LPS+H		22.08	0.5463	No
PBS vs. PBS+H		23.74	0.8487	No
PBS	Trial 2/2	14.97	-	-
PBS vs. LPS		15.76	0.9936	No
PBS vs. LPS+H		20.36	0.3636	No
PBS vs. PBS+H		13.05	0.9225	No
PBS	Trial 2/2 (Novel arm)	20.26	-	-
PBS vs. LPS		16.97	0.4828	No
PBS vs. LPS+H		12.50	0.0183	Yes *
PBS vs. PBS+H		13.51	0.0449	Yes *

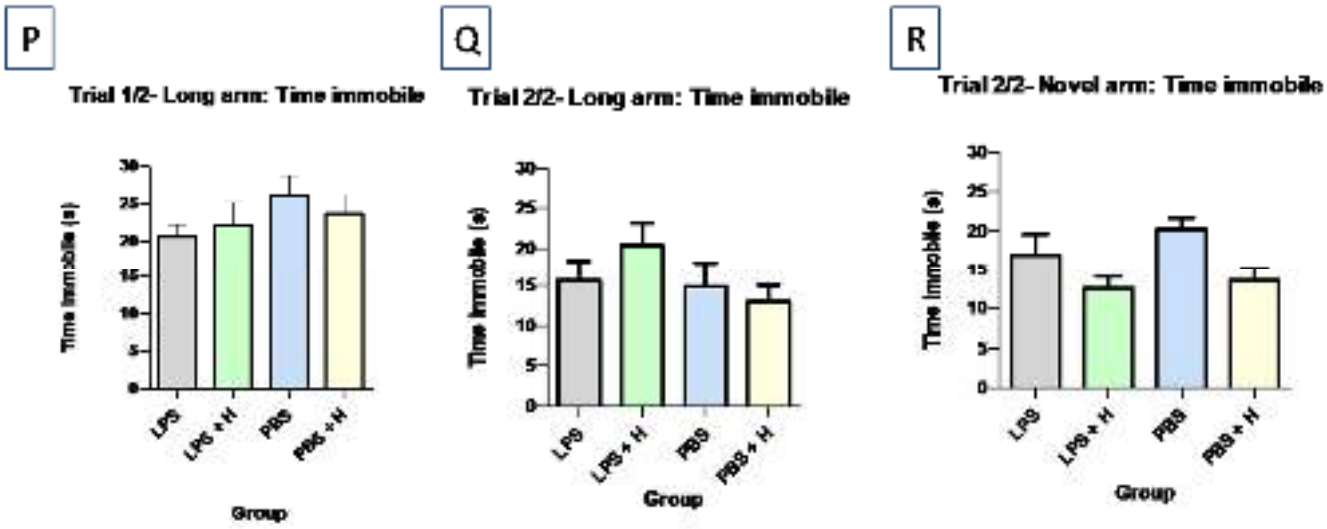

Figure 22 (P-R): Bar graph plot with mean ± SEM for time lapsed while the subject was immobile in the long and novel arm of the Y-maze chamber. Trial 1/2-Long arm shows the time mobile in the long arm during the exploration trial (P). Trial 2/2-Long arm shows the time mobile in the long arm during the testing/recognition trial (Q). Trial 2/2-Novel arm shows the time mobile in the novel arm during the testing/recognition trial (R).

Memory and learning deficits in the familiar arm of the y-maze were first evaluated by analyzing the number of head entries into the arm during the exploration and

testing/recognition trial as shown in **table 9** and **figure 23**. The number of head entries were not significantly different between the groups.

Table 9: A summary of the mean scores and p-values obtained when evaluating the average number of entries into the familiar arm of the Y-maze chamber during the exploration trial (Trial 1/2), testing/recognition trial (Trial 2/2) , in comparison to the novel arm (Trial 2/2-Novel arm).

Summary of the descriptive statistics of the number of head entries-familiar arm				
Group	**Trial**	**Mean**	**Adjusted P-value**	**Significant?**
PBS	Trial 1/2	5	-	-
PBS vs. LPS		5.1	0.9941	No
PBS vs. LPS+H		4.3	0.3636	No
PBS vs. PBS+H		5.1	0.9941	No
PBS	Trial 2/2	2.8	-	-
PBS vs. LPS		3.5	0.3227	No
PBS vs. LPS+H		3.1	0.8585	No
PBS vs. PBS+H		3.5	0.3227	No
PBS	Trial 2/2 (Novel arm)	7.5	-	-
PBS vs. LPS		8	0.8794	No
PBS vs. LPS+H		7.4	0.9987	No
PBS vs. PBS+H		7	0.8794	No

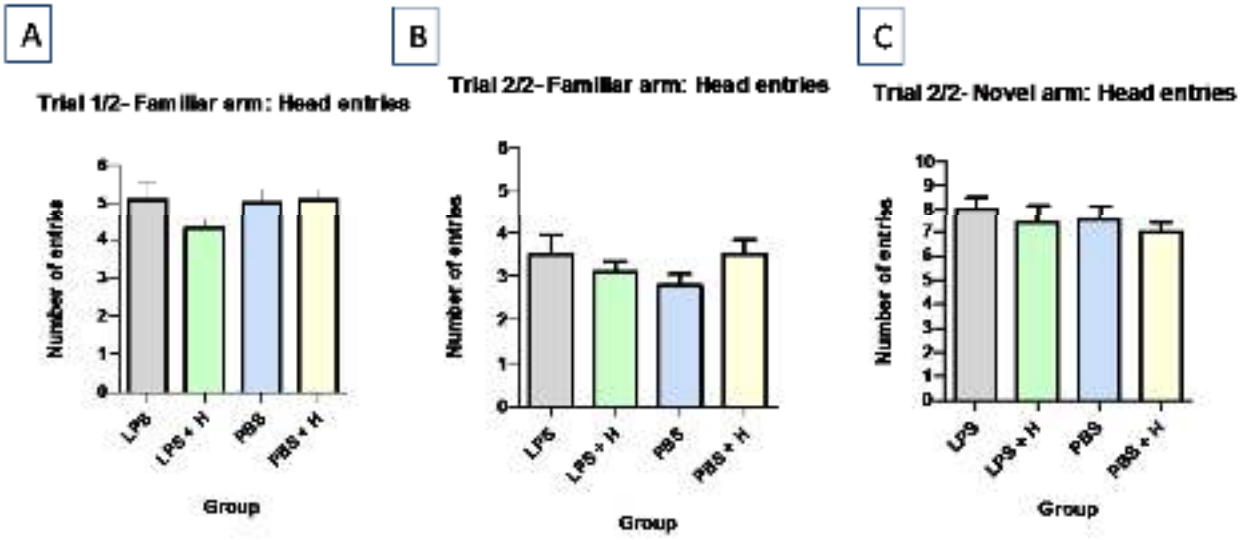

Figure 23 (A-C): Bar graph plot with mean ± SEM for the number of head entries into the familiar and novel arm of the Y-maze chamber. Trial 1/2-Familiar arm shows the average number head entries into the familiar arm during the exploration trial (A). Trial 2/2-Familiar arm shows the average number head entries into the familiar arm during the testing/recognition trial (B). Trial 2/2-Novel arm shows the average head entries into the novel arm during the testing/recognition trial (C).

Next, the time spent in the familiar arm was analyzed and presented in **table 10** and **figure 24**. A significant difference ($p<0.0072$) during the trial 2/2 in the familiar arm was noted when the PBS group was compared to the PBS + H group.

Table 10: A summary of the mean scores and p-values obtained when evaluating the average time spent in the familiar arm of the Y-maze chamber during the exploration trial (Trial 1/2), testing/recognition trial (Trial 2/2), in comparison to the novel arm (Trial 2/2-Novel arm).

Summary of the descriptive statistics of the time spent-familiar arm				
Group	**Trial**	**Mean**	**Adjusted P-value**	**Significant?**
PBS	Trial 1/2	45.23	-	-
PBS vs. LPS		54.11	0.1214	No
PBS vs. LPS+H		52.39	0.2529	No
PBS vs. PBS+H		55.80	0.0532	No
PBS	Trial 2/2	24.54	-	-
PBS vs. LPS		28.68	0.4728	No
PBS vs. LPS+H		28.42	0.5232	No
PBS vs. PBS+H		35.40	0.0072	Yes *
PBS	Trial 2/2 (Novel arm)	50.28	-	-
PBS vs. LPS		50.34	>0.9999	No
PBS vs. LPS+H		42.31	0.1664	No
PBS vs. PBS+H		44.69	0.4227	No

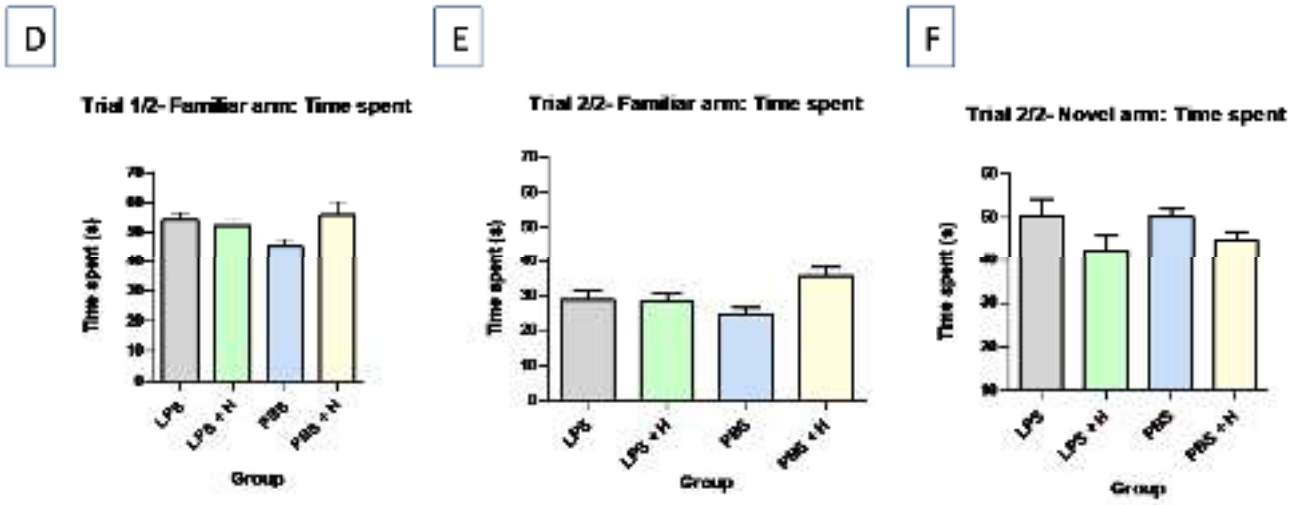

Figure 24 (D-F): Bar graph plot with mean ± SEM for the average time spent in the familiar and novel arm of the Y-maze chamber. Trial 1/2-Familiar arm shows the average time spent in the familiar arm during the exploration trial (D). Trial 2/2-Familiar arm shows the average time spent in the familiar

arm during the testing/recognition trial (E). Trial 2/2-Novel arm shows the average time spent in the novel arm during the testing/recognition trial (F).

Then, the average speed scored within the familiar arm was assessed and presented in **figure 25** and **table 11.** A significant difference ($p<0.0347$) during trial 2/2 in the novel arm was noted when the PBS group was compared to the PBS + H group.

Table 11: A summary of the mean scores and p-values obtained when evaluating the average speed of the subject in the familiar arm of the Y-maze chamber during the exploration trial (Trial 1/2), testing/recognition trial (Trial 2/2), in comparison to the novel arm (Trial 2/2-Novel arm).

Summary of the descriptive statistics of the average speed-familiar arm				
Group	**Trial**	**Mean**	**Adjusted P-value**	**Significant ?**
PBS	Trial 1/2	0.06800	-	-
PBS vs. LPS		0.05480	0.1035	No
PBS vs. LPS+H		0.05310	0.0577	No
PBS vs. PBS+H		0.05410	0.0818	No
PBS	Trial 2/2	0.07260	-	-
PBS vs. LPS		0.06420	0.4778	No
PBS vs. LPS+H		0.07080	0.9875	No
PBS vs. PBS+H		0.05710	0.0760	No
PBS	Trial 2/2 (Novel arm)	0.06290	-	-
PBS vs. LPS		0.07030	0.3504	No
PBS vs. LPS+H		0.07520	0.0567	No
PBS vs. PBS+H		0.07630	0.0347	Yes *

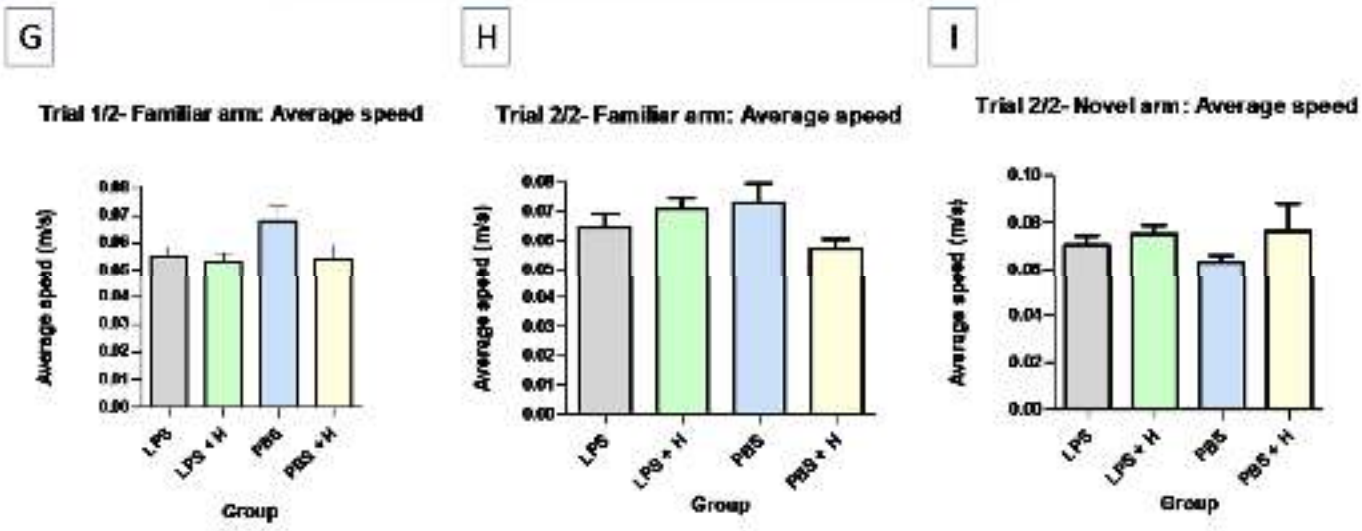

Figure 25 (G-I): Bar graph plot with mean ± SEM for the average speed of the subject in the familiar and novel arm of the Y-maze chamber. Trial 1/2-Familiar arm shows the average speed of the subject

in the familiar arm during the exploration trial (G). Trial 2/2-Familiar arm shows the average speed of the subject in the familiar arm during the testing/recognition trial (H). Trial 2/2-Novel arm shows the average speed of the subject in the novel arm during the testing/recognition trial (I).

The average number of visits into the familiar arm, as shown in **table 12** and **figure 26**, was recorded and compared between the exploration and testing trial. The number of visits were not significantly different between the groups.

Table 12: A summary of the mean scores and p-values obtained when evaluating the average number of visits into the familiar arm of the Y-maze chamber during the exploration trial (Trial 1/2), testing/recognition trial (Trial 2/2), in comparison to the novel arm (Trial 2/2-Novel arm).

Summary of the descriptive statistics of the average number of visits-familiar arm				
Group	**Trial**	**Mean**	**Adjusted P-value**	**Significant?**
PBS	Trial 1/2	10.21	-	-
PBS vs. LPS		10.27	>0.9999	No
PBS vs. LPS+H		12.08	0.5826	No
PBS vs. PBS+H		12.21	0.5327	No
PBS	Trial 2/2	9.220	-	-
PBS vs. LPS		10.86	0.6720	No
PBS vs. LPS+H		10.52	0.7993	No
PBS vs. PBS+H		11.27	0.5129	No
PBS	Trial 2/2 (Novel arm)	11.81	-	-
PBS vs. LPS		11.35	0.9753	No
PBS vs. LPS+H		9.650	0.2893	No
PBS vs. PBS+H		9.390	0.2095	No

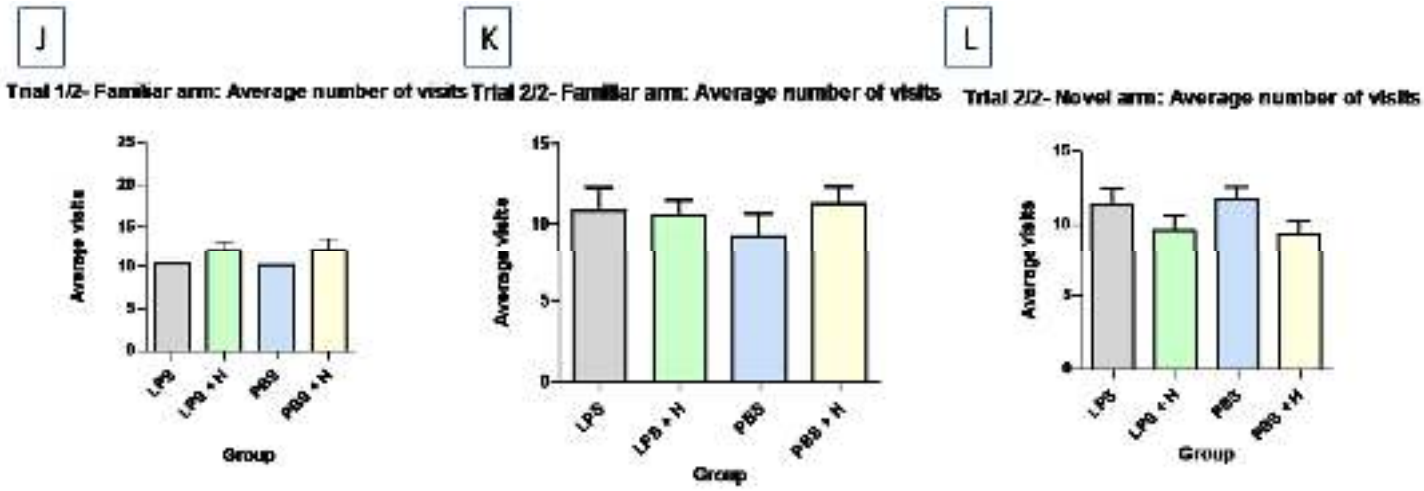

Figure 26 (J-L): Bar graph plot with mean ± SEM for the average number of visits into the familiar and novel arm of the Y-maze chamber. Trial 1/2-Familiar arm shows the average speed of the subject in the familiar arm during the exploration trial (J). Trial 2/2-Familiar arm shows the average speed of the subject in the familiar arm during the testing/recognition trial (K). Trial 2/2-Novel arm shows the average speed of the subject in the novel arm during the testing/recognition trial (L).

Lastly, the time spent in a state of motion and the time spent immobile was evaluated for inter-trial and inter-group comparison. This is shown in **table 13** and **table 14,** and graphically presented in **figure 27** and **figure 28.** The time mobile in the familiar arm and novel arm were not significantly different between the groups.

Table 13: A summary of the mean scores and p-values obtained when evaluating the time lapsed while the subject was mobile in the familiar arm of the Y-maze chamber during the exploration trial (Trial 1/2), testing/recognition trial (Trial 2/2) , in comparison to the novel arm (Trial 2/2-Novel arm).

Summary of the descriptive statistics of the time mobile-familiar arm				
Group	**Trial**	**Mean**	**Adjusted P-value**	**Significant?**
PBS	Trial 1/2	23.26	-	-
PBS vs. LPS		30.91	0.1215	No
PBS vs. LPS+H		28.29	0.4083	No
PBS vs. PBS+H		29.52	0.2426	No
PBS	Trial 2/2	14.33	-	-
PBS vs. LPS		14.84	0.9869	No
PBS vs. LPS+H		15.21	0.9394	No
PBS vs. PBS+H		16.87	0.4147	No
PBS	Trial 2/2 (Novel arm)	30.02	-	-
PBS vs. LPS		33.37	0.7187	No
PBS vs. LPS+H		29.81	>0.9999	No
PBS vs. PBS+H		31.19	0.9810	No

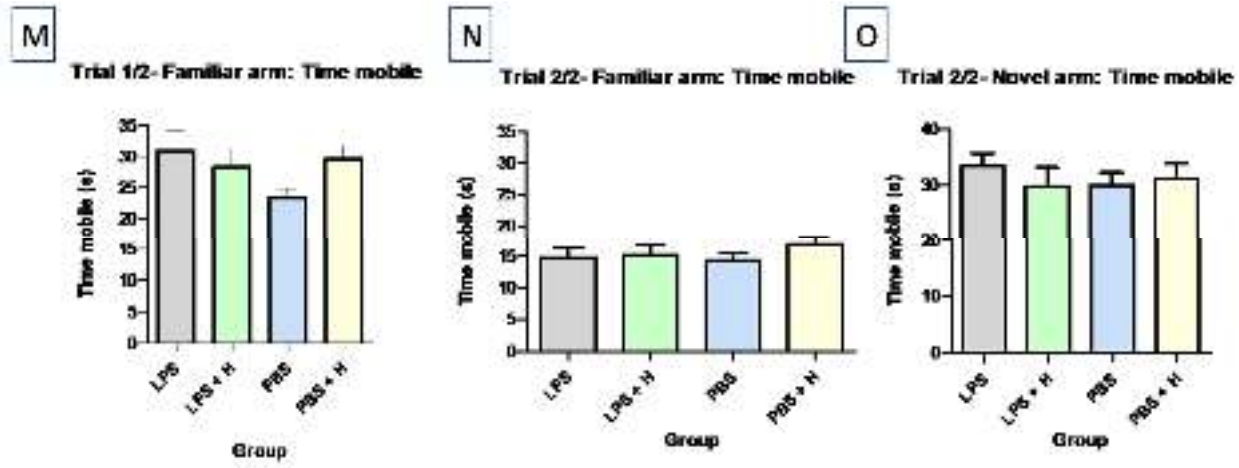

Figure 27 (M-O): Bar graph plot with mean ± SEM for time lapsed while the subject was mobile in the familiar and novel arm of the Y-maze chamber. Trial 1/2-Familiar arm shows the time mobile in the familiar arm during the exploration trial (M). Trial 2/2-Familiar arm shows the time mobile in the familiar arm during the testing/recognition trial (N). Trial 2/2-Novel arm shows the time mobile in the novel arm during the testing/recognition trial (O).

However, when time immobile was analyzed in **table 14** Significant differences in the familiar arm was noted when the PBS group was compared to the PBS + H ($p<0.0132$) group during trial 2/2. Significant differences were also observed in the novel arm when the PBS group was compared to the LPS + H ($p<0.0183$) and PBS + H ($p<0.0449$) groups.

Table 14: A summary of the mean scores and p-values obtained when evaluating the time lapsed while the subject was immobile in the familiar arm of the Y-maze chamber during the exploration trial (Trial 1/2), testing/recognition trial (Trial 2/2) , in comparison to the novel arm (Trial 2/2-Novel arm).

Summary of the descriptive statistics of the time immobile-familiar arm				
Group	**Trial**	**Mean**	**Adjusted P-value**	**Significant?**
PBS	Trial 1/2	21.97	-	-
PBS vs. LPS		23.19	0.9888	No
PBS vs. LPS+H		24.07	0.9481	No
PBS vs. PBS+H		26.32	0.6976	No
PBS	Trial 2/2	10.21	-	-
PBS vs. LPS		13.83	0.4268	No
PBS vs. LPS+H		13.24	0.5642	No
PBS vs. PBS+H		18.52	0.0132	Yes *
PBS	Trial 2/2 (Novel arm)	20.26	-	-
PBS vs. LPS		16.97	0.4828	No
PBS vs. LPS+H		12.50	0.0183	Yes *
PBS vs. PBS+H		13.51	0.0449	Yes *

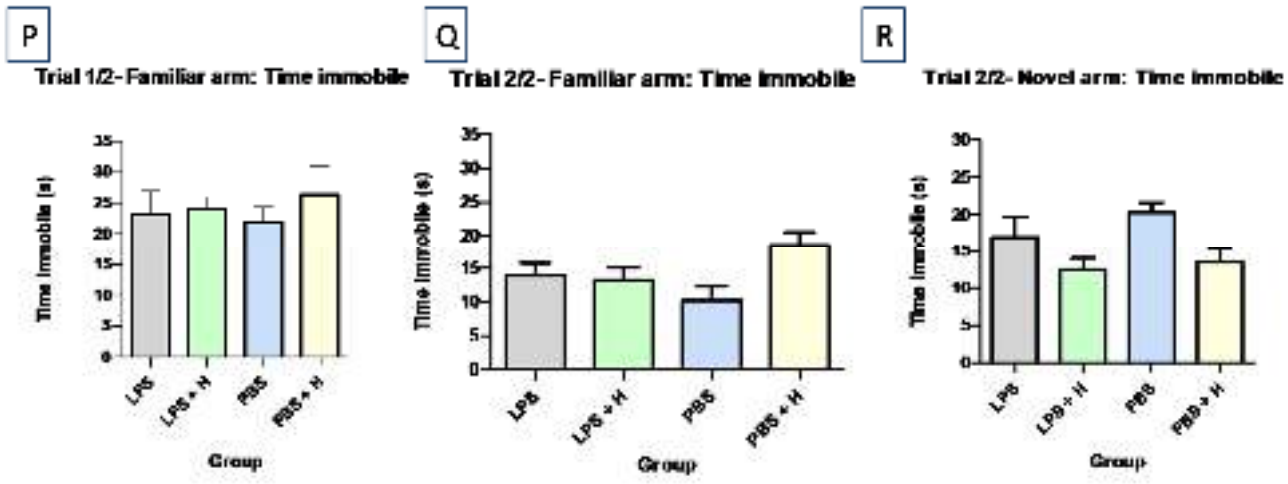

Figure 28 (P-R): Bar graph plot with mean ± SEM for time lapsed while the subject was immobile in the familiar and novel arm of the Y-maze chamber. Trial 1/2-Familiar arm shows the time mobile in the familiar arm during the exploration trial (P). Trial 2/2-Familiar arm shows the time mobile in the familiar arm during the testing/recognition trial (Q). Trial 2/2-Novel arm shows the time mobile in the novel arm during the testing/recognition trial (R).

4.4.2) Novel Object Recognition Task

After the training and testing trial were complete, the following parameters were considered for each block (object) A and block B:

i. Number of entries into the perimeter of the block.
ii. Mean visits.
iii. Time spent (overall time spent at/close to object).
iv. Time immobile (time spent while stationary observing/exploring object).
v. The first block entered.

For the training trial, both Block A and Block B (new block) held identical objects. For the testing trial, Block B (new block) held the novel object, whilst Block A remained the same.

For data analysis, the three experimental groups (LPS only vs. LPS and honey vs. PBS and honey) were compared to the control group (PBS only).

Firstly, the number of head entries into block A and block B during the training phase were analyzed and presented in **table 15 and figure 29.** As shown, The number of head entries was not significantly different across the groups.

Table 15: A summary of the mean scores and p-values obtained when evaluating the number of entries made within the perimeter of Block A and Block B, during the training trial.

Summary of the descriptive statistics of the number of entries during the training phase				
Group	**Trial**	**Mean**	**Adjusted P-value**	**Significant?**
PBS	Training Phase-Block A	5.5	-	-
PBS vs. LPS		6.8	0.5663	No
PBS vs. LPS+H		4.7	0.8412	No
PBS vs. PBS+H		6.1	0.9229	No
PBS	Training Phase-Block B	5.2	-	-
PBS vs. LPS		6.8	0.5655	No
PBS vs. LPS+H		5.6	0.9859	No
PBS vs. PBS+H		5.3	0.9997	No

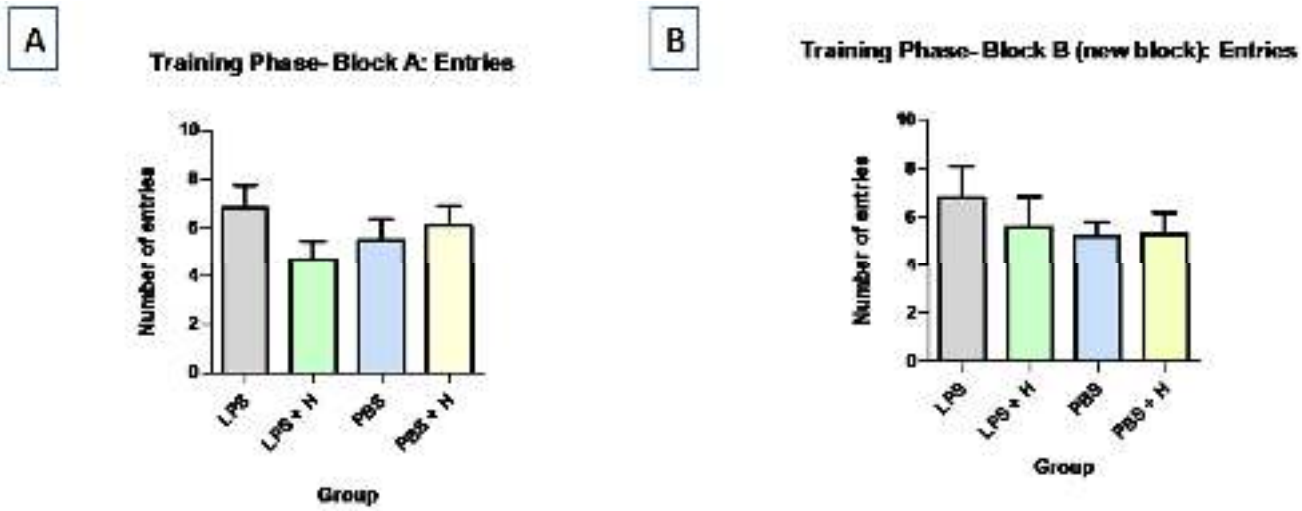

Figure 29 (A-B): Bar graph plot with mean ± SEM for the average number of entries made into the perimeter of Block A and Block B during the training trial of the NORT. The number of entries in Block A (A). The number of entries in Block B (B).

Next, the time spent immobile in block A and block B during the training phase was analyzed and presented in **table 16 and figure 30.** The time immobile was not significant between the groups.

Table 16: A summary of the mean scores and p-values obtained when evaluating time immobile (time spent while stationary exploring the object) within the perimeter of Block A and Block B, during the training trial.

Summary of the descriptive statistics of the time immobile in each block during the training phase				
Group	**Trial**	**Mean**	**Adjusted P-value**	**Significant?**
PBS	Training Phase-Block A	1.590	-	-
PBS vs. LPS		1.570	>0.9999	No
PBS vs. LPS+H		1.330	0.9925	No
PBS vs. PBS+H		2.630	0.7115	No
PBS	Training Phase-Block B	2.530	-	-
PBS vs. LPS		1.380	0.7172	No
PBS vs. LPS+H		4.450	0.3440	No
PBS vs. PBS+H		0.9500	0.4972	No

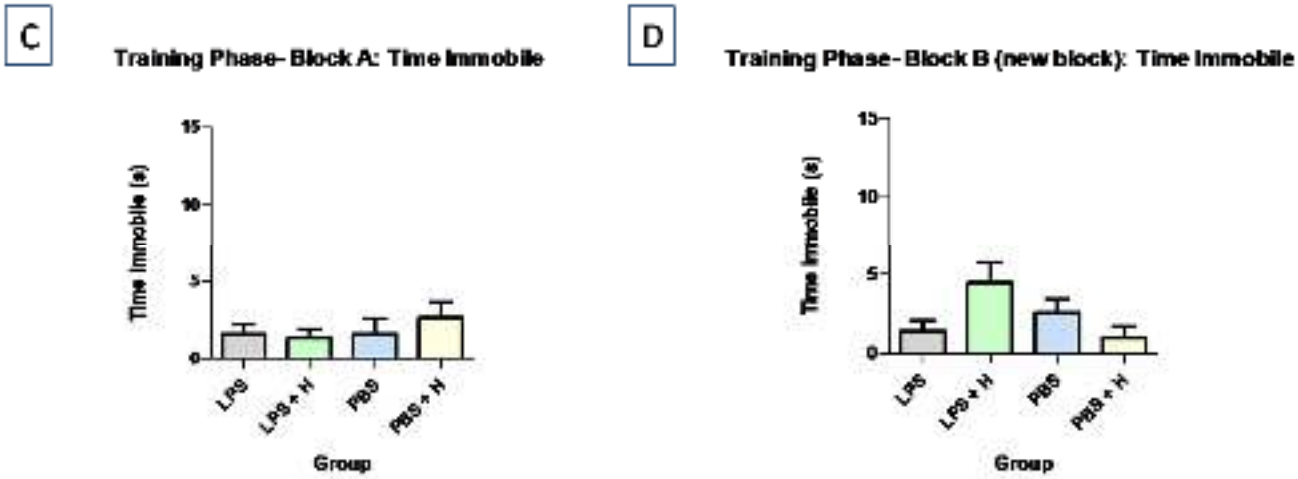

Figure 30 (C-D): Bar graph plot with mean ± SEM for the time immobile (time spent while stationary exploring the object) within the perimeter of Block A and Block B, during the training trial of the NORT. Time immobile in Block A (C). Time immobile in Block B (D).

Next, the average number of visits into block A and block B during the training phase was analyzed and presented in **table 17 and figure 31.** The number of visits were not significantly different across the groups.

Table 17: A summary of the mean scores and p-values obtained when evaluating the average number of visits made within the perimeter of Block A and Block B, during the training trial.

Summary of the descriptive statistics of the average number of visits in each block during the training phase				
Group	**Trial**	**Mean**	**Adjusted P-value**	**Significant?**
PBS	Training Phase-Block A	0.9700	-	-
PBS vs. LPS		1.010	0.9974	No
PBS vs. LPS+H		1.360	0.3152	No
PBS vs. PBS+H		1.290	0.4701	No
PBS	Training Phase-Block B	1.340	-	-
PBS vs. LPS		0.9000	0.4683	No
PBS vs. LPS+H		2.080	0.1097	No
PBS vs. PBS+H		1.430	0.9886	No

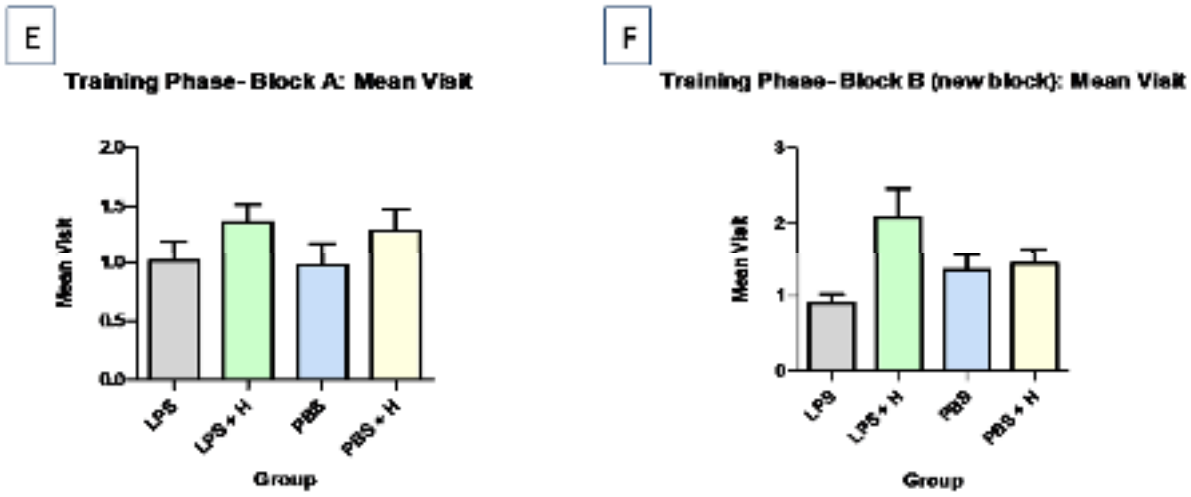

Figure 31 (E-F): Bar graph plot with mean ± SEM for the average number of visits made into the perimeter of Block A and Block B during the training trial of the NORT. The number of visits in Block A (E). The number of visits in Block B (F).

For the testing phase, a novel object was introduced into block B of the arena. To begin, the number of visits were analyzed during the testing/recognition phase of this assay. Data is presented in **table 18** and **figure 32**. A significant difference ($p<0.0044$) in the number of entries in block B was noted when the control group was compared to the LPS group during

the testing trial. This suggests that LPS treatment did not affect recognition memory in this trial since the LPS group entered the zone containing the novel object more often than the control group.

Table 18: A summary of the mean scores and p-values obtained when evaluating the number of entries made within the perimeter of Block A and Block B, during the testing trial

Summary of the descriptive statistics of the number of entries in each block during the testing phase				
Group	**Trial**	**Mean**	**Adjusted P-value**	**Significant?**
PBS	Testing Phase-Block A	4.5	-	-
PBS vs. LPS		6.9	0.1988	No
PBS vs. LPS+H		3.8	0.9171	No
PBS vs. PBS+H		5.8	0.6550	No
PBS	Testing Phase-Block B	4.0	-	-
PBS vs. LPS		7.5	0.0044	Yes *
PBS vs. LPS+H		4.3	0.9728	No
PBS vs. PBS+H		5.8	0.4541	No

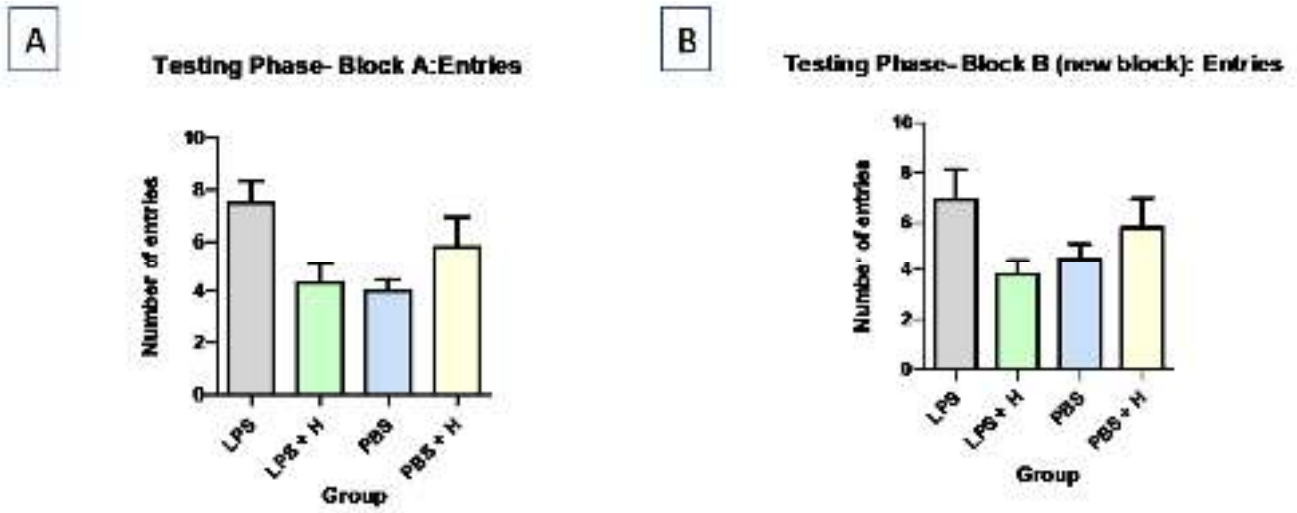

Figure 32 (G-H): Bar graph plot with mean ± SEM for the average number of entries made into the perimeter of Block A and Block B during the testing trial of the NORT. The number of entries in Block A (G). The number of entries in Block B (H).

Next, the time spent in block A and block B were analyzed during the testing phase and presented in **table 19** and **figure 33**. The time spent was not significantly different across the groups.

Table 19: A summary of the mean scores and p-values obtained when evaluating the average time spent within the perimeter of Block A and Block B, during the testing trial.

Summary of the descriptive statistics of the time spent in each block during the testing phase				
Group	**Trial**	**Mean**	**Adjusted P-value**	**Significant?**
PBS	Testing Phase-Block A	6.970	-	-
PBS vs. LPS		9.830	0.3162	No
PBS vs. LPS+H		[illegible]	[illegible]	No
PBS vs. PBS+H		8.670	0.7005	No
PBS	Testing Phase-Block B	6.570	-	-
PBS vs. LPS		9.310	0.8046	No
PBS vs. LPS+H		5.030	0.9549	No
PBS vs. PBS+H		11.12	0.4819	No

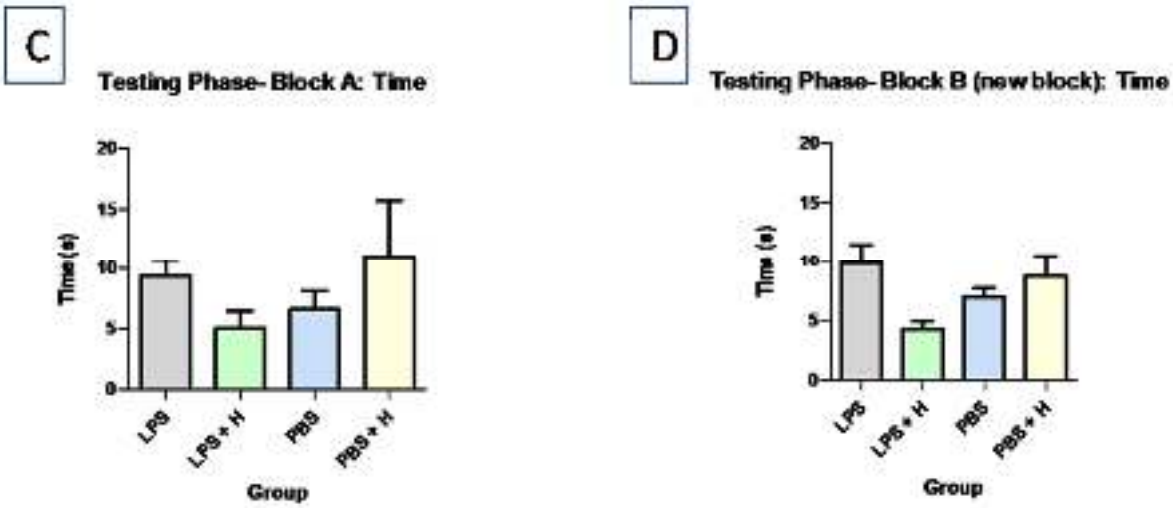

Figure 33 (C-D): Bar graph plot with mean ± SEM for the average time spent within the perimeter of Block A and Block B during the testing trial of the NORT. The number of entries in Block A (C). The number of entries in Block B (D).

Then, the average number of visits block A and block B were analyzed during the testing phase and presented in **table 20** and **figure 34**. The time spent was not significantly different across the groups. The number of visits were not significantly different across the groups.

Table 20: A summary of the mean scores and p-values obtained when evaluating the average number of visits made within the perimeter of Block A and Block B, during the testing trial.

Summary of the descriptive statistics of the average number of visits in each block during the testing phase				
Group	**Trial**	**Mean**	**Adjusted P-value**	**Significant?**
PBS	Testing Phase-Block A	1.710	-	-
PBS vs. LPS		1.470	0.7148	No
PBS vs. LPS+H		1.150	0.0966	No
PBS vs. PBS+H		1.570	0.9204	No
PBS	Testing Phase-Block B	1.520	-	-
PBS vs. LPS		1.270	0.7811	No
PBS vs. LPS+H		1.089	0.4332	No
PBS vs. PBS+H		1.480	0.9986	No

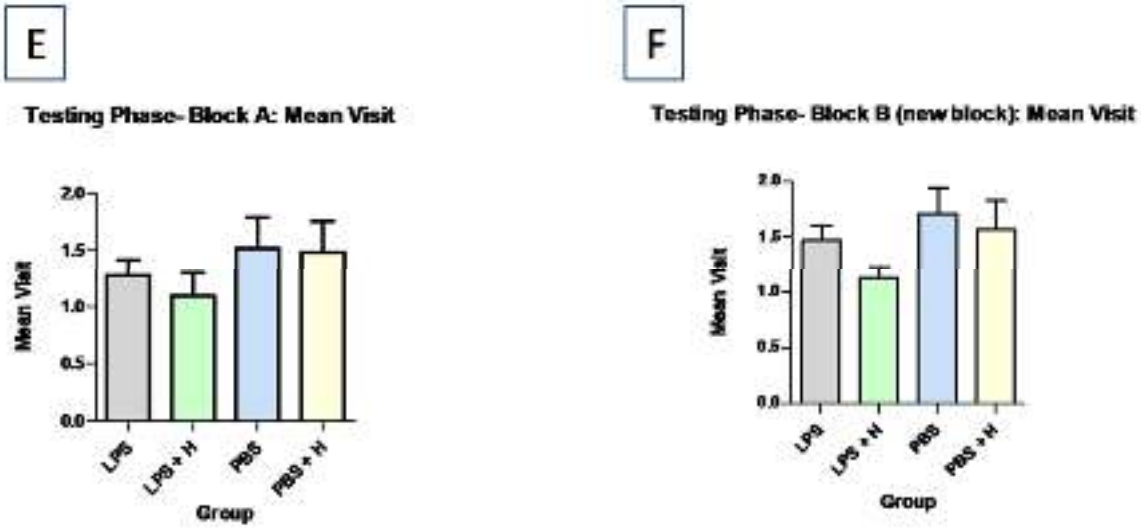

Figure 34 (E-F): Bar graph plot with mean ± SEM for the average number of visits made into the perimeter of Block A and Block B during the testing trial of the NORT. The number of visits in Block A (E). The number of visits in Block B (F).

Also, the time spent immobile inside block A and block B were analyzed during the testing phase and presented in **table 21** and **figure 35**. The time immobile was not significantly different between the groups.

Table 21: A summary of the mean scores and p-values obtained when evaluating time immobile (time spent while stationary exploring the object) within the perimeter of Block A and Block B, during the testing trial.

Summary of the descriptive statistics of the time immobile in each block during the testing phase				
Group	**Trial**	**Mean**	**Adjusted P-value**	**Significant?**
PBS	Testing Phase- Block A	3.150	-	-
PBS vs. LPS		4.360	0.7691	No
PBS vs. LPS+H		1.570	0.6062	No
PBS vs. PBS+H		5.030	0.4756	No
PBS	Testing Phase- Block B	2.370	-	-
PBS vs. LPS		3.190	0.9929	No
PBS vs. LPS+H		2.580	>0.9999	No
PBS vs. PBS+H		7.180	0.4506	No

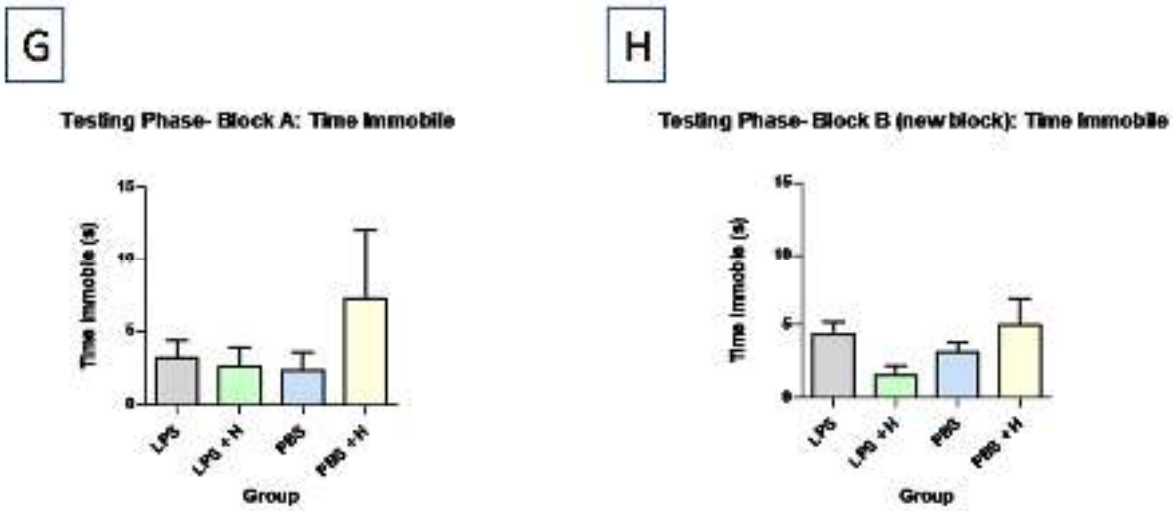

Figure 35 (G-H): Bar graph plot with mean ± SEM for the time immobile (time spent while stationary exploring the object) within the perimeter of Block A and Block B, during the testing trial of the NORT. Time immobile in Block A (G). Time immobile in Block B (H).

Lastly, the first zone entered (block explored first) during the training and testing trial was also noted and illustrated in **figure 36**. It was predicted that the novel (Block B) object would be visited first, before the familiar (Block A) object during the testing trial. Results of the training phase indicate that all three experimental groups explored block A first, while the control group explored block B first. However, this was contrasted during the testing phase. The LPS-treated group and control group

explored block B, containing the novel object, first. The LPS + H group showed no preference in the object first explored. And, the PBS + H group explored block A, containing the familiar object, first.

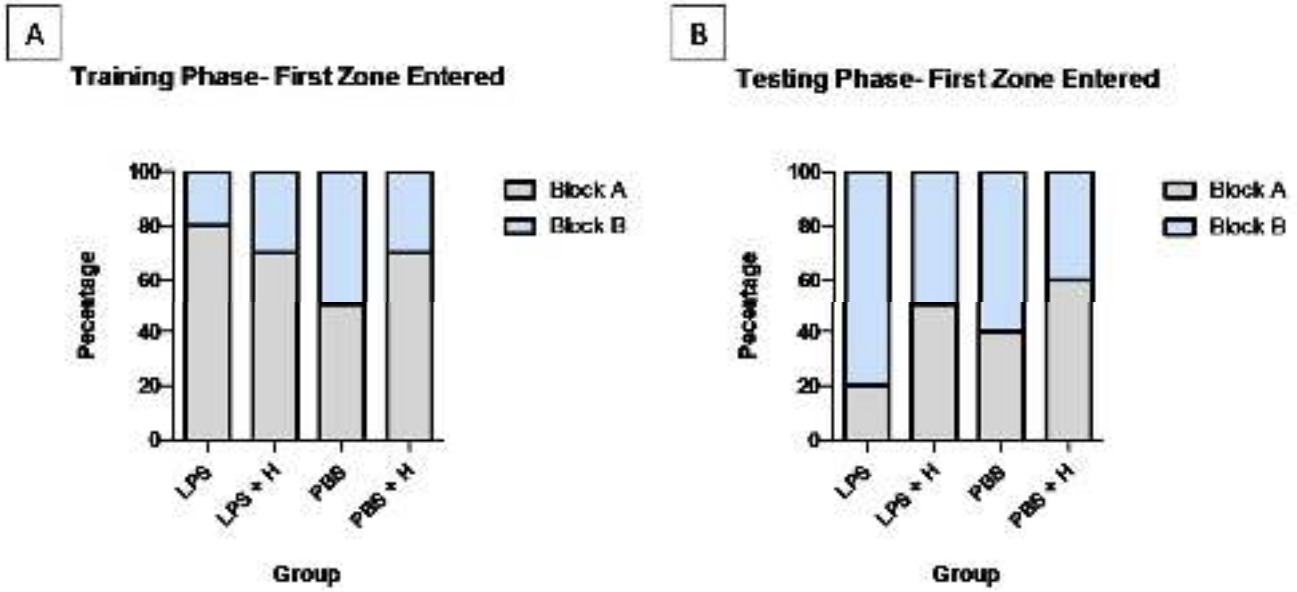

Figure 36 (A-B): A vertically stacked bar graph plot showing the proportion of the first zone entered (object explored first) upon commencement of the NORT trial. First zone entered during the training trial (A). First zone entered during the testing trial (B). In the training trial, all the experimental groups explored Block A (grey) first, at the start of the trial. However, during the testing trial, a majority of subjects in the LPS group and PBS explored Block B (blue), which contained the novel object, first. Surprisingly, the LPS + H group showed equal preference for both the familiar and novel object. The PBS + H group showed bias towards to the familiar object.

Altogther, the results of this assay suggest that low systemic LPS does not cause impairments in learning and recognition memory.

4.4.3) Open-Field Analysis

Habituation was not required for this assay. To begin, the number of head within the outer zone during the training phase were analyzed and presented in **table 22 and figure 37.** As shown, the number of head entries was not significantly different across the groups.

Table 22: A summary of the mean scores and p-values obtained when evaluating the number of entries completed by the subject in the outer zone of the open-field arena during the testing trial.

Summary of the descriptive statistics of the number of entries within the outer zone during the testing phase				
Group	Trial	Mean	Adjusted P-value	Significant?
PBS	Testing Phase	6.30	-	-
PBS vs. LPS		8.30	0.1271	No
PBS vs. LPS+H		5.10	0.4891	No
PBS vs. PBS+H		5.60	0.8223	No

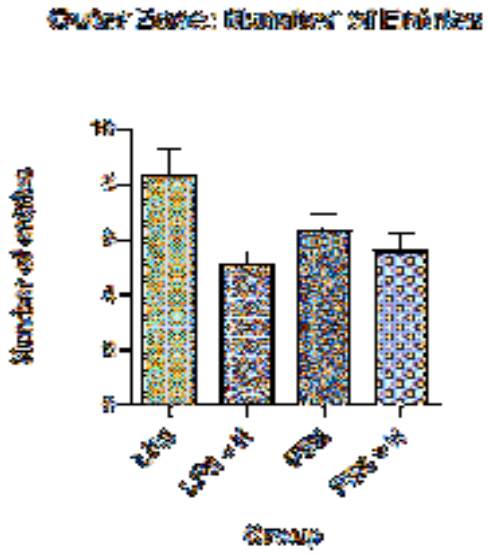

Figure 37: A bar graph plot with mean ± SEM showing the number of entries completed in the outer zone of the open-field arena during the testing trial.

Next, the average speed within the outer zone during the training phase were analyzed and presented in **table 23 and figure 38.** The average speed was not significantly different between the groups.

Table 23: A summary of the mean scores and p-values obtained when evaluating the average speed undertaken by the subject in the outer zone of the open-field arena during the testing trial.

Summary of the descriptive statistics of the average speed within the outer zone during the testing phase				
Group	Trial	Mean	Adjusted P-value	Significant?
PBS	Testing Phase	0.08160	-	-
PBS vs. LPS		0.08790	0.7665	No
PBS vs. LPS+H		0.08810	0.7503	No
PBS vs. PBS+H		0.09050	0.5450	No

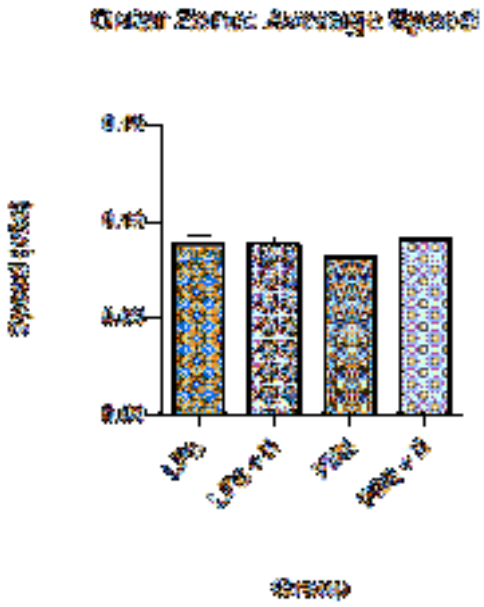

Figure 38: A bar graph plot with mean ± SEM showing the average speed undertaken by the subject in the outer zone of the open-field arena during the testing trial.

Then, the average number of visits in the outer zone during the training phase were analyzed and presented in **table 24 and figure 39.** The average number of visits was not significantly different between the groups

Table 24: A summary of the mean scores and p-values obtained when evaluating the average number of visits in the outer zone of the open-field arena during the testing trial.

Summary of the descriptive statistics of the average number of visits within the outer zone during the testing phase				
Group	**Trial**	**Mean**	**Adjusted P-value**	**Significant?**
PBS	Testing Phase	30.21	-	-
PBS vs. LPS		23.68	0.5961	No
PBS vs. LPS+H		37.31	0.5343	No
PBS vs. PBS+H		36.62	0.6092	No

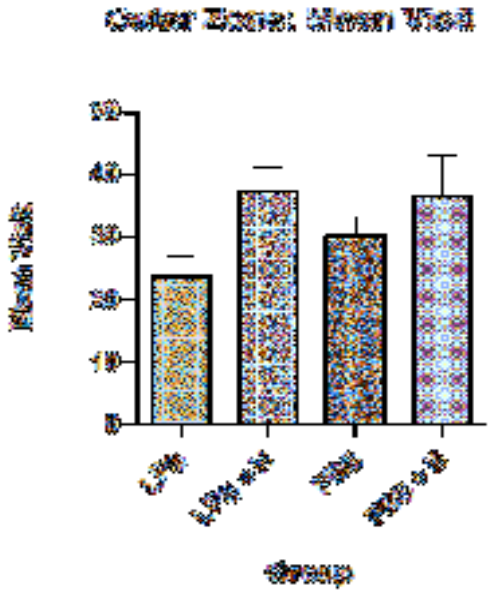

Figure 39: A bar graph plot with mean ± SEM showing the average number of visits in the outer zone of the open-field arena during the testing trial.

Then, the average speed within the outer zone during the training phase were analyzed and presented in **table 25** and **figure 40.** Again, the average was not significantly different between the groups.

Table 25: A summary of the mean scores and p-values obtained when evaluating the time spent in the outer zone of the open-field arena during the testing trial.

Summary of the descriptive statistics of the time spent in the outer zone during the testing phase				
Group	**Trial**	**Mean**	**Adjusted P-value**	**Significant?**
PBS	Testing Phase	172.2	-	-
PBS vs. LPS		171.3	0.8984	No
PBS vs. LPS+H		173.7	0.6914	No
PBS vs. PBS+H		172.5	0.9952	No

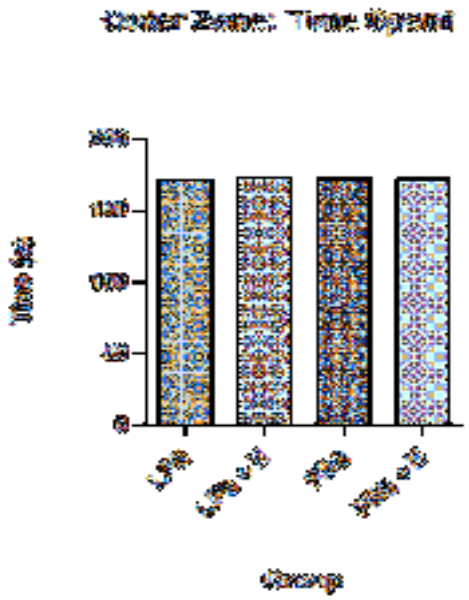

Figure 40: A bar graph plot with mean ± SEM showing the time spent completed by subject in the outer zone of the open-field arena during the testing trial.

Further, the number of lines crossed within the outer zone during the training phase was analyzed and presented in **table 26** and **figure 41.** Again, the average was not significantly different between the groups.

Table 26: A summary of the mean scores and p-values obtained when evaluating the number of line crossings in the outer zone of the open-field arena during the testing trial.

Summary of the descriptive statistics of the number of line crossings in the outer zone during the testing phase				
Group	**Trial**	**Mean**	**Adjusted P-value**	**Significant?**
PBS	Testing Phase	69.7	-	-
PBS vs. LPS		73.1	0.9049	No
PBS vs. LPS+H		73.9	0.8395	No
PBS vs. PBS+H		76.8	0.5333	No

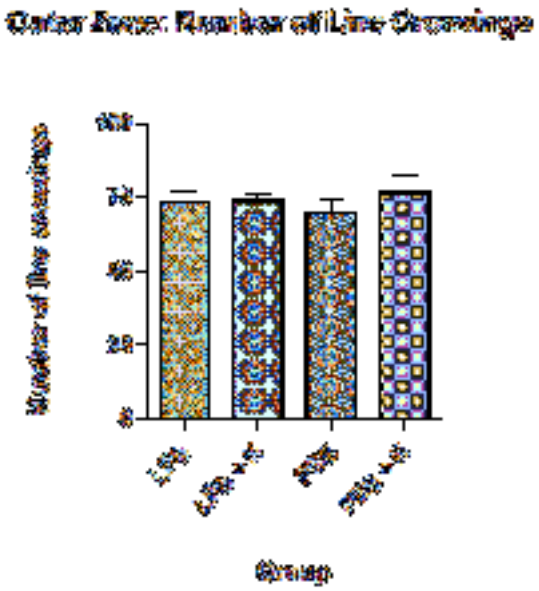

Figure 41: A bar graph plot with mean ± SEM showing the number of line crossings completed by subject in the outer zone of the open-field arena during the testing trial.

For the middle zone, the number of head entries made within was analyzed and presented in **table 27 and figure 42.** Results show that the average was not significantly different between the groups.

Table 27: A summary of the mean scores and p-values obtained when evaluating the number of entries in the middle zone of the open-field arena during the testing trial.

Summary of the descriptive statistics of the number of entries in the middle zone during the testing phase				
Group	**Trial**	**Mean**	**Adjusted P-value**	**Significant?**
PBS	Testing Phase	6.6	-	-
PBS vs. LPS		8.6	0.1907	No
PBS vs. LPS+H		4.9	0.3040	No
PBS vs. PBS+H		5.7	0.7567	No

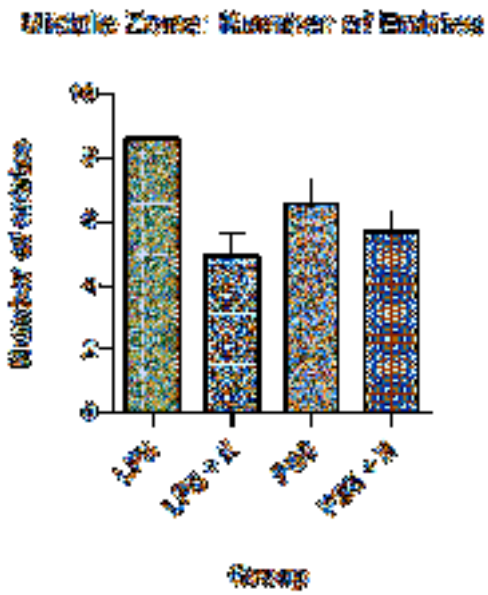

Figure 42: A bar graph plot with mean ± SEM showing the number of entries in the middle zone of the open-field arena during the testing trial.

Next, the time spent in the middle zone during the training phase was analyzed and presented in **table 28 and figure 43.** Data suggests that the time spent was not significantly different between the groups.

Table 28: A summary of the mean scores and p-values obtained when evaluating the time spent in the middle zone of the open-field arena during the testing trial.

Summary of the descriptive statistics of the time spent in the middle zone during the testing phase				
Group	**Trial**	**Mean**	**Adjusted P-value**	**Significant?**
PBS	Testing Phase	6.980	-	-
PBS vs. LPS		8.130	0.7921	No
PBS vs. LPS+H		5.550	0.6711	No
PBS vs. PBS+H		7.0	>0.9999	No

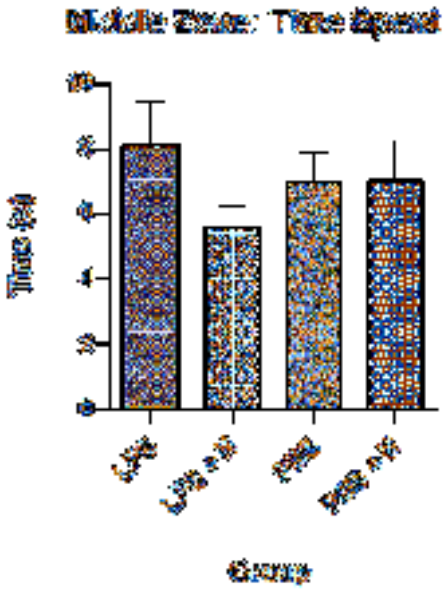

Figure 43: A bar graph plot with mean ± SEM showing the time spent in the middle zone of the open-field arena during the testing trial.

Next, the average speed detected in the middle zone during the training phase was analyzed and presented in **table 29 and figure 44.** Data suggests that the average speed was not significantly different between the groups.

Table 29: A summary of the mean scores and p-values obtained when evaluating the average speed undertaken in the middle zone of the open-field arena during the testing trial.

Summary of the descriptive statistics of the average speed in the middle zone during the testing phase				
Group	**Trial**	**Mean**	**Adjusted P-value**	**Significant?**
PBS	Testing Phase	0.2680	-	-
PBS vs. LPS		0.2530	0.9132	No
PBS vs. LPS+H		0.2713	0.9988	No
PBS vs. PBS+H		0.2526	0.9070	No

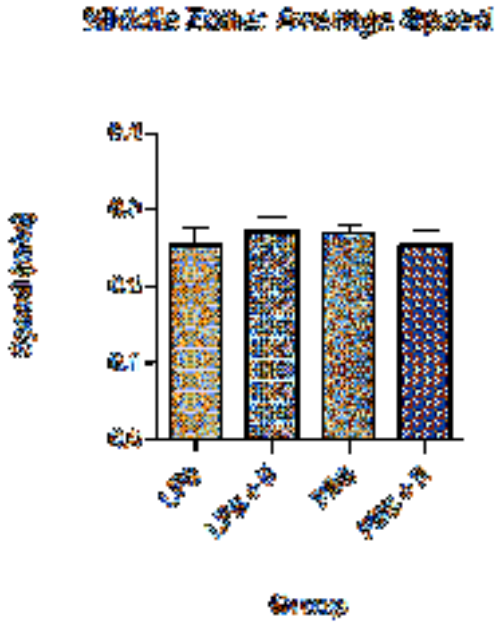

Figure 44: A bar graph plot with mean ± SEM showing the average speed in the middle zone of the open-field arena during the testing trial.

Finally, the number of lines crossed within the middle zone during the training phase was analyzed and presented in **table 30** and **figure 45.** Data suggests that the average speed was not significantly different between the groups.

Table 30: A summary of the mean scores and p-values obtained when evaluating the number of line crossings completed by the subject in the middle zone of the open-field arena during the testing trial.

Summary of the descriptive statistics of the number of lines crossed in the middle zone during the testing phase				
Group	**Trial**	**Mean**	**Adjusted P-value**	**Significant?**
PBS	Testing Phase	11.90	-	-
PBS vs. LPS		13.70	0.7071	No
PBS vs. LPS+H		9.4	0.4752	No
PBS vs. PBS+H		10.70	0.8842	No

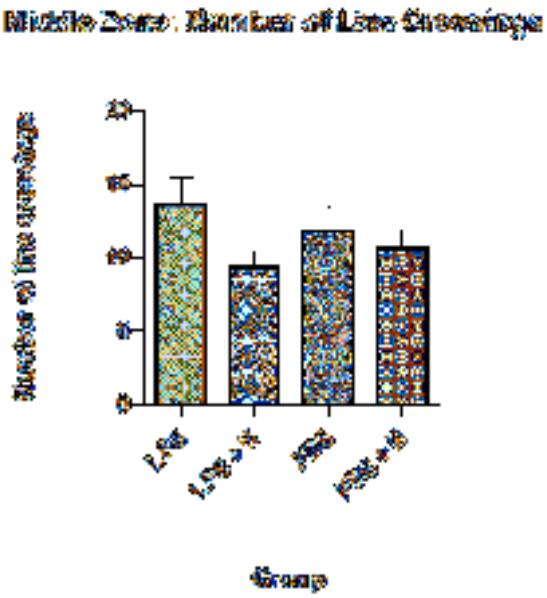

Figure 45: A bar graph plot with mean ± SEM showing the number of line crossings completed by subject in the middle zone of the open-field arena during the testing trial.

For the central zone, the number of head entries made was analyzed and presented in **table 31** and **figure 46.** Results show that the average was not significantly different between the groups.

Table 31: A summary of the mean scores and p-values obtained when evaluating the number of entries completed by the subject in the central zone of the open-field arena during the testing trial.

Summary of the descriptive statistics of the number of entries in the central zone during the testing phase				
Group	**Trial**	**Mean**	**Adjusted P-value**	**Significant?**
PBS	Testing Phase	1.2	-	-
PBS vs. LPS		1.3	0.9916	No
PBS vs. LPS+H		0.8	0.6854	No
PBS vs. PBS+H		0.9	0.8320	No

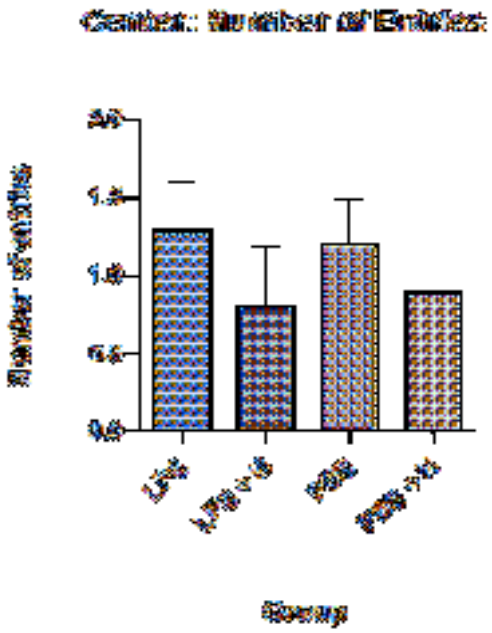

Figure 46: A bar graph plot with mean ± SEM showing the number of entries completed by subject in the central zone of the open-field arena during the testing trial.

Then, the time spent in the central zone was analyzed and presented in **table 32 and figure 47.** Results show that the time spent was not significantly different between the groups.

Table 32: A summary of the mean scores and p-values obtained when evaluating the time spent in the central zone of the open-field arena during the testing trial.

Summary of the descriptive statistics of the time spent in the central zone during the testing phase				
Group	**Trial**	**Mean**	**Adjusted P-value**	**Significant?**
PBS	Testing Phase	0.82	-	-
PBS vs. LPS		0.64	0.9479	No
PBS vs. LPS+H		0.71	0.9870	No
PBS vs. PBS+H		0.47	0.7334	No

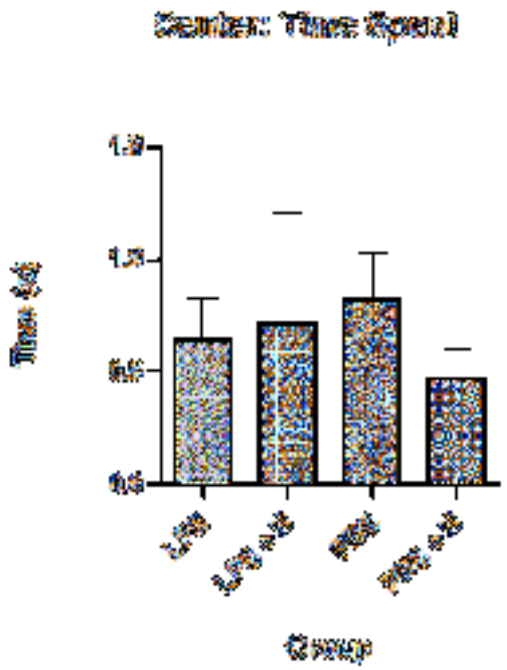

Figure 47: A bar graph plot with mean ± SEM showing the time spent in the central zone of the open-field arena during the testing trial.

Furthermore, the average speed in the central zone was analyzed and presented in **table 33 and figure 48.** Results show that the average speed was not significantly different between the groups**.**

Table 33: A summary of the mean scores and p-values obtained when evaluating the average speed undertaken in the central zone of the open-field arena during the testing trial.

Summary of the descriptive statistics of the average speed in the central zone during the testing phase				
Group	**Trial**	**Mean**	**Adjusted P-value**	**Significant?**
PBS	Testing Phase	0.2063	-	-
PBS vs. LPS		0.2994	0.3101	No
PBS vs. LPS+H		0.2983	0.4517	No
PBS vs. PBS+H		0.2689	0.6156	No

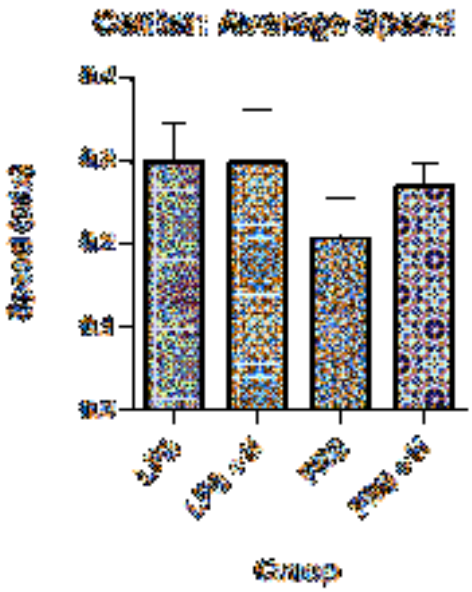

Figure 48: A bar graph plot with mean ± SEM showing the average speed undertaken in the central zone of the open-field arena during the testing trial.

Next, the average number of visits in the central zone was analyzed and presented in **table 34 and figure 49.** Results show that the average number of visits was not significantly different between the groups.

Table 34: A summary of the mean scores and p-values obtained when evaluating the average number of visits in the central zone of the open-field arena during the testing trial.

Summary of the descriptive statistics of the average number of visits in the central zone during the testing phase				
Group	**Trial**	**Mean**	**Adjusted P-value**	**Significant?**
PBS	Testing Phase	0.7750	-	-
PBS vs. LPS		0.4429	0.2784	No
PBS vs. LPS+H		0.6750	0.9580	No
PBS vs. PBS+H		0.5286	0.5105	No

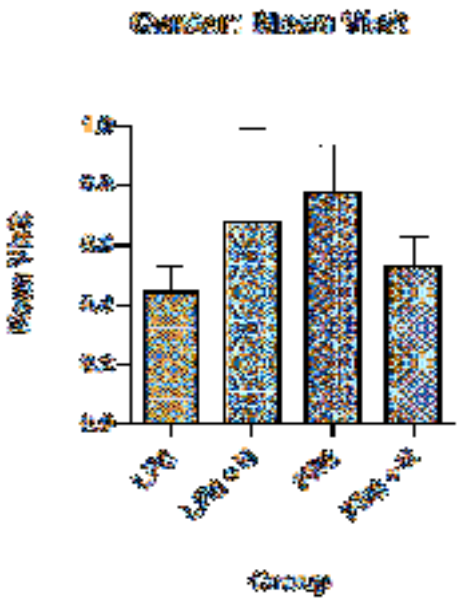

Figure 49: A bar graph plot with mean ± SEM showing the average number of visits in the central zone of the open-field arena during the testing trial.

To conclude, the number of lines crossed in the central zone was analyzed and presented in **table 35** and **figure 50.** Results show that the average number of visits was not significantly different between the groups.

Table 35: A summary of the mean scores and p-values obtained when evaluating the number of line crossings in the central zone of the open-field arena during the testing trial.

Summary of the descriptive statistics of the number of line crossings in the central zone during the testing phase				
Group	Trial	Mean	Adjusted P-value	Significant?
PBS	Testing Phase	1.1	-	-
PBS vs. LPS		1.3	0.9382	No
PBS vs. LPS+H		0.8	0.8278	No
PBS vs. PBS+H		0.9	0.9382	No

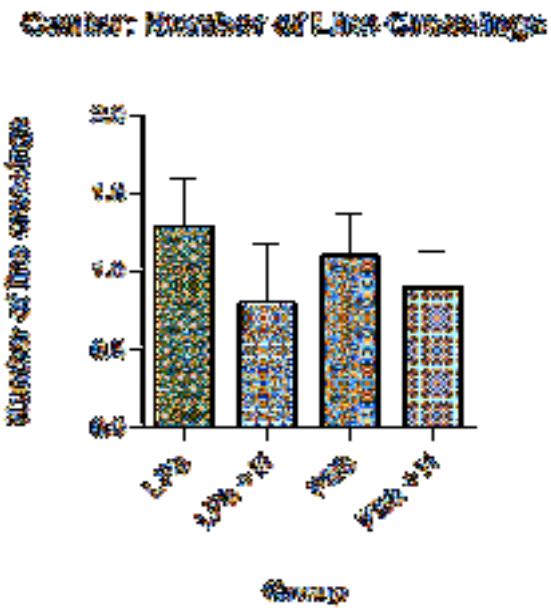

Figure 50: A bar graph plot with mean ± SEM showing the number of line crossings in the central zone of the open-field arena during the testing trial.

Altogether, the open-field analysis indicates that ten-day systemic exposure to 0.1 M LPS was not potent enough to induce anxiety-like behaviour and locomotor impairments.

4.5 Discussion

Neurodegenerative diseases are characterized by a crippling intellectual decline. The development of murine models has been exceptionally important because they have been adopted to assess neurodegeneration with qualities like those in the human brain.[228] Models

that restate different features of AD, including deficits in cognitive areas disturbed in patients provide fundamental tools for extensive research into the diseases and provide beneficial means for effective screening *in vivo*.[228] As yet, the exact aetiology of neurodegeneration remains unclear.[229]

Presently, there are no therapies available to cure AD.[230] Medications that are available on the market are disease-modifying, in that they target the inherent cause of the disease.[230] This suggests an earnest requirement for effective pre-clinical, and new remedial approaches for the disease.[231]

Changes to features of cognitive behaviour can provide meaningful markers of neurodegeneration, and they can reveal signs relating to the disease prognosis, treatment, and complications. To identify signs of cognitive decline and/or group differences in behaviour between healthy subjects and those exposed to systemic LPS. This chapter investigated three behavioural tests commonly used in the laboratory to assess such impairments, and its association to neuroinflammation in a homogenous group of Sprague Dawley rats. The results of the control group (PBS only) were compared to the three experimental groups (LPS vs. LPS + H vs. PBS + H). Only significant results will be discussed.

4.6.1) Y-maze Test

Collectively, the findings reveal no statistical significance in the differences between the control and experimental groups, and thus no conclusive association between acute LPS-induced systemic neuroinflammation and spatial recognition. However, when comparing just the means of each group, per parameter, notable differences are seen.

Statistical analysis showed a significant difference in the average speed between the control group and PBS + H group (mean=0.07630, $p<0.0347$) in novel arm during the testing trial (**table 5**). Although speculative, these results suggest that honey may facilitate increased short-term spatial working memory by alleviating symptoms of memory decline in rodents, hence the PBS + H group showed preference to the novel arm and moved about at a higher speed than the other groups. This is supported by a study by Akanmu *et al*., (2011), who examined the neurological impacts of Nigerian honey using the Y-maze paradigm, and concluded that honey improved spatial working memory in mice.[232] Examination of the time spent in motion in the long arm (**table 7**) during the testing trial indicated that in general, all four groups spent much more time in motion inside the novel arm than they did in the long arm (although not significant). The amount of time that the subjects remained in motion in the

novel arm, was suggestive of their short-term spatial working memory ability. Surprisingly, upon further scrutiny of the mean scores during the testing trial in the long arm, significant differences were noted when the control group was compared to LPS (mean=8.780, $p<0.0440$) and PBS + H (mean=8.320, $p<0.0237$) group. The motion-time profile of these two groups when evaluated against the training trial in the long arm and testing trial in the novel arm could be suggestive of weakened spatial memory consolidation processes in the LPS populations. This is consistent with previous findings that LPS administration impairs cognitive ability and exploratory behaviour.[229] Furthermore, **table 8** reveals significant differences in the time that the LPS + H (mean=12.50, $p<0.0183$) and PBS + H (mean=13.51, $p<0.0449$) groups remained immobile in the novel arm. A possible explanation to why the honey-fed experimental groups showed increased mobility (less time immobile) in the novel arm is that honey improves spatial memory, thus they explored the novel arm with greater enthusiasm and mobility. Examination of the time spent in the familiar arm (**table 10**) during the testing trial showed a significant difference between the control group and PBS + H group (mean=35.40, $p<0.0072$), where the PBS + H group spent more time in the familiar arm than they did in the novel arm. However, non-conclusive associations can be drawn from these results. On the other hand, data shown in **table 5** indicates a significant difference in the average speed undertaken by the PBS + H (mean=0.07630, $p<0.0347$) group in the novel arm during the testing trial. The PBS + H group explored by novel arm at a greater pace than the other three groups, which may suggest that honey consumption induces hyperactivity in rodents. This is consistent with findings of Marwitz and colleagues[233] who concluded that rats exposed to a Western-style Diet, comprising high sugar and saturated fats, exhibit behaviours characteristic to hyperactive-impulsive type ADHD. Lastly, observations of the time lapsed while the subjects were immobile show that the PBS + H group (mean=18.52, $p<0.0132$) spent significantly more time immobile in the familiar arm during the testing trial, than the control group **(table 14)**. Plausible justifications for this observation can't be made. When time immobile in the novel arm was examined, it was noted that both the LPS + H (mean=12.50, $p<0.0183$) and PBS + H (mean=13.51, $p<0.0449$) groups spent significantly less time immobile in the novel arm than the control group. Again, this emphasizes previous findings that a high-sugar diet (honey) contributes to hyperactivity and impulsivity in Sprague Dawley rats.[233]

4.6.2) Novel Object Recognition Test

Collectively, the findings reveal no statistical significance in the differences between the control and experimental groups. These observations are consistent with findings by De La Torre[234] that indicated that male C57BL/6 mice exhibit decreased speed (cm/s) and distance (cm) after LPS exposure. However, when the number of entries in Block B (which contained the novel object) during the testing trial were analyzed, a significant difference between the LPS group (mean=7.5, $p<0.0044$) and the control group (mean=4.0) was observed (**table 18**). This indicates that the LPS group exhibited more curiosity in the novel object by exploring it more frequently than the control group. Similarly, analysis of the first zone entered **(figure 35)** during the testing trial shows that LPS group and PBS group explored Block B first, which contained the novel object. Surprisingly, the LPS + H group showed equal preference for the familiar and novel object. Meanwhile the PBS + H group showed bias towards to the familiar object. Conclusions by Czerniawski J *et al*., (2015) indicate that even though the subjects were able to differentiate a familiar object from a novel one, LPS-induced neuroinflammation does not hinder memory recall in every hippocampal-dependant task, but instead it may distinctly interfere with tasks that demand context discrimination.[235] For the most part, the results obtained in this assessment may be attributed to the age (ten-weeks old) of the subjects which limits them from displaying significant cognitive dysfunction, and recognition memory. However, studies have reported that significant brain development in rats occurs until 9 weeks of age, and CNS myelination of limbic structures occurs until 6 weeks of age.[236,237] Alternatively, the two-minute trial period may have not been sufficient for memory consolidation and recall, which consequently resulted in the task not being sensitive enough to identify subtle differences between the groups.

4.6.3) Open-field Test

Taken together, the outcomes reveal that there were no significant differences between the control group and experimental groups. This implies that LPS-induced neuroinflammation does not induce anxiety or motor deficits of rodents. This is supported by Bassi and colleagues[238] who concluded that LPS administration up to 200 µg/kg does not cause motor dysfunction. Given that this study sought to simulate a period of sustained inflammation that may arise naturally in healthy individuals, a low concentration of LPS treatment administered regularly was sufficient. In summary, a study by Tanaka, *et al*., (2012) identified four factors that may explain differences underlying rodent behaviour in the open-maze paradigm.[239]

These include activity, sequential organization, diversive exploration and inspective exploration.[239] The authors suggest that this four-factor model be used in drug efficacy and psychiatric studies, to ensure systematic and consistent characterization of rodent behaviour.

4.6 Conclusion

Research has validated the importance of LPS-induced murine models of neuroinflammation in understanding the pathological mechanisms underlying neurodegeneration.[229] Compounding reports reveal that the administration of LPS promotes neuroinflammation, coupled with damage to the BBB and memory dysfunction.[96] The administration of LPS has been shown to reduce cognitive ability in animals and cause a complex range of behaviours including weight loss, depression, reduced mobility, and intensified anxiety and sleepiness.[228,240,241]

Sufficient evidence has been collected in this chapter to deduce that 0.1 M LPS systemically administered at a 0.1 mg/ml concentration and a volume of 0.1 ml/kg for a period of 10 days does not cause significant cognitive dysfunction in Sprague Dawley rats. This may be attributed to a considerable number of elements that affect the results observed in behavioural testing, such as group selection, task complexity, individuality, data analysis, animal-investigator interactions and repetition.[242,] At the same time, there are several factors that can impact animal response to LPS administration like the dosage of LPS given, type of LPS exposure, route of exposure, and period of exposure.[243] For example, if it is administered acutely, prior to training, it impairs cue-fear conditioning, whereas chronic administration of LPS, has been found to impair spatial memory and promote memory and learning deficits. [244] A single intraperitoneal injection of LPS in a dose of 100 µg/kg in adult male Wistar rats, impaired memory object recognition.[245] Shaw *et al.*[246] reported that a single intraperitoneal injection of LPS in a dose of 250 µg/kg impaired hippocampal dependent spatial learning in the Morris water maze behavioral test. In another study, in adult male Wistar rats, a single injection of LPS in a dose of 1mg/kg, impaired cognitive performance in the Barnes Maze test and in the inhibitory avoidance test.[247] Therefore, to mimic a period of sustained inflammation, repeated exposure to low dose LPS (concentration of 0.1mg/ml) was determined using reference articles.

Group selection and randomization can influence the cognitive and sensory-motor abilities of each group.[242] In this study, the sample groups were categorized by weight range. This may have impacted mobility performance in the behavioural tests in such a way that the heavier

cohort had fewer entries into the arms/blocks, showed longer periods of immobility (which may have been incorrectly interpreted as increased exploratory behaviour) and completed the task at slower speeds when compared to lighter group. Task complexity may challenge subject performance if the task is too easy or too demanding.[242] Although speculative, results from the NORT and open-field test, which show no significant differences between the control and experimental groups, may suggest a negative impact possibly caused by the notion that the tasks were too complex for the low dosage of LPS and short exposure time. Furthermore, it is important to note that the subjects are individuals and will consequently behave differently despite the treatment method selected.[242] Animal-investigator interactions, which includes the experience level of the investigator and their degree of comfort working with rodents, may have an adverse effect on the results. In this study, the principal investigator was a novice at animal studies, and therefore, may have unintentionally induced fear and anxiety in the subjects causing their performance to deviate from the predicted outcomes. Altogether, it is conceivable that the non-significant differences observed in this study may be attributed to the factors listed above, in addition to the suggestion that acute neuroinflammation plays a protective role in the body.[248,249,250]

To confirm whether or not the LPS treatment induced histological changes similar to what is observed in AD-dementia, amyloid formation and deposition into the hippocampus was examined by enzyme-linked immunosorbent assay (ELISA) specific for the $A\beta_{42}$ isoform, which is considered to be the most toxic.

5

Chapter 5: Measuring total amyloid-βeta$_{42}$

5.1 Chapter Objectives

This chapter will address the methods and results pertinent to the following objective;

- Assessing the progression of amyloid β (Aβ) formation by measuring the amount (concentration) of soluble Aβ$_{42}$ levels in the hippocampal tissue of aged Sprague-Dawley rats using a sandwich-ELISA.

5.2 Introduction

The aggregation of soluble amyloid oligomers and deposition into fibrils and plaques is a pathogenic phenomenon central to AD dementia. The most prevalent amyloid β peptides comprise 40 (Aβ$_{40}$) and 42 (Aβ$_{42}$) amino acids.[19] Despite the fact that the Aβ$_{40}$ peptides are produced in larger quantities than Aβ$_{42}$, Aβ$_{42}$ isoforms account for a larger portion of amyloid aggregates in the brain because of its tendency to misfold-which renders it more toxic.[251] Nonetheless, extracellular Aβ is transported from the blood to the brain and vice versa. Translocation into the brain is facilitated by carrier-receptor transport across the BBB whilst degradation occurs by proteins such as astrocytes, plasmin and apolipoprotein E (ApoE).[252,253,254,255] The concentration of soluble Aβ peptides in the CNS plays a significant role in the production of toxic oligomers, and this concentration is profoundly regulated by Aβ transport across the BBB.[256] Moreover, recent studies show that soluble Aβ aggregates trigger neuronal dysfunction and activate microglia.[257] And neurotoxic Aβ oligomers activate gliosis, which stimulates the release of pro-inflammatory mediators by astrocytes and microglia *in vitro*.[258] Essentially, enzyme-linked immunosorbent assay (ELISA) is a simple technique used to detect the concentration of Aβ in plasma, the brain and CSF.[259]

ELISA is a plate-based analytical procedure used in biochemistry to quantitatively determine the concentration of soluble substances in solution.[260] The assays is conducted in 96-well polystyrene plates which bind antibodies. Multiple wells per plate allow for several samples to be run at once. The bottom surface of each well of the plate is pre-coated with the antigen of interest. Plates are purchased with the wells already coated and the concentration of the fixed antigen differs for each ELISA kit therefore the detection range / sensitivity of the

antigen-antibody complex is always indicated. During the analysis an intense colour change indicates a higher concentration of antibody (i.e. protein) present. For the analysis, the generated data is evaluated in comparison to a standard curve (optical density vs. log concentration) and the antibody of interest is quantified.

5.3 Methods and Materials

All the samples were prepared at the Laboratory of Microscopy and Microanalysis unit, University of Pretoria, Prinshof campus. In this study, the concentration of soluble $A\beta_{42}$ present in the hippocampal tissue was determined. Commercially available ELISA kit from Elabscience® catalogue number E-EL-R1402 was used.

5.3.1) Sample preparation

After termination, the right hemisphere was used for ELISA. On an ice-cold metal plate, the right hemisphere was separated into the cortex, cerebellum, and hippocampus. The hippocampus was extracted and placed inside an empty round bottom Eppendorf tube. The tube was immersed in liquid nitrogen for snap freezing and the tissue was maintained in dry ice until final storage in a -80°C freezer until the assay was conducted. The hippocampal tissue was brought to room temperature before it was homogenized in EzLys™ tissue protein extraction reagent (purchased from Biocom Africa) containing DNAse 1 protease inhibitor cocktail (purchased from Sigma®, South Africa).

5.3.2) Soluble $A\beta_{42}$ Assay

Brain homogenate: The tissue sample was weighed by recording the weight of the empty eppendorf tube and subtracting that from the weight of the tube containing the right hemisphere. For each gram of tissue to be homogenized, 10-15 ml of cold tissue protein extraction reagent and 100-150 U of DNAse I protease inhibitor was added. The tissue was homogenized with 15 strokes using Dounce disposable homogenizer. The sample was then centrifuged at 10,000 ϑ at 4°C for 10 minutes. The supernatant was collected, aliquotted and used to quantify the amount of soluble $A\beta_{42}$ protein present in the hippocampal tissue.

Reagent preparation: All reagents were brought to room temperature before use. To prepare the wash buffer, 30 mL wash buffer concentrate was diluted in 720 mL of distilled water. To prepare standard working buffer; the standard was centrifuged at 10,000 ϑ for 1 minute

followed by the addition of 1.0 mL of reference standard and sample diluent. This was gently mixed and allowed to stand for 10 minutes before serial dilutions of the gradient 1000, 500, 250, 125, 62.5, 31.25, 15.63, 0 pg/mL were made. To prepare biotinylated detection antibody solution, 100x concentrated biotinlyated detection antibody was diluted to 1x working solution with biotinylated detection antibody diluent. To prepare HRP solution, 100x concentrated HRP conjugate was diluted to 1x working solution with concentrated HRP conjugate diluent.

Assay procedure: Standard working solution was added to all the wells of the first two columns (100 µL each well). Next, 100 µL of sample was added to the other appropriate wells and the plate was covered and incubated for 90 minutes at 37°C. The solution was drained and 100 µL of biotinylated detection antibody working solution was added to each well. The plate was covered, gently mixed, and incubated for one hour at 37°C. The solution was removed and 350 µL of wash buffer was added to each well, allowed to soak for two minutes before it was decanted and pat dry using clean absorbent paper. This step was repeated three times. Then, 100 µL of HRP conjugate working solution was added to each well; the plate was covered and incubated for 30 minutes at 37°C. The solution was removed, and the wells washed five times with wash buffer. To facilitate antibody detection, 90 µL of substrate reagent was added to each well and the plate was covered and incubated for 15 minutes at 37°C in the dark. Finally, 50 µL stop solution was added to each well and gently mixed. The optical density (OD value) of each well was determined, using a BioTek® Epoch microplate reader set to 450 nm absorbance. The generated data was plotted on an optical density vs. log concentration curve and then compared to standards to quantify soluble $A\beta_{42}$ present in the hippocampal tissue.

5.4 Results

All statistical analyses were completed using GraphPad™ Prism (version 9.2.0) for Windows (GraphPad™ Software, San Diego, California USA). The data was analysed using one-way ANOVA. The p-value was set at $p < 0.05$, with a 95% confidence interval.

To characterize the effects of LPS-induced neuroinflammation on total $A\beta_{42}$ quantity in the hippocampus, the control group (PBS only) was compared to the three experimental groups (LPS only vs. LPS + H vs. PBS + H). Biochemical analysis indicated that there are no significant differences between the four groups. **Table 36** and **figure 51** are a representative summary and graph of the quantity of soluble $A\beta_{42}$ present.

Table 36: A summary of the soluble $A\beta_{42}$ mean scores ± standard deviation (SD) per sample group.

Total $A\beta_{42}$ (pg/mL)			
Group	Mean ± SD	p-value	Significant? (yes/no)
PBS	0.1528 ± 0.1959		
PBS + H	0.1695 ± 0.2306	0.8585	no
LPS	0.1142 ± 0.1592		
LPS + H	0.1164 ± 0.1583		

The p-value (**table 36**) indicates that the quantity of $A\beta_{42}$ detected in the hippocampi of the experimental group did not significantly differ from the amount detected in the control group after LPS-induced neuroinflammation.

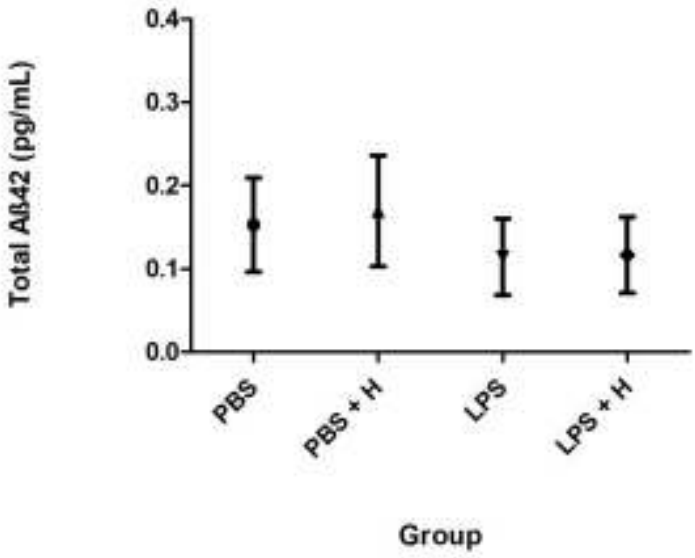

Figure 51: A dot plot (mean ± SEM) graph showing quantity of $A\beta_{42}$ peptide found in the hippocampal area using $A\beta_{42}$ sandwich ELISA . The p-value indicates that the of soluble Aβ present in the hippocampus did not signifantly differ between the groups.

Results reveal no statistical differences in $A\beta_{42}$ levels among the groups. However, when comparing just the means of each group, notable differences were seen.

5.5 Discussion

The deposition and aggregation of soluble $A\beta_{42}$ fibrils into plaques in the brain are known to contribute to the pathogenesis of AD.[261] Various neurodegenerative diseases exhibit an inflammatory element.[262] It is possible that chronic or acute systemic inflammation provides means by which $A\beta_{42}$ plaques steadily increase in the brain, consequently resulting to it's association with cognitive dysfunction.[263] However, the key components linking acute inflammatory activities, syntheisis of soluble $A\beta_{42}$ peptides, $A\beta_{42}$ plaque deposition and cognitive decline remain unclear.[263]

The objective of this chapter was to quantitively determine the level of $A\beta_{42}$ present in the hippocampal tissue of each group, following LPS-induced systemic neuroinflammation. According to findings in **table 36**, no significant differences were detected in $A\beta_{42}$ level among the four groups. This suggests that the SC administration of 0.1 M LPS systemically administered at a 0.1 mg/ml concentration and a volume of 0.1 ml/kg for a period of 10 days does not significantly elevate $A\beta_{42}$ levels in the hippocampal region of Sprague Dawley rats. This is consistent with reports by Mechnikov[264] that pre-conditioning with low-dose LPS causes physiological inflammation –which is characterized by the removal of cellular debris, tissue repair, and thus return to CNS homeostasis and protection- as opposed to a pathological immune response which contributes to neurodegenerative diseases.[265] In the AD model, LPS pre-conditioning was shown to improve cognitive impairment by hindering amyloid formation and aggregation.[266,267,268] This is due to low-dose LPS pre-conditioning inhibits the expression of pro-inflammatory agents, such as IL-β and TNF-α.[268] In addition, it leads to the preferential activation of anti-inflammatory microglia instead of pro-inflammatory microglia.[269] Although speculative, the concept of "physiological inflammation" may provide insight to the observations of these results.

5.6 Conclusion

The sandwich ELISA used to quantify $A\beta_{42}$ levels showed that LPS did not produce increased $A\beta_{42}$ levels. Instead, it appears that the administered LPS may have triggered an anti-inflammatory response. However, assays which detect markers of pro- and anti-inflammatory mechanisms would provide a useful tool to confirm the results from this study. Also, it is imperative to note that the cytokine profile in the brain and blood are influenced by different doses of LPS.[265]

Pre-conditioning with LPS is said to induce neuroprotection by promoting anti-inflammatory and anti-oxidative processes, and autography.[265] Being that LPS is amply present in traditional remedies and foods ingested by humans[270,271,272], it is clear that humans consume LPS regularly. This suggests that a higher dose of LPS may have steered the innate immune response to LPS, away from physiological to a pathogical response that eventually results in amyloid accumulation. Therefore, it is valuable for future studies to examine the pro- and anti-inflammatory effects at increasing doses of LPS, in order to further elucidate the shift from regulated inflammation to pathological inflammation.

6

Chapter 6: Immunofluorescence Assay

6.1 Chapter Objectives

This chapter will address the methods and results pertinent to the following objectives:

- Determine the number of astrocytes present in the hippocampal tissue of Sprague-Dawley rats by immunofluorescence staining with glial fibrillary acidic protein (GFAP) antibody using confocal microscopy and ImageJ.

- Identify astrocyte activity (astrogliosis) in the hippocampal tissue of Sprague-Dawley rats by measuring fluorescent intensity using a GFAP antibody using confocal microscopy and ImageJ.

- Identify microglial activity (microgliosis) in the hippocampal tissue of Sprague-Dawley rats by co-labeling tissue sections with Iba1 and CD68 antibodies and counting the number of Iba1 positive cells using confocal microscopy and ImageJ and measuring the fluorescent intensity of co-localized Iba1 and CD68 positive cells using ImageJ.

- Identify the protective effects of honey on the astrocyte and microglial expression/quantity in the hippocampal tissue of Sprague-Dawley rats using ImageJ.

- Identify the presence and fluorescent intensity of fibril amyloid proteins in the hippocampal tissue of Sprague-Dawley rats by measuring fluorescent intensity using Thioflavin-T stain using confocal microscopy and ImageJ.

6.2 Introduction

Immunohistochemistry (IHC) forms an important component of diagnostic pathology, drug development, and research methodology, especially in the fields of neuropathology, hematopathology and oncopathology.[273] It is a commonly used approach for examining protein expression and distribution in health and pathohistological studies.[273] The use of IHC

techniques to examine tissue samples provides details that otherwise can't be attained using standard hematoxylin and eosin (H & E) stains, on pathways that contribute to pathological states.[273] Tissue samples are either embedded in paffarin wax or frozen for microtome or cryostat sectioning, respectively, followed by subsequent staining and visualization by light or confocal microscopy. The technique uses antigen-antibody reactions to identify antigens of interest in biological samples, that are subsequently visualized by a chromogenic-substrate marker.[274] Additionally, the technique maintains the composition, cellular and structural integrity of the tissue.[274] Therefore, it is a valuable assay with a diverse series of applications that include the; identification of infectious agents in tissue samples, classification and diagnosis of neuropathologies, and diagnosis of muscular dystrophies. Also, IHC can be used to determine the functions of gene products, and serves as a predictive marker for cancer progression.[273]

Immunofluorescence (IF) assay is a specialized subcategory of IHC, that is split into two types; direct and indirect IF. This technique uses a fluorescent dye to capture antibody binding, intracellular processes and cellular structures under fluorescent microscopy.[274] The antigen of interest binds to a fluorochrome-tagged antibody that emits light when a reaction is present.[275] This light is captured by fluorescent microscopes attached with filters specific for the wavelength of light emited.[275] Some advantages of IF (compared to IHC) include: higher resolution imaging and stability of fluorescent-labelled tissue as well as the ability to label multiple antigens at a time.[276] Lastly, the enzymatic nature of IHC techniques prevents the quantitative analysis of results, whilst the opposite is true for the IF approach. In fact, modern high-output techniques are facilitated by fluorescent detection, for rapid and quantitative microscopy.[277]

Previous research has shown that GFAP is mostly expressed by astrocytes.[278] Additionally, ionized calcium-binding adapter molecule 1 (Iba-1) is distinctly expressed in microglia and macrophages.[279] It is induced by cytokines and IFNs and contributes to inflammation.[280] Therefore, GFAP and Iba-1 are recognized as biomarkers of astrocytes and microglial cells.[281] An investigation by Kang, J [281] aimed at elucidating the role of LPS in regulating activations of neuroglia in the cerebral cortex used anti-GFAP and anti-Iba-1 fluorescent antibodies to observe Iba-1 and GFAP positive microglia and astocytes. To assess the expression value of these antibodies, they quantified the expression as a ratio of the intensity of the control group, and found that the LPS-treated group expressed greater levels of both antibodies. Moreover, Belfiore and colleagues co-labeled hippoacampal sections with CD68

and Iba-1 antibodies to identify microglial activation.[282] Activation was defined as the co-localization of CD68 and Iba-1. Also, they found that the quantity of microglia showing co-localized binding was greater in the LPS-treated group.

In this study, whole brain sections of the left hemisphere were prepared for IF staining with antibodies specific for microglia (anti-CD68 and anti-Iba1) and astrocytes (anti-GFAP). Microscope slides were visualized by fluorescent confocal microscopy. Quantitative data was generated and interpreted using ImageJ software (ImageJ 1.52a, National Institutes of Health, USA) and the results of the experimental groups were compared to the control group. The efficacy of honey as a protective/mopping agent was determined by comparing the quantitative results of the intervention (honey) group to the experimental groups. In line with the foregoing literature in chapter 2, it was anticipated that honey will suppress microglial and astrocyte reactivity.

6.3 Methods and Materials

All tissue samples were prepared at the Laboratory of Microscopy and Microanalysis unit, University of Pretoria, Prinshof campus, following completion of the this first trial of the study, as indicated in **figure 9** . A detailed list of the reagents used in this chapter can be found in **addendum 6.**

6.3.1) Antibodies used for the immunoflorescence

Purchased from Abcam: Anti-GFAP antibody (ab33922,1:1000 dilution); anti-Iba1 antibody (ab5076, 1:1000 dilution); anti-CD68 antibody (ab31630, 1:800 dilution); Thioflavin T stain (T3516, 20µM).

6.3.2) Tissue collection and preservation

Subjects were terminated by inhalation of Isfor® followed by perfusion with saline and 4% formaldehyde, which was then followed by decapitation. The brain was carefully removed from the skull and bisected into the right and left hemisphere. The left hemisphere was dropped and fixed in 4% formaldehyde solution for 48 hours at room temperature.

6.3.3) Tissue processing

The tissue was rinsed with 0.1 M phosphate buffered saline (PBS) three times for 10 minutes each to remove formaldehyde precipitates. It was then placed in 15% sucrose solution until it sank to the bottom. The sucrose solution was replaced with a 30% sucrose solution containing 0.05% sodium azide. The tissue was stored at 4°C until sectioning. Sagittal sections of 30 µm were sectioned using a cryostat set to -20°C.

6.3.4) Free-floating sections

Cryo-protection: All four sides of a 96-well plate were labelled for each brain and cryo-protectant medium was prepared using 125 ml glycerine, 150 ml ethylene glycol and 250 ml 0.1 M PO_4. With the use of a multi-channel pipette, the wells were filled with cryo-protectant and stored at 4°C.

Sectioning: Tissue sectioning was performed using a cryostat (Leica CM 1850,Leica Biosystems) set at -20°C. Sections of 30 µm sections were prepared and floated in wells containing cryo-protectant.

ThT staining: 10 mM stock solution was prepared by dissolving 31.8 mg ThT powder in 0.1M PBS.

Permeabilization: The slides were incubated in 0.1 M TBS containing 0.3% Triton X-100, three times for 15 minutes. Tris buffered saline (TBS) was prepared from 26.44 g trizma hydrochloride, 3.88 g trizma base and 18 g sodium chloride + 2 L ddH_2O. The buffer was removed and the sections were blocked.

Preparation of TBS+: Add 1.25 ml Triton X-100 to 500 ml 0.1 M TBS.

Blocking: Sections were incubated in a blocking buffer prepared using 38 ml TBS+, 0.3 M glycine and 2 ml bovine serum albumin (BSA) for one hour with gentle agitation. The blocking solution was removed and the sections were rinsed in 0.1 M TBS, three times for 15 minutes each.

Immunostaining: The primary antibodies (GFAP, Iba-1, and CD68) were diluted according to manufacturer suggestions. Antibodies were diluted in TBS+. Each well was filled with the solution and incubated in the fridge at 4°C for 72 hours. This was aspirated and sections were washed in 0.1 M TBS three times for 15 minutes each.

Mounting: The sections were mounted on a 1 mm thick clear glass slide (Labocare® microscope slides) and allowed to air dry for less than one minute. Fluoromount™ aqueous mounting medium (Sigma-Aldrich) was used to mount the sections. These were placed flat overnight and stored in a dark slide box, at 4°C, until visualization with a Zeiss LSM 880 confocal laser scanning microscope (Carl Zeiss Microscopy GmbH, Jena, Germany).

6.3.5) Quantitative analysis using ImageJ

Sample analysis involved capturing a series of micrographs that represented features of interest to the study. A minimum of ten representative micrographs per sample was taken to show the general overview of the sample at low magnification (40x objective with a 1.5x digital zoom). Features of interest were identified and further series of micrographs were taken that showed these features at progressively higher magnifications. The following properties were noted:

1. Fluorescent intensity of GFAP stained sections for each subject in all three sample groups using ImageJ.
2. The number of GFAP stained cells in each sample using ImageJ.
3. The number of Iba1 positive cells in each sample using ImageJ
4. Fluorescent intensity of CD68 stained sections for each subject in all three sample groups using ImageJ.
5. Co-localization of Iba1 positive cells with CD68 stained lysosomal cells using ImageJ.
6. Fluorescent intensity of ThT stained cells using ImageJ.

To quantify co-localization in the confocal micrographs , ten images per rat were quantified and averaged. To count astrocytes and microglia, GFAP and Iba1- stained sections were visualized using a 10x and 40x objective with a 1.5x digital zoom. Micrographs were transferred to ImageJ for cell counting.

6.3.5.1) Cell counting with ImageJ

Astrocyte activity: Automated counting was employed. The image to be analysed was opened, and the cells to be counted were highlighted. The background was subtracted accordingly. Customization (i.e. size or circularity of particles to be counted) of the analysis tool was made accordingly, the image was processed and the results were obtained. The boxes next to the information of interest were checked and all the relevant data was recorded. The results log was saved on a excel spreadsheet.

Microglial activity: Manual counting was employed. After installing the Cell Counter plug-ins, the image was opened. The plug-in tool was selected and two new windows were opened, a counter window with the image on top of a row of buttons, and another with a results window where cells tallied. To begin counting, “type 1” or “type 2” at the bottom of the counter window was selected followed by a direct click on the cell/object to be counted. After counting, the results button was selected and a total for each cell type plus a grand total of all clicks at the bottom of the results window was generated. The results were saved on a excel spreadsheet.

6.3.5.2) Intensity quantification with ImageJ

To get the intensity of a defined area within the image; ImageJ program was opened. Using the toolbar, the “analyze” tool was selected followed by “set measurements”. The boxes next to the information of interest were checked (i.e. area, diameter and intensity). To create a plot of intensity values across features in the image, the “analyze” and “plot profile” tools were used. The background was subtracted accordingly. Customization of the analysis tool was made accordingly, the image was processed and the results were obtained. The results log were saved on a excel spreadsheet.

6.4 Results

The data is presented as microphotographs of hippocampal sections, which show the fluorescent profiles observed. Microphotographs of each sample group were captured and used to compare the experimental groups to the control group. The samples were visualized using a 40x and 10x objective, during which the fluorescent trends and cell counts were noted. ImageJ was used to determine the fluorescent intensity observed in addition to performing cell counts. To calculate fluorescent intensity, the corrected total cell fluorescence (CTCF) was used to reliably compare the groups. Statistical tests were completed using GraphPad™ Prism (version 9.2.0) for Windows (GraphPad™ Software, San Diego, California USA). The Shapiro-Wilk normality test was used to establish that the dataset was normally distributed. The dataset was analyzed using one-way ANOVA. Post-hoc checks with Dunnett’s multiple comparisons test were used to compare the three experimental groups to the control group. The p-value was set at $p < 0.05$, with a 95% confidence interval. The results were represented as mean ± standard error of mean (SEM). Error bars indicate SEM.

To characterize the effects of LPS-induced neuroinflammation on hippocampal astrocytes, microglia, and amyloid presence, the control group was compared to the three experimental

groups by immunostaining with GFAP, Iba1 antibodies (and CD68 for colabelling) and ThT stain respectively. Analysis of the mean scores, per group revealed non-significant differences between them, although notable differences in fluorescent intensity and quantity of cells was observed between the groups and thus discussed.

6.4.1) Astrocytes

Sections stained with the GFAP antibody emitted a blue fluorescencethat is observable on the microphotographs of **figure 51 (A-D)**.

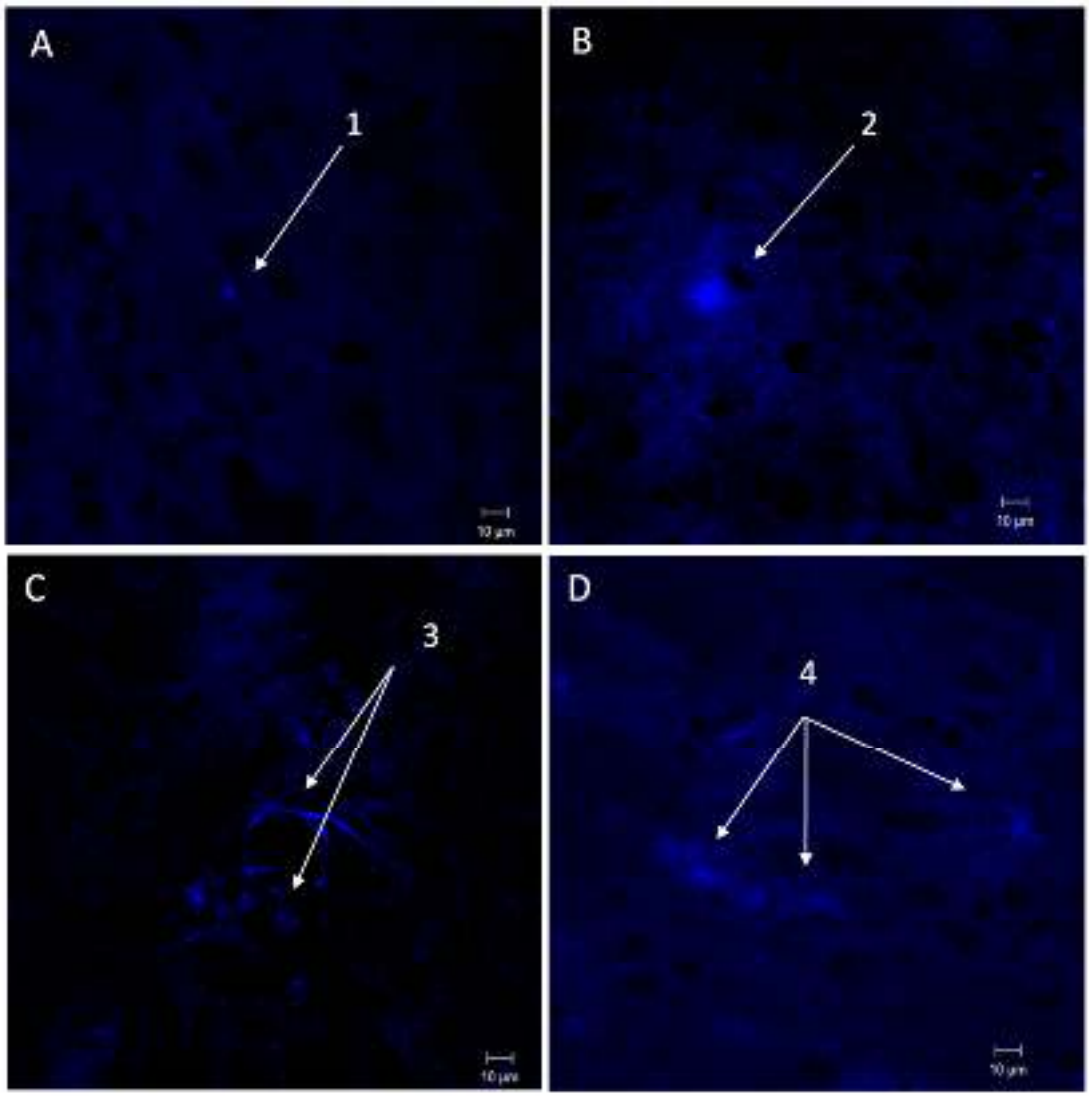

Figure 52 (A-D): Hippocampal microphotographs from the four groups stained with anti-GFAP. Scale bar was set at 10 µm. (A) Microphotograph from the control group. (Label 1) An astrocyte cell emitting slight fluorescence. (B) Microphotograph from the PBS + H group. (Label 2) An astrocyte cell emitting more fluorescence than the control group. (C) Microphotograph from the LPS group. (Label 3)

Astrocytes showing a greater degree of fluorescence and cell quantity than the control group. (D) Microphotograph from the LPS + H group. (Label 4) Astrocytes emitting more fluorescence and cell quantity than the control group.

A summary of the descriptive statistics of the fluorescent intensity observed when the hippocampal tissue was stained with anti-GFAP antibody is shown in **table 37.** Analysis of the CTCF values show that fluorescent intensity was not significantly different between the groups.

Table 37: A summary of the mean CTCF scores and p-values obtained when evaluating the fluorescent intensity of the four groups after immunostaining with anti-GFAP.

Astrocyte Immunostaining			
Group	Mean CTCF	Adjusted p-value	Significant?
PBS	35186	-	-
PBS vs. PBS + H	43382	0.5701	No
PBS vs. LPS	49168	0.2665	No
PBS vs. LPS + H	48426	0.3053	No

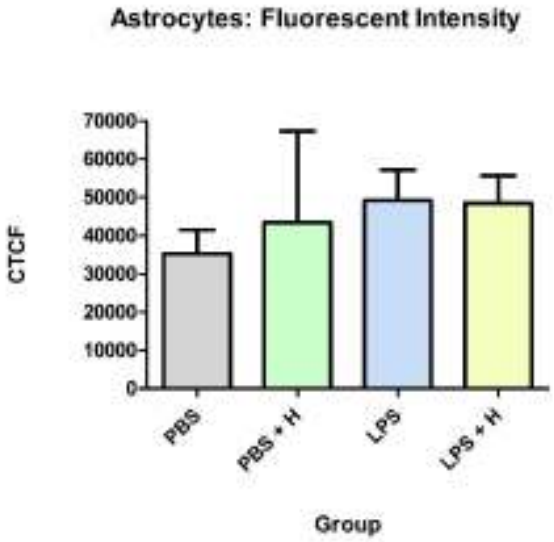

Figure 53: Bar graph plot with mean and standard error of mean (SEM) for the fluorescent intensity of astrocytes (expressed as CTCF score) across all four groups.

6.4.2) Microglia

Sections stained with anti-Iba-1 antibody emitted a red fluorescencethat is observable on the micrographs of **figure 54 (A-D)**. Here, activation was defined as an increase in fluorescent intensity, indicated by the CTCF value, and density of microglia, indicated by cell counts **(table 41).** Data shows that the fluorescent intensity of the LPS group was significantly higher than the control group. This indicates that low, systemic LPS exposure induced the activation of microglia.

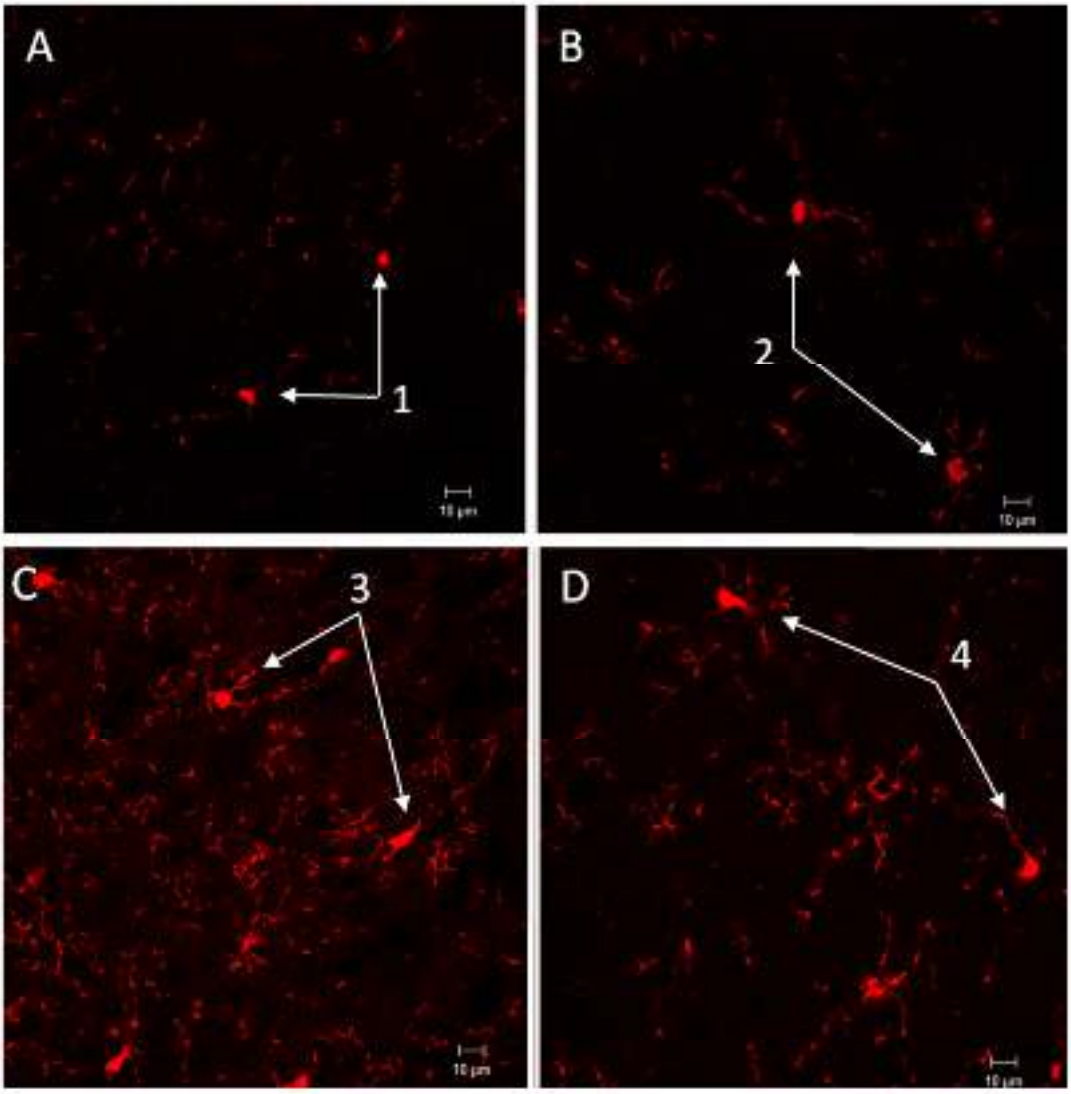

Figure 54 (A-D): Hippocampal microphotographs of the four groups stained with anti-Iba1. Scale bar was set at 10 µm. (A) Micrograph from the control group. (Label 1) Microglia showing slight activation (fluorescence). (B) Microphotograph from the PBS + H group. (Label 2) Microglia showing more activation than the control group. (C) Microphotograph from the LPS group. (Label 3) Microglia showing a significanty higher degree of fluorescence and cell quantity than the control group. (D)

Microphotograph from the LPS + H group. (Label 4) Microglia showing a fair degree of fluorescence and cell quantity than the control group.

Table 38: A summary of the mean CTCF scores and p-values obtained when sections were immunolabeled with anti-Iba-1 evaluating the fluorescent intensity of the four groups.

Microglia Immunostaining			
Group	Mean CTCF	Adjusted p-value	Significant?
PBS	84380	–	-
PBS vs. PBS + H	42923	0,3029	No
PBS vs. LPS	244103	<0.9999	Yes
PBS vs. LPS + H	98180	0,7883	No

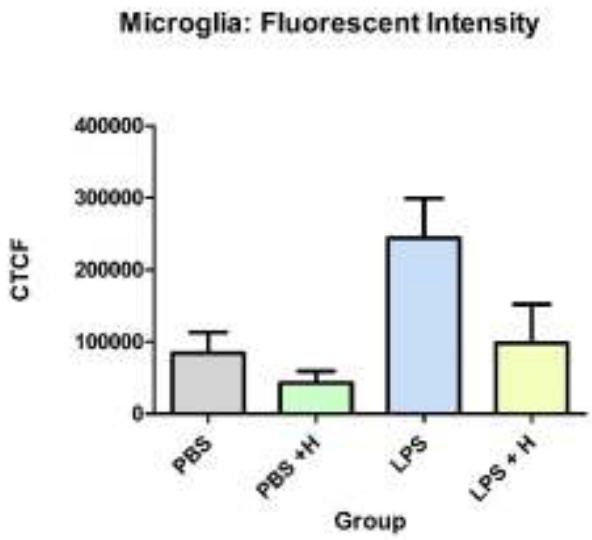

Figure 55: Bar graph plot with mean and standard error of mean (SEM) for the fluorescent intensity of microglia (expressed as CTCF score) across all four groups.

6.4.3) Colocalization - Microglial Activation

Sections co-labelled with Iba1 and CD68 antibody emitted a combination fluorescencethat is observable as a orange on the micrographs of **Figure 56 (A-D)**. Here, microglial activation was defined as the co-localization of Iba-1-positive cells and CD68-positive cells. Data showed that no significant differences in microglial activation was present between the experimental and control groups.

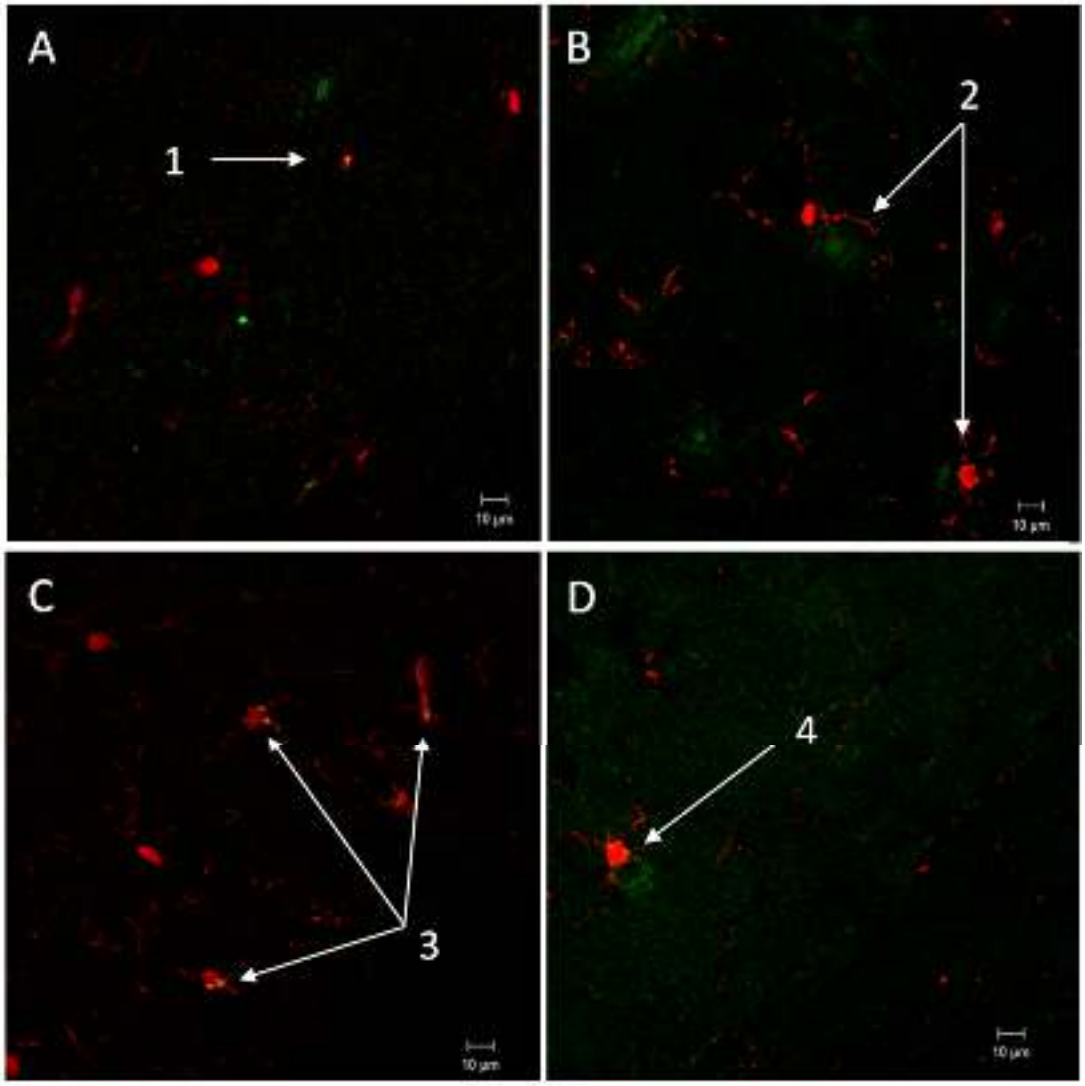

Figure 56 (A-D): Hippocampal micrographs from the four groups co-stained with anti-Iba1 and CD68. Scale bar was set at 10 µm. (I) Micrograph from the control group. (Label 1) Microglia showing minimal activation. (J) Micrograph from the PBS + H group. (Label 2) Microglia in close-proximity to CD68-labelled lysosomes. (K) Micrograph from the LPS group. (Label 3) CD68 positive microglia cells indicating a degree of microglial activation and cell quantity than the control group. (L) Micrograph from the LPS + H group. (Label 4) A CD68 positive microglia cell indicating a degree of microglial activation than the control group.

A comparison of the mean CTCF values, presented in **table 39**, show that the fluorescent intensity of Iba-1 and CD68-positive cells between the groups were not significantly different.

Table 39: A summary of the mean CTCF scores and p-values obtained when evaluating the fluorescent intensity of the four groups after co-staining with anti-Iba1 and CD68.

Co-localization immunostaining			
Group	Mean CTCF	Adjusted p-value	Significant?
PBS	8832	-	-
PBS vs. PBS + H	10991	0,575	No
PBS vs. LPS	19861	0,666	No
PBS vs. LPS + H	12903	0,610	No

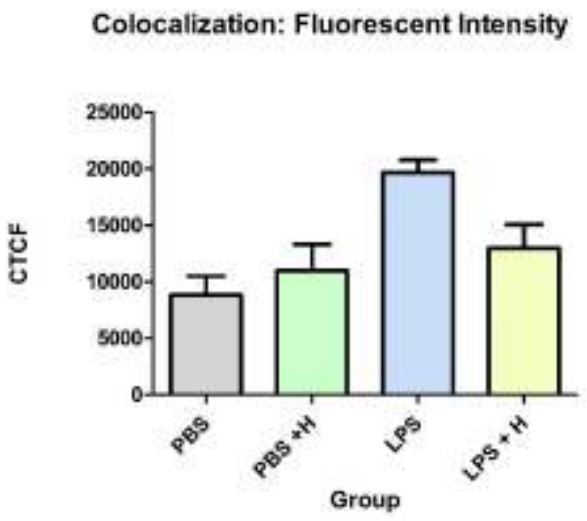

Figure 57: Bar graph plot with mean and standard error of mean (SEM) for the fluorescent intensity of activated microglia (expressed as CTCF score) across all four groups.

6.4.4) Thioflavin T

Sections stained with ThT stain emitted a green fluorescenceobservable on the representative Micrographs of **Figure 58 (A-D)**. Here, amyloid progression was determined by the comparing the CTCF values of the experimental groups to the control group.

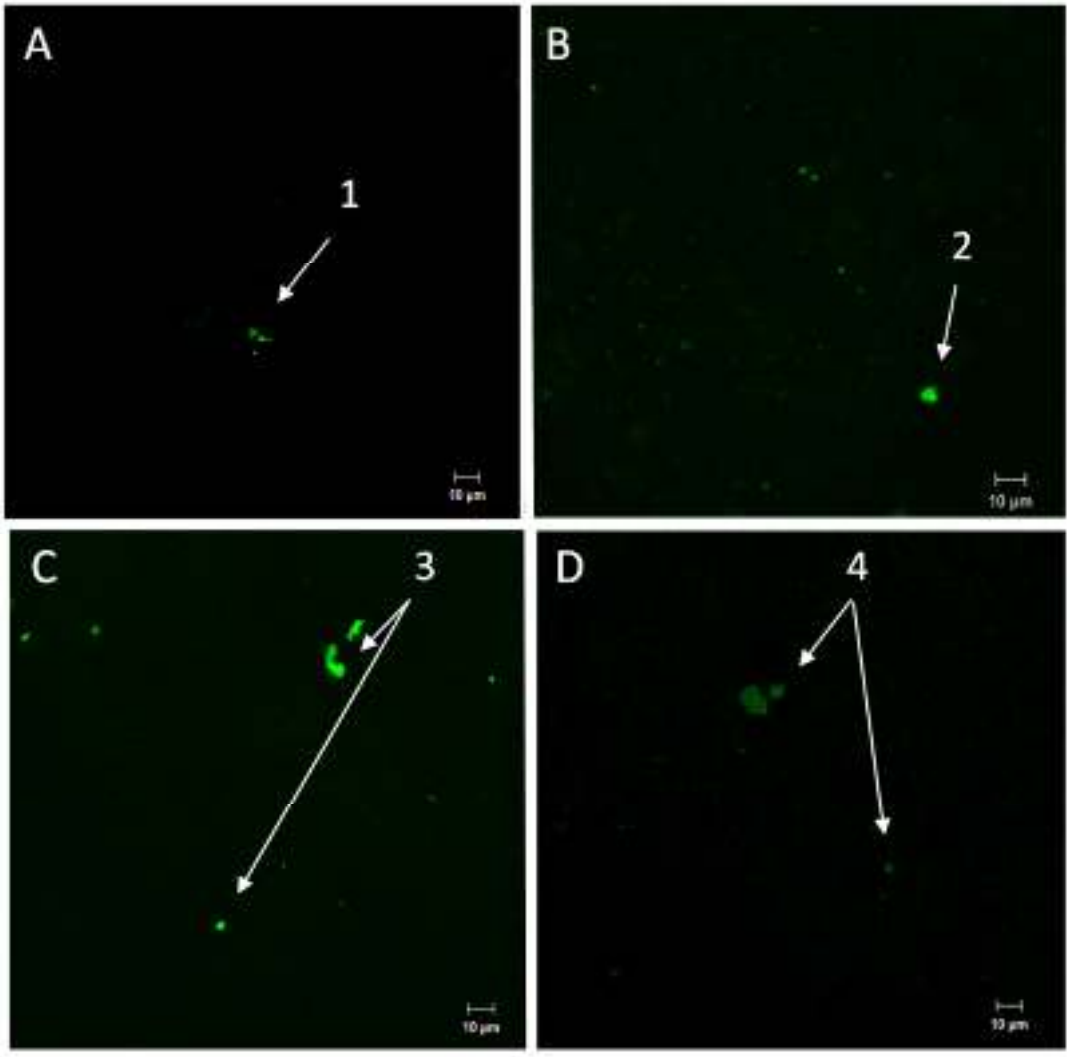

Figure 58 (A-D): Hippocampal Micrographs of the four groups stained with ThT. Scale bar was set at 10 µm. (M) Micrograph from the control group. (Label 1) Aβ fibrils staining positive with ThT. (N) Microphotograph from the PBS + H group. (Label 2) An amyloid fibril showing more fluorscent intensity than the control group. (O) Micrograph from the LPS group. (Label 3) Aβ fibrils appear to be increased than the control group. (P) Micrograph from the LPS + H group. (Label 4) Aβ fibrils showing less fluorescence and cell quantity than the LPS group.

A comparison of the mean CTCF values, presented in **table 40**, show that the fluorescent intensity of ThT-positive cells between the groups was not significantly different.

Table 40: A summary of the mean CTCF scores and p-values obtained when evaluating the fluorescent intensity of the four groups after immunostaining with ThT.

Thioflavin T Immunostaining			
Group	Mean CTCF	Adjusted p-value	Significant?
PBS	1093	-	-
PBS vs. PBS + H	2059	0,408	No
PBS vs. LPS	4253	0,301	No
PBS vs. LPS + H	3384	0,386	No

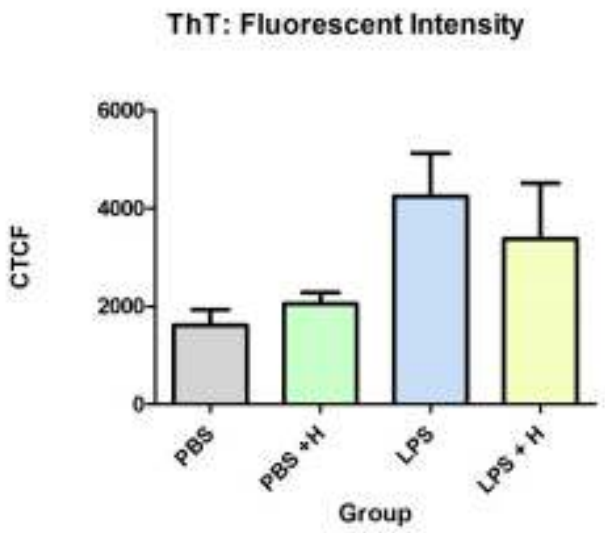

Figure 59: Bar graph plot with mean and standard error of mean (SEM) for the fluorescent intensity of amyloid fibrils (expressed as CTCF score) across all four groups. No significant differences were detected for the fluorescence intensities between the groups.

6.4.5) Cell counts

The dataset in **table 41** was analyzed using one-way ANOVA. Post-hoc checks with Dunnett's multiple comparisons test were used to compare the three experimental groups to the control group. The p-value was set at $p < 0.05$, with a 95% confidence interval.

Table 41: A summary of the number of cells observed in the micrographs for each IF analysis performed. Significant differences in the number of cells observed between the PBS control group and LPS group apply both astrocytes and microglia.

Antibody/Dye	p-value	Significant? (yes/no)
GFAP	0.0207	yes
Iba-1	0.0041	yes
Iba-1 and CD68 (co-localization)	0.6038	no
ThT	0.1342	no

6.5 Discussion

There is a rising interest in the study of neuroinflammation and the role in neuropathology, therefore, the use for reliable biomarkers of inflammation are important for diagnosis. Moreover, inflammatory biomarkers were found in the rat brain even two years after exposure to AD-inducing pathogens.[283] In this study, popular biomarkers of inflammation were used to identify the impact of systemic LPS on the profile of neuroglial cells implicated in AD pathology.

6.5.1) Astrocytes

Collectively, the findings reveal no statistical significance in the differences between the control and experimental groups, and thus no conclusive association between LPS-induced systemic neuroinflammation and astrocyte activity. However, when comparing just the mean fluorescence (CTCF score) of each group, notable differences were seen.

Taken as a whole, results in **table 37** show that there were no differences in fluorescent intensity, thus astrocyte activation, between the groups. Although speculative, it suggests that LPS exposure did not have a major effect on the activity of astrocytes. Furthermore, the groups treated with honey did not show decreased astrocyte activation, as anticipated.

These findings are contradictory to previous research which suggest that honey is an effective neuroprotective agent against the effects of LPS-induced neuroinflammation. It is known that honey contains phenol and hydrogen peroxide elements which inhibit the spread of infectious agents[217,284], like LPS, that can cause a leaky gut, spread into circulation and the CNS where it triggers neuroinflammation.[285] Secondly, Ali and colleagus examined the *in vitro* effects of honey on the viability of astrocytes exposed to oxidative stress and found that honey at 1% (v/v) concentration inhibits apoptosis.[286]

On the hand, our findings are supported Mohr, K whose investigation into the discrepancy of GFAP as a glial marker showed that there is a discrepancy between species and experimental models that limit the use of GFAP as a marker for neuroglial cell activation.[287] This provides insight to the non-significant differences observed in fluorescence (activation) expressed by the groups.

6.5.2) Microglia

Findings from **table 38** reveal a statistical significance in the differences between the control group and LPS group ($p<0.0001$). The LPS group (mean= 244103, $p<0.0001$) displayed a considerable degee of fluorescent intensity which suggests that LPS-induced systemic neuroinflammation facilitates microglial activation.[288] The activation of microglia facilitates restoration and homeostasis in the neuron microenvironment.[289] Since microglia are known to play a vital function of degrading apoptotic cells and aggregated proteins [290], in addition to multiplying in number and reactivity within close proximity to Aβ plaques[291], the outcomes observed were expected. Microglia are one of the first cells to be activated during neuroinflmammation[289], which further validates the signifant fluorescent differences observed between the control and LPS group. Activated microglia show varied interactions with Aβ proteins and neuronal pathways, which result in wide-ranging effects on the progression of AD, based on the stage of disease and individual vulnerability.[292] The mechanisms linking systemic inflammation and microglial activation remain unclear however, age is a key factor regulating the degree of microglial activation following systemic inflammation.[293] These findings are consistent with reports by Norden and colleagues who observed an increase in Iba-1 immunoreactivity 24 hours after LPS exposure.[294] Interestingly, they also found that repeated LPS exposure was linked to immune and behavioural tolerance, and a minimized inflammatory microglial profile opposed to observations of acute LPS exposure.

Furthermore, the fluorescent intensity observed in LPS + H group (mean=98160, $p=0.7683$) was not significantly different from the intensity observed in both the control and LPS group. This is contradicted with findings by Candiracci, M *et al*. (2012) who report that 0.5 µg/mL and 1µg/mL honey flavonoid extract sourced from unprocessed multifloral honey strongly hinders the secretion of proinflammatory cytokines and reduces the quantity of degenerated neuronal cells in the hippocampus.[295] Our findings differ from previous research possibly due to the origin of honey used and the short exposure time, which might have been insufficient to influence microglial activation.

6.5.3) Colocalization - Microglial Actvitation

It is known that CD68 levels are higher in reactive microglia and extensively reduced in resting microglia[296]. The results indicate that there were no significant differences between the control group and experimental groups. Although **figure 55 (C)** illustrates an increased number of Iba1-positive microglial cells as well as activated (Iba1 and CD68 positive)

microglia when compared to the control group **figure 55 (A)**, in addition to the statistical differences between the PBS group (mean=8832) and LPS group (mean=19661, p=0.698), conclusive associations cannot be derived. The Iba and CD68 antibodies are commonly used as microglial markers, however, due to heterogeneity in gene regulation, they may recognize different activation stages of microglia.[297] This may possibly explain the low amount of activated microglia (Iba1 and CD68 positive) seen in **figure 55 (C)** in comparison the amount of microglia observed in **figure 54 (C).**

6.5.4) Thioflavin T

The aggregation of soluble Aβ proteins influences AD progression, which may result in synaptic aberration and subsequent neurodegeneration.[290] On the other hand, astrocytes may, in principle, contribute to Aβ production since they increase β-secretase and APP in pathology states, however, this has not been validated.[298] To quantitatively examine fibril Aβ deposition in the hippocampal region, ThT stain was used as an Aβ biomarker for which fluorescent intensity was determined and used to compare between the four groups. Changes in intensity levels were used as a marker of fibril synthesis or degradation, where a decline was attributed to the reduction of fibril synthesis caused by the neuroprotective effects of honey.

Results showed that there was noticeable green fluorescencein the hippocampal area of all four groups **figure 57 (A-D)**. The synthesis and deposition of Aβ peptides occurs in healthy brains without causing cognitive decline.[299,300] This may provide insight for the presence of Aβ proteins observed in the control group **(figure 57 A)**.

Emergence to AD then, is regulated by the synthesis and degradation of Aβ proteins and how well they are eliminted from the brain.[300] The results in **table 40,** though not significant, reveal that 10 days after s.c injection of LPS, Aβ deposition was the highest in the LPS group (mean=4253, p=0.301). This observation suggests that the period of exposure to LPS or the concentration of LPS administered was enough to impact amyloid formation or deposition in the hippocampus.

The results in **table 40** suggest that honey treatment did not have a mopping effect on amyloid formation. This is inconsistent with findings by Wan and colleagues which report that honey significantly reduces LPS-induced neuronal loss and presents anti-inflammatory potential against oxidative stress and Aβ protein deposition.[301]

6.6 Conclusion

Research has validated the importance of glial cells in neuroinflammation and neurodegeneration.[301] Compounding data present strong evidence that astrocytes actively facilitate the pathogenesis of AD.[302] Additionlly, microglia have become the focal point amongst researchers as the cells have been implicated in neurodegeneration. This is attributed to the fact that microglia have the ability to upregulate neuroinflammation, causing subsequent neuronal death.[303] Lastly, foregoing literature highlights the role, significance and pathogenesis of amyloid proteins in AD. Taken as a whole, it is imperative to examine the activity of the glial cells in neuroinflammation models *in vivo.*

Sufficient evidence has been collected in this chapter to deduce that 0.1 M LPS systemically administered at a 0.1 mg/ml concentration and a volume of 0.1 ml/kg for a period of 10 days does not cause significant astrogliosis, microgliosis and amyloid deposition in Sprague Dawley rats.

Literature may be used to explain the lack of significant differences in these observations. Firstly, there exists inter- and intra-regional differences between astrocyte populations, which translates into heterogenous functional features.[302] Secondly, though GFAP has been regarded a reliable biomarker for astrocytes, not all astrocytes positively bind to GFAP.[302] Finally, astrocytes can provide neuroprotective effects at various stages of AD.[302] Both activated astrocytes and microglia, when exposed to Aβ proteins, release transforming growth factor (TGF-β) which functions to protect neuronal cells from amyloid toxicity and stimulate the removal of Aβ.[302] Altogether, this implies that the activated astrocytes came to a peak level and undertook an adaptive state.

Numerous lines of evidence suggest that microglia are instrumental in AD progression.[304] The findings presented in this study reveal that LPS-induced neuroinflammation significantly stimulates microglial activation in LPS rodent populations. However, depending on the stage of disease, activated microglia operate in both beneficial and deleterious ways.[304] Therefore, the degree of activation and, thus, their influence on pathogenesis may be contingent on the type and duration of injury, in addition to the CNS area under examination.[305,306,307] Also, while Iba1 antibody is commonly used to identify microglia, it does not specify microglial polarization since both pro- and anti-inflammatory microglia express Iba1.[304]

The ThT stain was used to assess fibril amyloid deposition, however, ThT also has several intrinsic disadvantages including poor BBB penetration and short emission wavelength.[308] Notably, it has been shown that distinct fibril structural configurations, derived from the same protein, can exhibit varying ThT fluorescent intensities.[309,310,311] Furthermore, the signal intensity can be regulated by a other agents present in solution, through fluorescence quenching or molecular interactions.[312,313] Additionally, the binding of ThT is not restricted to Aβ fibrils but it extends to certain resident proteins.[314] Lastly, fibrils are capable of binding to ThT through various binding modes with varying affinities.[315]

Chapter 7: Integrated discussion and conclusion

Substantial research is currently underway to find a cure for AD globally. Many remarkable advances have been successful in this effort, and it is probable that available treatments will soon shift from symptomatic to curative, thus decreasing the rate of progression towards AD and improving the quality of life in elderly populations. What seems to be lacking in this global undertaking is the comprehensive understanding of the biological pathways and molecular mediators contributing to the aetiology of AD.

The aim of this study was to investigate a concept that has been gaining recognition in neurodegenerative conditions, namely the influence of LPS-induced neuroinflammation on AD-like symptoms in the hippocampal region. These are symptoms resulting in damaged cortical structures, functions, and subsequent cognitive decline. Consequently, it is important to elucidate the role of bacterial agents natural to the GIT, specifically LPS, in inflammation because the chronic release of such agents has been implicated in BBB damage and AD development. In this study, it was noted that systemically distributed 0.1 M LPS does not induce pathological neuroinflammation in the hippocampus. Observations from the assays (behavioural and biochemical) conducted in this study suggest that neuroinflammation did occur in subjects that received LPS, however, examination of the findings imply that this reaction was neuro-protective rather than disease-causing. As discussed in foregoing literature, acute inflammation is beneficial to the immune system since it initiates mechanisms involved in neuro-immune conditioning and cellular repair.[77]

The results obtained from the various behavioural assessments (y-maze, NOR, and open-field test) show that cognitive abilities were not severely affected by LPS. Although analysis of results from the y-maze experiment indicate that the PBS + H group maintained high speeds while exploring the novel arm, it appears that honey may have a role in spatial and working memory. Albeit not conclusive, it is supported by Gasparrini's investigations into the protective impact of Manuka honey on LPS-treated macrophages that show that honey inhibits LPS-induced inflammatory molecules and TLR_4 /NF-kβ signaling.[316] In line with literature, this means that an innate immune response may have been supressed by the Manuka honey since it is known that honey has anti-tumor, anti-oxidant and anti-inflammatory properties.[316,317,318] It is important to note, however, that the composition and physiochemical properties of honey are contingent on its floral source and origin.[319] Factors such as the

phenolic and flavonoid content, peroxidase activity, type of sugars present and pH differs among honey subtypes.[320] This may have posed a limitation on the remedial effects observed in this study. Nonetheless, this presents an opportunity for future studies to evaluate the effects of Tualang honey, Malaysian honey and Nigerian honey on LPS-induced systemic inflammation using both a low and high dose of LPS. Then, assess the anti-inflammatory effects of Manuka honey.

It is evident that a diverse array of variables influence behavioural and physiological performance.[321] These limiting factors can be broadly categorized into empirical, animal and experimental factors.[321] Some empirical factors that may have influenced observations of this study include: the sequence which the assays were performed, measures of health at the beginning of the study, environmental factors that influence innate behaviour, method for measuring performance. It is recommended that the sequence of the assays proceed from the least stressful to the most stressful. In this study, the Y-maze test was performed first, followed by the NOR task and open-field test, respectively. Since the open-field test is the most facile assay of all three, it should have been conducted first, followed by the NOR task and finally, the Y-maze analysis.[321] Also, starting with measures of health eliminates the possibility of health confounds effecting physical performance. Moreover, animal factors such as sex, age and vendor source play a role in behavioural performance.[321] The population of subjects used in this study comprised 10-week old, male Sprague-Dawley rats sourced from one vendor. Considering that AD is prevalent among older human populations, rodents of an older age may have presented results similar to what is seen in humans. Also, investigating the effects of LPS-induced neuroinflammation in both sexes may provide insight to the role of gender in neuroinflammation. Lastly, since there are variations in the methods for measuring and evulating performance, data from this study may be subject to differences in interpretation of previous studies.

To assess the progression of amyloid deposition, the quantity of soluble $A\beta_{42}$ was measured by sandwich ELISA. The negative results observed from this assay may be linked to the lack of specificity of the type of amyloid peptide detected. Since Aβ peptides are naturally present and harmless in the brain, and the progression to plaque deposition and AD rises from the aggregation of peptides into fibrils then plaques; the assay used was unable to distinguish the structure of $A\beta_{42}$, thus toxicity, detected. The results show that in totality, the quantity of $A\beta_{42}$ in the hippocampus was not affected by LPS-induced neuroinflammation. However, this

does not reveal whether the ratio of Aβ peptides, fibrils and plaques differed between the three experimental groups. This is an important variable because the presence of Aβ plaques has profound effects on pathology than the presence of Aβ peptides. Techniques such as western blot, in conjunction with ELISA, may be used to qualitatively determine Aβ deposition and verify results from ELISA. Alternatively, more sophisticated techniques such as magnetic resonance spectroscopy can be used to detect Aβ plaques, however, this was not feasible in this study. [322] This is because the quantification of Aβ using ELISA is mostly used in transgenic rodent models, so not much data is available to support results obtained from wild-type rodents.[259] Therefore, it is imperative to examine the effects of LPS-induced neuroinflammation on glial cells that are directly implicated in AD pathology namely astrocytes and microglia.

According to the conventional hypothesis, astrocytes and microglia are major contributors to neuropathologies. These macrophage-like cells are involved in brain homeostatic activities involving neurogenesis, BBB intrigrity, neurotransmitters and synapse growth.[323] Apart from homeostasis, microglia and astrocytes contribute to inflammation by assuming the role of CNS-resident immune cells.[324] Pathogens like LPS trigger the activation of these cells, and the phenotype (repair or intensify damage) adopted by the cells thereof is regulated by the nature and severity of damage, presence of anatagonistic mediators and activation status of other macrophages.[324]

Results from this present study revealed a significant difference in the quantity of activated microglia in the LPS group than the control group, who showed normal levels of microglia. It has been alluded that activated microglia recruit astrocytes, which then exacerbate the brain's inflammatory response to amyloid proteins resulting in cytokine-mediated inflammation.[324] Consistent with this present study, the concentration of microglia increased significantly compared to astrocytes, which are the most prevalent in the brain.[118] This suggests that microglia respond to LPS injury within a shorter period of time than astrocytes. Also, the considerable increase in microglial cells compared to astrocyte cells in the LPS groups, suggest that an Aβ plaque formation did not occur, because astrocytes show a tendency to co-localize with Aβ plaques.[118] In view of this, we can further deduce that in this study, the integrity of BBB was not severely compromised by systemic LPS, as indicated by a non-significant difference in $A\beta_{42}$ concentration observed in the ELISA. The significant increase of microglia in the LPS groups was expected. This is because a mere single injection

of LPS is known to increase microglial density in Sprague Dawley rats.[263] Also, seeing that only microglia greatly increased in quantity, it is plausible that the inflammatory response triggered, was a physiological reaction, aimed at brain repair and homeostasis.[263] However, the categorization of the immune response observed requires the analysis of pro- and anti-inflammatory mediators. To overcome this limitation, it is advisable to combine the assays of this study with assays like ELISA to confirm the presence and quantity of inflammatory mediators produced by the activated microglial cells like IL1-α, TNFα and complement component 1q (C1q), all of which are capable of inducing reactive astrogliosis themself.[325]

In conclusion, it is suggested that a low dose of systemic LPS may induce neuroprotective molecular interactions that increase the density of microglia in the hippocampus, without significantly influencing astrocytes or the formation of amyloid proteins. Furthermore, honey may be an effective mopping agent that suppresses these molecular interactions, preventing cognitive deterioration and weakened physical abilities.

Bibliography

1. Gale SA, Acar D, Daffner KR. Dementia. The American Journal of Medicine. 2018 Oct 1;131(10):1161–9.

2. World Health Organization [Online] (available at https://www.who.int/news-room/fact-sheets/detail/dementia) [Internet]. 2019. Available from: https://www.who.int/news-room/fact-sheets/detail/dementia

3. Alzheimer's Association. Stages of Alzheimer's Disease. Alzheimer's Association. 2018. p. 1–3.

4. Maass A, Berron D, Harrison TM, Adams JN, La Joie R, Baker S, et al. Alzheimer's pathology targets distinct memory networks in the ageing brain. Brain : a journal of neurology. 2019;142(8):2492–509.

5. Wimo A, Guerchet M, Ali GC, Wu YT, Prina AM, Winblad B, et al. The worldwide costs of dementia 2015 and comparisons with 2010. Alzheimer's and Dementia. 2017;13(1):1–7.

6. Alzheimer's SA NPC [Internet]. [cited 2019 Dec 17]. Available from: https://alzheimers.org.za/prevalence-of-dementia/

7. Potocnik FC V. Dementia. South African Journal of Psychiatry. 2013 Aug 30;19(3).

8. Vanderheyden WM, Lim MM, Musiek ES, Gerstner JR. Alzheimer's Disease and Sleep–Wake Disturbances: Amyloid, Astrocytes, and Animal Models. The Journal of Neuroscience. 2018;38(12):2901–10.

9. Floden AM, Darland DC, Karki S, Combs CK, Kulas JA, Rojanathammanee L, et al. APP Regulates Microglial Phenotype in a Mouse Model of Alzheimer's Disease. Journal of Neuroscience. 2016;36(32):8471–86.

10. Pignataro A, Middei S. Trans-Synaptic Spread of Amyloid-β in Alzheimer's Disease: Paths to β-Amyloidosis. Vol. 2017, Neural Plasticity. 2017.

11. Sengupta U, Nilson AN, Kayed R. The Role of Amyloid-β Oligomers in Toxicity, Propagation, and Immunotherapy. EBioMedicine. 2016;6:42–9.

12. Chen GF, Xu TH, Yan Y, Zhou YR, Jiang Y, Melcher K, et al. Amyloid beta: Structure, biology and structure-based therapeutic development. Vol. 38, Acta Pharmacologica Sinica. 2017. p. 1205–35.

13. Bayer TA, Wirths O. Intracellular accumulation of amyloid-beta - A predictor for synaptic dysfunction and neuron loss in Alzheimer's disease. Frontiers in Aging Neuroscience. 2010;2(MAR):1–10.

14. Walsh DM, Selkoe DJ. Aβ Oligomers – a decade of discovery. Journal of Neurochemistry. 2007 Jun 1;101(5):1172–84.

15. Ono K, Takahashi R, Ikeda T, Yamada M. Cross-seeding effects of amyloid β-protein and α-synuclein. Journal of Neurochemistry. 2012 Sep 1;122(5):883–90.

16. Hasegawa K, Yamaguchi I, Omata S, Gejyo F, Naiki H. Interaction between Aβ(1−42) and Aβ(1−40) in Alzheimer's β-Amyloid Fibril Formation in Vitro. Biochemistry. 1999 Nov 1;38(47):15514–21.

17. Jan A, Gokce O, Luthi-Carter R, Lashuel HA. The ratio of monomeric to aggregated forms of Abeta40 and Abeta42 is an important determinant of amyloid-beta aggregation, fibrillogenesis, and toxicity. The Journal of biological chemistry. 2008/08/11. 2008 Oct 17;283(42):28176–89.

18. Jarrett JT, Berger EP, Lansbury PT. The carboxy terminus of the .beta. amyloid protein is critical for the seeding of amyloid formation: Implications for the pathogenesis of Alzheimer's disease. Biochemistry. 1993 May 11;32(18):4693–7.

19. Baldassarre M, Baronio CM, Morozova-Roche LA, Barth A. Amyloid β-peptides 1-40 and 1-42 form oligomers with mixed β-sheets. Chemical Science. 2017;8(12):8247–54.

20. Yan Y, Wang C. Abeta40 protects non-toxic Abeta42 monomer from aggregation. Journal of molecular biology. 2007 Jun;369(4):909—916.

21. Pauwels K, Williams TL, Morris KL, Jonckheere W, Vandersteen A, Kelly G, et al. Structural basis for increased toxicity of pathological aβ42:aβ40 ratios in Alzheimer disease. The Journal of biological chemistry. 2011/12/08. 2012 Feb 17;287(8):5650–60.

22. Hamley IW. The Amyloid Beta Peptide: A Chemist's Perspective. Role in Alzheimer's and Fibrillization. Chemical Reviews. 2012 Oct 10;112(10):5147–92.

23. Gharibyan AL, Zamotin V, Yanamandra K, Moskaleva OS, Margulis BA, Kostanyan IA, et al. Lysozyme Amyloid Oligomers and Fibrils Induce Cellular Death via Different Apoptotic/Necrotic Pathways. Journal of Molecular Biology. 2007;365(5):1337–49.

24. Lee C-C, Sun Y, Huang HW. How type II diabetes-related islet amyloid polypeptide damages lipid bilayers. Biophysical journal. 2012 Mar 7;102(5):1059–68.

25. Bamberger ME, Harris ME, McDonald DR, Husemann J, Landreth GE. A cell surface receptor complex for fibrillar beta-amyloid mediates microglial activation. The Journal of neuroscience : the official journal of the Society for Neuroscience. 2003;23(7):2665–74.

26. Butterfield DA, Drake J, Pocernich C, Castegna A. Evidence of oxidative damage in Alzheimer's disease brain: central role for amyloid β-peptide. Trends in Molecular Medicine. 2001 Dec 1;7(12):548–54.

27. Hiltunen M, Natunen T, Kemppainen S, Marttinen M, Tanila H, Haapasalo A, et al. Molecular Mechanisms of Synaptotoxicity and Neuroinflammation in Alzheimer's Disease. Frontiers in Neuroscience. 2018;12(December):1–9.

28. AVILA J. Role of Tau Protein in Both Physiological and Pathological Conditions. Physiological Reviews. 2004;84(2):361–84.

29. Goedert M, Spillantini MG, Jakes R, Rutherford D, Crowther RA. Multiple isoforms of human microtubule-associated protein tau: sequences and localization in neurofibrillary tangles of Alzheimer's disease. Neuron. 1989 Oct 1;3(4):519–26.

30. Zhang Y, Tian Q, Zhang Q, Zhou X, Liu S, Wang J-Z. Hyperphosphorylation of microtubule-associated tau protein plays dual role in neurodegeneration and neuroprotection. Pathophysiology. 2009 Oct 1;16(4):311–6.

31. Pîrşcoveanu DFV, Pirici I, Tudorică V, Bălşeanu TA, Albu VC, Bondari S, et al. Tau protein in neurodegenerative diseases – a review. Vol. 58, Romanian Journal of Morphology and Embryology. 2017. p. 1141–50.

32. Grundke-Iqbal I, Iqbal K, Tung YC, Quinlan M, Wisniewski HM, Binder LI. Abnormal phosphorylation of the microtubule-associated protein tau (tau) in Alzheimer cytoskeletal pathology. Proceedings of the National Academy of Sciences of the United States of America. 1986 Jul;83(13):4913–7.

33. Gendron TF, Petrucelli L. The role of tau in neurodegeneration. Molecular neurodegeneration. 2009 Mar 11;4:13.

34. Iqbal C-XG and K. Hyperphosphorylation of Microtubule-Associated Protein Tau: A Promising Therapeutic Target for Alzheimer Disease. Vol. 15, Current Medicinal Chemistry. 2008. p. 2321–8.

35. Avila J. Our Working Point of View of Tau Protein. Journal of Alzheimer's Disease. 2018;62(3):1277–85.

36. Hernández-Zimbrón LF, Díaz-Hung M-L, Pérez-Garmendia R, Gevorkian G, Quiroz-Mercado H, Gorostieta-Salas E. Beta Amyloid Peptides: Extracellular and Intracellular Mechanisms of Clearance in Alzheimer's Disease. Update on Dementia. 2016;(September).

37. Braak H, Braak E. Braak H, Braak E. Neuropathological staging of Alzheimer-related changes. Acta Neuropathol (Berl) 82: 239-259. Vol. 82, Acta neuropathologica. 1991. 239–259 p.

38. Smith AD. Imaging the progression of Alzheimer pathology through the brain. Proceedings of the National Academy of Sciences of the United States of America. 2002 Apr 2;99(7):4135–7.

39. Bature F, Guinn BA, Pang D, Pappas Y. Signs and symptoms preceding the diagnosis of Alzheimer's disease: A systematic scoping review of literature from 1937 to 2016. BMJ Open. 2017;7(8).

40. Thies B, Trojanowski JQ, Vinters H V, Montine TJ. National Institute on Aging-Alzheimer's Association guidelines for the. 2013;8(1):1–13.

41. Vinters H V, Hyman BT. Digest on data on persons with disabilities. 2013;123(1):1–11.

42. Hurtz S, Chow N, Watson AE, Somme JH, Goukasian N, Hwang KS, et al. Automated

and manual hippocampal segmentation techniques: Comparison of results, reproducibility and clinical applicability. NeuroImage: Clinical. 2019;21:101574.

43. Wu JW, Hussaini SA, Bastille IM, Rodriguez GA, Mrejeru A, Rilett K, et al. Neuronal activity enhances tau propagation and tau pathology in vivo. Nature neuroscience. 2016;19(8):1085.

44. Kaufman SK, Del Tredici K, Thomas TL, Braak H, Diamond MI. Tau seeding activity begins in the transentorhinal/entorhinal regions and anticipates phospho-tau pathology in Alzheimer's disease and PART. Acta neuropathologica. 2018;136(1):57–67.

45. Adams JN, Maass A, Harrison TM, Baker SL, Jagust WJ. Cortical tau deposition follows patterns of entorhinal functional connectivity in aging. eLife. 2019 Sep 2;8:e49132.

46. Squire LR, Stark CEL, Clark RE. The medial temporal lobe. Annual review of neuroscience. 2004 Jun 24;27(1):279–306.

47. Kordower JH, Chu Y, Stebbins GT, DeKosky ST, Cochran EJ, Bennett D, et al. Loss and atrophy of layer II entorhinal cortex neurons in elderly people with mild cognitive impairment. Annals of Neurology. 2001 Feb 1;49(2):202–13.

48. Wood R; Chan D. The hippocampus, spatial memory and Alzheimer's disease. Advances in clinical neuroscience and rehabilitation. 2015;15(2):5–7.

49. Gosche KM, Mortimer JA, Smith CD, Markesbery WR, Snowdon DA. Hippocampal volume as an index of Alzheimer neuropathology: findings from the Nun Study. Neurology. 2002;58(10):1476–82.

50. Mortimer JA, Gosche KM, Riley KP, Markesbery WR, Snowdon DA. Delayed recall, hippocampal volume and Alzheimer neuropathology: findings from the Nun Study. Neurology. 2004;62(3):428–32.

51. Morrison JH, Hof PR. Life and Death of Neurons in the Aging Brain. Science. 1997 Oct 17;278(5337):412–9.

52. Morra JH, Tu Z, Apostolova LG, Green AE, Avedissian C, Madsen SK, et al. Automated 3D mapping of hippocampal atrophy and its clinical correlates in 400 subjects with Alzheimer's disease, mild cognitive impairment, and elderly controls. Human brain

mapping. 2009 Sep;30(9):2766–88.

53. Cui R, Liu M. Hippocampus analysis based on 3D CNN for Alzheimer's disease diagnosis. In: Procspie. 2018. p. 108065O. (Society of Photo-Optical Instrumentation Engineers (SPIE) Conference Series; vol. 10806).

54. Gilbert PE, Brushfield AM. The role of the CA3 hippocampal subregion in spatial memory: a process oriented behavioral assessment. Progress in neuro-psychopharmacology & biological psychiatry. 2009/04/16. 2009 Aug 1;33(5):774–81.

55. Anand KS, Dhikav V. Hippocampus in health and disease: An overview. Annals of Indian Academy of Neurology. 2012;15(4):239–46.

56. Bonfanti L, Peretto P. Adult neurogenesis in mammals – a theme with many variations. European Journal of Neuroscience. 2011 Sep 1;34(6):930–50.

57. Stella F, Cerasti E, Si B, Jezek K, Treves A. Self-organization of multiple spatial and context memories in the hippocampus. Neuroscience & Biobehavioral Reviews. 2012;36(7):1609–25.

58. Toyoda H, Li X-Y, Wu L-J, Zhao M-G, Descalzi G, Chen T, et al. Interplay of Amygdala and Cingulate Plasticity in Emotional Fear. Neural Plasticity. 2011/09/07. 2011;2011:1–9.

59. Harricharan R, Thaver V, Russell VA, Daniels WMU. Tat-induced histopathological alterations mediate hippocampus-associated behavioural impairments in rats. Behavioral and Brain Functions. 2015;11(1):1–11.

60. Braak H, Braak E. Neuropathological stageing of Alzheimer-related changes. Acta neuropathologica. 1991;82(4):239–59.

61. Braak H, Braak E, Bohl J. Staging of Alzheimer-related cortical destruction. European neurology. 1993;33(6):403–8.

62. Bobinski M, De Leon MJ, Wegiel J, Desanti S, Convit A, Saint Louis LA, et al. The histological validation of post mortem magnetic resonance imaging-determined hippocampal volume in Alzheimer's disease. Neuroscience. 1999;95(3):721–5.

63. Jack CR, Dickson DW, Parisi JE, Xu YC, Cha RH, O'brien PC, et al. Antemortem MRI findings correlate with hippocampal neuropathology in typical aging and dementia. Neurology. 2002;58(5):750–7.

64. Viswanathan A, Greenberg SM. Cerebral amyloid angiopathy in the elderly. Annals of neurology. 2011 Dec;70(6):871–80.

65. Kinney JW, Bemiller SM, Murtishaw AS, Leisgang AM, Salazar AM, Lamb BT. Inflammation as a central mechanism in Alzheimer's disease. Vol. 4, Alzheimer's and Dementia: Translational Research and Clinical Interventions. Elsevier Inc.; 2018. p. 575–90.

66. Ferreira ST, Clarke JR, Bomfim TR, De Felice FG. Inflammation, defective insulin signaling, and neuronal dysfunction in Alzheimer's disease. Alzheimer's & Dementia. 2014;10(1, Supplement):S76–83.

67. Lull ME, Block ML. Microglial activation and chronic neurodegeneration. Neurotherapeutics. 2010;7(4):354–65.

68. Ferrero-Miliani L, Nielsen O, Skytt Andersen P, Girardin SE. Chronic inflammation: Importance of NOD2 and NALP3 in interleukin-1β generation. Vol. 147, Clinical and experimental immunology. 2007. 227–235 p.

69. Akira S, Uematsu S, Takeuchi O. Pathogen Recognition and Innate Immunity. Cell. 2006 Feb 24;124(4):783–801.

70. Rubartelli A, Lotze MT. Inside, outside, upside down: damage-associated molecular-pattern molecules (DAMPs) and redox. Trends in Immunology. 2007 Oct 1;28(10):429–36.

71. Tang D, Kang R, Coyne CB, Zeh HJ, Lotze MT. PAMPs and DAMPs: signals 0s taht spur autophagy and inmunity. Immunol Rev. 2013;249(1):158–75.

72. Glick D, Barth S, Macleod KF. Autophagy: cellular and molecular mechanisms. The Journal of pathology. 2010 May;221(1):3–12.

73. Takeuchi O, Akira S. Pattern Recognition Receptors and Inflammation. Cell. 2010 Mar 19;140(6):805–20.

74. Nathan C, Ding A. Nonresolving Inflammation. Cell. 2010;140:871–82.

75. Nathan C, Ding A. Nonresolving Inflammation. Vol. 140, Cell. 2010. p. 871–82.

76. DiSabato DJ, Quan N, Godbout JP. Neuroinflammation: the devil is in the details. Journal of Neurochemistry. 2016;139(Suppl 2):136–53.

77. Wee Yong V. Inflammation in Neurological Disorders: A Help or a Hindrance? The Neuroscientist. 2010 Aug 1;16(4):408–20.

78. Akiyama H, Barger S, Barnum S, Bradt B, Bauer J, Cole GM, et al. Inflammation and Alzheimer's disease. Vol. 21, Neurobiology of Aging. 2000. p. 383–421.

79. Wyss-Coray T, Mucke L. Inflammation in neurodegenerative disease - A double-edged sword. Vol. 35, Neuron. 2002. p. 419–32.

80. Netea MG, Balkwill F, Chonchol M, Cominelli F, Donath MY, Giamarellos-Bourboulis EJ, et al. A guiding map for inflammation. Nature Immunology. 2017.

81. Dubový P, Klusáková I, Hradilová Svíženská I. Inflammatory profiling of Schwann cells in contact with growing axons distal to nerve injury. BioMed Research International. 2014/04/27. 2014;2014:691041.

82. Y.S. K, T.H. J. Microglia, major player in the brain inflammation: Their roles in the pathogenesis of Parkinson's disease. Experimental and Molecular Medicine. 2006 Aug 1;38(4):333–47.

83. Najjar S, Pahlajani S, De Sanctis V, Stern JNH, Najjar A, Chong D. Neurovascular Unit Dysfunction and Blood-Brain Barrier Hyperpermeability Contribute to Schizophrenia Neurobiology: A Theoretical Integration of Clinical and Experimental Evidence. Frontiers in psychiatry. 2017 May 23;8:83.

84. Kumar A. Editorial: Neuroinflammation and Cognition. Frontiers in Aging Neuroscience. 2018;10(December):1–3.

85. Sankowski R, Mader S, Valdés-Ferrer SI. Systemic Inflammation and the Brain: Novel Roles of Genetic, Molecular, and Environmental Cues as Drivers of Neurodegeneration . Vol. 9, Frontiers in Cellular Neuroscience . 2015. p. 28.

86. Varatharaj A, Galea I. The blood-brain barrier in systemic inflammation. Brain, Behavior, and Immunity. 2017;60:1–12.

87. Abbott NJ. Astrocyte–endothelial interactions and blood–brain barrier permeability*. Journal of Anatomy. 2002 Jun 1;200(6):629–38.

88. Holmes C, Cunningham C, Zotova E, Woolford J, Dean C, Kerr S, et al. Systemic inflammation and disease progression in Alzheimer disease. Neurology. 2009 Sep 8;73(10):768–74.

89. Weintraub MK, Kranjac D, Eimerbrink MJ, Pearson SJ, Vinson BT, Patel J, et al. Peripheral administration of poly I:C leads to increased hippocampal amyloid-beta and cognitive deficits in a non-transgenic mouse. Behavioural Brain Research. 2014;266:183–7.

90. Erickson MA, Hartvigson PE, Morofuji Y, Owen JB, Butterfield DA, Banks WA. Lipopolysaccharide impairs amyloid β efflux from brain: altered vascular sequestration, cerebrospinal fluid reabsorption, peripheral clearance and transporter function at the blood-brain barrier. Journal of neuroinflammation. 2012 Jun 29;9:150.

91. Roher AE, Kuo Y-M, Esh C, Knebel C, Weiss N, Kalback W, et al. Cortical and leptomeningeal cerebrovascular amyloid and white matter pathology in Alzheimer's disease. Molecular medicine (Cambridge, Mass). 2003;9(3–4):112–22.

92. Erickson MA, Banks WA. Blood-brain barrier dysfunction as a cause and consequence of Alzheimer's disease. Journal of cerebral blood flow and metabolism : official journal of the International Society of Cerebral Blood Flow and Metabolism. 2013/08/07. 2013 Oct;33(10):1500–13.

93. Blair LJ, Frauen HD, Zhang B, Nordhues BA, Bijan S, Lin YC, et al. Tau depletion prevents progressive blood-brain barrier damage in a mouse model of tauopathy. Acta neuropathologica communications. 2015 Jan 31;3:8.

94. Zenaro E, Piacentino G, Constantin G. The blood-brain barrier in Alzheimer's disease. Neurobiology of Disease. 2017;107:41–56.

95. Liu C, Cui G, Zhu M, Kang X, Guo H. Neuroinflammation in Alzheimer's disease:

chemokines produced by astrocytes and chemokine receptors. International journal of clinical and experimental pathology. 2014 Dec 1;7(12):8342–55.

96. Noh H, Jeon J, Seo H. Systemic injection of LPS induces region-specific neuroinflammation and mitochondrial dysfunction in normal mouse brain. Neurochemistry International. 2014;69:35–40.

97. Mason, PhD P, Mason P. Introduction to the Nervous System. In: Rea PBT-CA of the CN, editor. Medical Neurobiology. San Diego: Academic Press; 2013. p. 3–20.

98. Blackburn D, Sargsyan S, Monk PN, Shaw PJ. Astrocyte function and role in motor neuron disease: A future therapeutic target? Glia. 2009 Sep 1;57(12):1251–64.

99. Simons M, Nave KA. Oligodendrocytes: Myelination and axonal support. Cold Spring Harbor Perspectives in Biology. 2016;8(1).

100. Campbell K, Götz M. Radial glia: multi-purpose cells for vertebrate brain development. Trends in Neurosciences. 2002 May 1;25(5):235–8.

101. Ochoa-Cortes F, Turco F, Linan-Rico A, Soghomonyan S, Whitaker E, Wehner S, et al. Enteric Glial Cells: A New Frontier in Neurogastroenterology and Clinical Target for Inflammatory Bowel Diseases. Inflammatory bowel diseases. 2015/12/18. 2016 Feb;22(2):433–49.

102. Wilcock D, Gordon MN, Morgan D, Tan J, Rojiani AM. Dynamic Complexity of the Microglial Activation Response in Transgenic Models of Amyloid Deposition: Implications for Alzheimer Therapeutics. Journal of Neuropathology & Experimental Neurology. 2005 Sep 1;64(9):743–53.

103. Edison P, Donat CK, Sastre M. In vivo Imaging of Glial Activation in Alzheimer's Disease. Frontiers in neurology. 2018 Aug 7;9:625.

104. Akiyama H, Barger S, Barnum S, Bradt B, Bauer J, Cole GM, et al. Inflammation and Alzheimer's disease. Neurobiology of aging. 2000;21(3):383–421.

105. Nayak D, Roth TL, McGavern DB. Microglia Development and Function. Annual Review of Immunology. 2014/01/22. 2014;32(1):367–402.

106. Askew K, Li K, Olmos-Alonso A, Garcia-Moreno F, Liang Y, Richardson P, et al. Coupled Proliferation and Apoptosis Maintain the Rapid Turnover of Microglia in the Adult Brain. Cell reports. 2017 Jan 10;18(2):391–405.

107. Newcombe EA, Camats-Perna J, Silva ML, Valmas N, Huat TJ, Medeiros R. Inflammation: the link between comorbidities, genetics, and Alzheimer's disease. Journal of Neuroinflammation. 2018;15(1):1–26.

108. Pocock JM, Kettenmann H. Neurotransmitter receptors on microglia. Trends in Neurosciences. 2007 Oct 1;30(10):527–35.

109. Lee YB, Nagai A, Kim SU. Cytokines, chemokines, and cytokine receptors in human microglia. Journal of Neuroscience Research. 2002 Jul 1;69(1):94–103.

110. Thameem Dheen S, Kaur C, Ling E-A. Microglial Activation and its Implications in the Brain Diseases. Current Medicinal Chemistry. 2007;14(11):1189–97.

111. Regen F, Hellmann-Regen J, Costantini E, Reale M. Neuroinflammation and Alzheimer's Disease: Implications for Microglial Activation. Current Alzheimer Research. 2017;14(11):1140–8.

112. Hickman SE, Allison EK, El Khoury J. Microglial Dysfunction and Defective -Amyloid Clearance Pathways in Aging Alzheimer's Disease Mice. Journal of Neuroscience. 2008 Aug 13;28(33):8354–60.

113. Zilka N, Kazmerova Z, Jadhav S, Neradil P, Madari A, Obetkova D, et al. Who fans the flames of Alzheimer's disease brains? Misfolded tau on the crossroad of neurodegenerative and inflammatory pathways. Vol. 9, Journal of Neuroinflammation. BioMed Central; 2012. p. 47.

114. Mrak RE. Microglia in Alzheimer brain: A neuropathological perspective. International Journal of Alzheimer's Disease. 2012.

115. Baik SH, Kang S, Son SM, Mook-Jung I. Microglia contributes to plaque growth by cell death due to uptake of amyloid β in the brain of Alzheimer's disease mouse model. Glia. 2016 Dec 1;64(12):2274–90.

116. Haim L Ben, Rowitch D. Functional diversity of astrocytes in. Nature Publishing Group.

2016 Dec 1;18:31.

117. Turner MD, Nedjai B, Hurst T, Pennington DJ. Cytokines and chemokines: At the crossroads of cell signalling and inflammatory disease. Biochimica et Biophysica Acta (BBA) - Molecular Cell Research. 2014;1843(11):2563–82.

118. Sofroniew M V, Vinters H V. Astrocytes: biology and pathology. Acta neuropathologica. 2009/12/10. 2010 Jan;119(1):7–35.

119. Sofroniew M V. Astrogliosis. Cold Spring Harbor Perspectives in Biology. 2015;7(2):a020420–a020420.

120. Iglesias J, Morales L, Barreto GE. Metabolic and Inflammatory Adaptation of Reactive Astrocytes: Role of PPARs. Molecular Neurobiology. 2017;54(4):2518–38.

121. Magistretti PJ, Allaman I. A Cellular Perspective on Brain Energy Metabolism and Functional Imaging. Neuron. 2015 May 20;86(4):883–901.

122. Vasile F, Dossi E, Rouach N. Human astrocytes: structure and functions in the healthy brain. Brain structure & function. 2017/03/09. 2017;222(5):2017–29.

123. Dallérac G, Rouach N. Astrocytes as new targets to improve cognitive functions. Progress in Neurobiology. 2016;144:48–67.

124. Araque A, Carmignoto G, Haydon PG, Oliet SHR, Robitaille R, Volterra A. Gliotransmitters travel in time and space. Neuron. 2014 Feb 19;81(4):728–39.

125. Dossi E, Vasile F, Rouach N. Human astrocytes in the diseased brain. Brain Research Bulletin. 2018;136:139–56.

126. Olabarria M, Noristani HN, Verkhratsky A, Rodríguez JJ. Age-dependent decrease in glutamine synthetase expression in the hippocampal astroglia of the triple transgenic Alzheimer's disease mouse model: Mechanism for deficient glutamatergic transmission? Molecular Neurodegeneration. 2011 Jul 30;6(1):55.

127. Serrano-Pozo A, Gómez-Isla T, Growdon JH, Frosch MP, Hyman BT. A Phenotypic Change But Not Proliferation Underlies Glial Responses in Alzheimer Disease. The American Journal of Pathology. 2013;182(6):2332–44.

128. Heneka MT, Carson MJ, El Khoury J, Landreth GE, Brosseron F, Feinstein DL, et al. Neuroinflammation in Alzheimer's disease. The Lancet Neurology. 2015 Apr;14(4):388–405.

129. Ding S, Fellin T, Zhu Y, Lee S-Y, Auberson YP, Meaney DF, et al. Enhanced astrocytic Ca2+ signals contribute to neuronal excitotoxicity after status epilepticus. The Journal of neuroscience : the official journal of the Society for Neuroscience. 2007 Oct 3;27(40):10674–84.

130. Araque A, Parpura V, Sanzgiri RP, Haydon PG. Glutamate-dependent astrocyte modulation of synaptic transmission between cultured hippocampal neurons. European Journal of Neuroscience. 1998 Jun 1;10(6):2129–42.

131. Halassa MM, Fellin T, Haydon PG. The tripartite synapse: roles for gliotransmission in health and disease. Trends in Molecular Medicine. 2007 Feb 1;13(2):54–63.

132. Lee L, Kosuri P, Arancio O. Picomolar amyloid-β peptides enhance spontaneous astrocyte calcium transients. Journal of Alzheimer's disease : JAD. 2014;38(1):49–62.

133. Argaw AT, Asp L, Zhang J, Navrazhina K, Pham T, Mariani JN, et al. Astrocyte-derived VEGF-A drives blood-brain barrier disruption in CNS inflammatory disease. The Journal of clinical investigation. 2012/06/01. 2012 Jul 2;122(7):2454–68.

134. Kostianovsky AM, Maier LM, Anderson RC, Bruce JN, Anderson DE. Astrocytic Regulation of Human Monocytic/Microglial Activation. The Journal of Immunology. 2014 Oct 15;181(8):5425–32.

135. Kato S, Gondo T, Hoshii Y, Takahashi M, Yamada M, Ishihara T. Confocal observation of senile plaques in Alzheimer's disease: Senile plaque morphology and relationship between senile plaques and astrocytes. Pathology International. 1998 May 1;48(5):332–40.

136. Burda JE, Sofroniew M V. Reactive gliosis and the multicellular response to CNS damage and disease. Neuron. 2014 Jan 22;81(2):229–48.

137. Sofroniew M V. Multiple Roles for Astrocytes as Effectors of Cytokines and Inflammatory Mediators. The Neuroscientist. 2013 Oct 8;20(2):160–72.

138. Alexander C, Rietschel ET. Invited review: Bacterial lipopolysaccharides and innate immunity. Journal of Endotoxin Research. 2001 Jun 1;7(3):167–202.

139. https://microbeonline.com/lipopolysaccharide-lps-of-gram-negative-bacteria-characteristics-and-functions/ [Internet]. Available from: https://microbeonline.com/lipopolysaccharide-lps-of-gram-negative-bacteria-characteristics-and-functions/

140. Arenas J. The Role of Bacterial Lipopolysaccharides as Immune Modulator in Vaccine and Drug Development. Endocrine, Metabolic & Immune Disorders-Drug Targets. 2012;12(3):221–35.

141. Klein G, Raina S. Regulated Assembly of LPS, Its Structural Alterations and Cellular Response to LPS Defects. International Journal of Molecular Sciences. 2019;20(2):356.

142. Anspach FB. Endotoxin removal by affinity sorbents. Journal of Biochemical and Biophysical Methods. 2001;49(1):665–81.

143. Reyes RE. Mechanisms of O-Antigen Structural Variation of Bacterial Lipopolysaccharide (LPS). In: González CR, editor. Rijeka: IntechOpen; 2012. p. Ch. 3.

144. Huang JX, Azad MAK, Yuriev E, Baker MA, Nation RL, Li J, et al. Molecular Characterization of Lipopolysaccharide Binding to Human α-1-Acid Glycoprotein. Journal of lipids. 2012/12/20. 2012;2012:475153.

145. Martínez-Sernández V, Orbegozo-Medina RA, Romarís F, Paniagua E, Ubeira FM. Usefulness of ELISA methods for assessing LPS interactions with proteins and peptides. PLoS ONE. 2016;11(6):1–17.

146. Silipo A, Leone MR, Lanzetta R, Parrilli M, Lackner G, Busch B, et al. Structural characterization of two lipopolysaccharide O-antigens produced by the endofungal bacterium Burkholderia sp. HKI-402 (B4). Carbohydrate Research. 2012;347(1):95–8.

147. Netea MG, van Deuren M, Kullberg BJ, Cavaillon J-M, Van der Meer JWM. Does the shape of lipid A determine the interaction of LPS with Toll-like receptors? Trends in

Immunology. 2002 Mar 1;23(3):135–9.

148. Steimle A, Autenrieth IB, Frick JS. Structure and function: Lipid A modifications in commensals and pathogens. Vol. 306, International Journal of Medical Microbiology. Elsevier GmbH.; 2016. p. 290–301.

149. Medzhitov R. Approaching the Asymptote: 20 Years Later. Immunity. 2009 Jun 19;30(6):766–75.

150. Elass-Rochard E, Legrand D, Salmon V, Roseanu A, Trif M, Tobias PS, et al. Lactoferrin inhibits the endotoxin interaction with CD14 by competition with the lipopolysaccharide-binding protein. Infection and Immunity. 1998;66(2):486–91.

151. Kim SJ, Kim HM. Dynamic lipopolysaccharide transfer cascade to TLR4/MD2 complex via LBP and CD14. BMB reports. 2017/02/28. 2017;50(2):55–7.

152. Tan Y, Kagan JC. A cross-disciplinary perspective on the innate immune responses to bacterial lipopolysaccharide. Molecular cell. 2014 Apr 24;54(2):212–23.

153. Yan SR, Qing G, Byers DM, Stadnyk AW, Al-Hertani W, Bortolussi R. Role of MyD88 in diminished tumor necrosis factor alpha production by newborn mononuclear cells in response to lipopolysaccharide. Infection and immunity. 2004 Mar;72(3):1223–9.

154. Schumann RR. Old and new findings on lipopolysaccharide-binding protein: a soluble pattern-recognition molecule. Biochemical Society Transactions. 2011;39(4):989–93.

155. B.S. Park (a) H.M. Kim (a), B.S. Choi (a), H. Lee (b) and J-O. Lee (a,c), Nature 458, 1191 (2009). DHS (a), (a) Department of Chemistry Daejeon (Korea) K, (b) Department of Biology Daejeon (Korea) CNU, (c) Institute of BioCentury Daejeon (Korea) K. The structural basis of LPS recognition by the TLR4-MD-2 complex. Nature. 2009 Mar 1;458:1191.

156. Knapp S, de Vos AF, Florquin S, Golenbock DT, van der Poll T. Lipopolysaccharide Binding Protein Is an Essential Component of the Innate Immune Response to Escherichia coli Peritonitis in Mice. Infection and Immunity. 2003 Dec 1;71(12):6747 LP – 6753.

157. Hansen GH, Rasmussen K, Niels-Christiansen L-L, Danielsen EM.

Lipopolysaccharide-binding protein: localization in secretory granules of Paneth cells in the mouse small intestine. Histochemistry and Cell Biology. 2009;131(6):727–32.

158. Shreiner AB, Kao JY, Young VB. The gut microbiome in health and in disease. Current opinion in gastroenterology. 2015 Jan;31(1):69–75.

159. Turnbaugh PJ, Ley RE, Hamady M, Fraser-Liggett CM, Knight R, Gordon JI. The human microbiome project. Nature. 2007 Oct 18;449(7164):804–10.

160. Cho I, Blaser MJ. The human microbiome: at the interface of health and disease. Nature reviews Genetics. 2012 Mar 13;13(4):260–70.

161. Bonaz B, Bazin T, Pellissier S. The vagus nerve at the interface of the microbiota-gut-brain axis. Vol. 12, Frontiers in Neuroscience. 2018. p. 1–9.

162. Barko PC, McMichael MA, Swanson KS, Williams DA. The Gastrointestinal Microbiome: A Review. Journal of veterinary internal medicine. 2017/11/24. 2018;32(1):9–25.

163. Sochocka M, Donskow-Łysoniewska K, Diniz BS, Kurpas D, Brzozowska E, Lesze J. The gut microbiome alterations and inflammation-driven pathogenesis of alzheimer's disease—a critical review. Molecular Neurobiology. 2018;56(3):1841–51.

164. Grice EA, Segre JA. The Human Microbiome: Our Second Genome. Annual Review of Genomics and Human Genetics. 2012/06/06. 2012;13(1):151–70.

165. Thursby E, Juge N. Introduction to the human gut microbiota. The Biochemical journal. 2017 May 16;474(11):1823–36.

166. Hooper L V, Littman DR, Macpherson AJ. Interactions between the microbiota and the immune system. 2012/06/06. Vol. 336, Science. 2012. p. 1268–73.

167. Maynard CL, Elson CO, Hatton RD, Weaver CT. Reciprocal interactions of the intestinal microbiota and immune system. Nature. 2012 Sep 13;489(7415):231–41.

168. Logsdon AF, Erickson MA, Rhea EM, Salameh TS, Banks WA. Gut reactions: How the blood–brain barrier connects the microbiome and the brain. Experimental Biology and Medicine. 2018;243(2):159–65.

169. E.M.M. Q. Microbiota-Brain-Gut Axis and Neurodegenerative Diseases. Current Neurology and Neuroscience Reports. 2017;17(94).

170. Lechuga S, Ivanov AI. Disruption of the epithelial barrier during intestinal inflammation: Quest for new molecules and mechanisms. Biochimica et biophysica acta Molecular cell research. 2017/03/18. 2017 Jul;1864(7):1183–94.

171. Dinan TG, Cryan JF. Gut instincts: microbiota as a key regulator of brain development, ageing and neurodegeneration. The Journal of physiology. 2016/12/04. 2017 Jan 15;595(2):489–503.

172. Bonaz BL, Bernstein CN. Brain-Gut Interactions in Inflammatory Bowel Disease. Gastroenterology. 2013 Jan 1;144(1):36–49.

173. Kowalski K, Mulak A. Brain-gut-microbiota axis in Alzheimer's disease. Journal of Neurogastroenterology and Motility. 2019;25(1):48–60.

174. Eisenstein M. Microbiome: Bacterial broadband. Nature. 2016 May 18;533(7603):S104–6.

175. Franceschi C, Garagnani P, Parini P, Giuliani C, Santoro A. Inflammaging: a new immune–metabolic viewpoint for age-related diseases. Nature Reviews Endocrinology. 2018;14(10):576–90.

176. Köhler CA, Maes M, Slyepchenko A, Berk M, Solmi M, Carvalho KLL and AF. The Gut-Brain Axis, Including the Microbiome, Leaky Gut and Bacterial Translocation: Mechanisms and Pathophysiological Role in Alzheimer's Disease. Vol. 22, Current Pharmaceutical Design. 2016. p. 6152–66.

177. Logsdon AF, Erickson MA, Rhea EM, Salameh TS, Banks WA. Gut reactions: How the blood-brain barrier connects the microbiome and the brain. Experimental biology and medicine (Maywood, NJ). 2017/11/23. 2018 Jan;243(2):159–65.

178. Kodukula K, Faller D V, Harpp DN, Kanara I, Pernokas J, Pernokas M, et al. Gut Microbiota and Salivary Diagnostics: The Mouth Is Salivating to Tell Us Something. BioResearch open access. 2017 Oct 1;6(1):123–32.

179. Cherny I, Rockah L, Levy-Nissenbaum O, Gophna U, Ron EZ, Gazit E. The Formation

of Escherichia coli Curli Amyloid Fibrils is Mediated by Prion-like Peptide Repeats. Journal of Molecular Biology. 2005;352(2):245–52.

180. Abreu MT, Fukata M, Arditi M. TLR Signaling in the Gut in Health and Disease. The Journal of Immunology. 2014 Apr 15;174(8):4453–60.

181. Wekerle H. Brain Autoimmunity and Intestinal Microbiota: 100 Trillion Game Changers. Trends in Immunology. 2017 Jul 1;38(7):483–97.

182. Luo A, Leach ST, Barres R, Hesson LB, Grimm MC, Simar D. The microbiota and epigenetic regulation of t helper 17/regulatory T cells: In search of a balanced immune system. Vol. 8, Frontiers in Immunology. Frontiers Media S.A.; 2017. p. 417.

183. A.T. T, J.P. C, J.J. K, Y. Y, C.C. H, N. H, et al. Endothelial TLR4 and the microbiome drive cerebral cavernous malformations. Nature. 2017 May 10;545(7654):305–10.

184. Banks WA, Gray AM, Erickson MA, Salameh TS, Damodarasamy M, Sheibani N, et al. Lipopolysaccharide-induced blood-brain barrier disruption: Roles of cyclooxygenase, oxidative stress, neuroinflammation, and elements of the neurovascular unit. Journal of Neuroinflammation. 2015 Nov 25;12(1):223.

185. Jaeger LB, Dohgu S, Sultana R, Lynch JL, Owen JB, Erickson MA, et al. Lipopolysaccharide alters the blood-brain barrier transport of amyloid beta protein: a mechanism for inflammation in the progression of Alzheimer's disease. Brain, behavior, and immunity. 2009/02/06. 2009 May;23(4):507–17.

186. I. UM. Anatomy of the periodontium: A biological basis for radiographic evaluation of periradicular pathology. Journal of Dentistry and Oral Hygiene. 2014;6(7):70–6.

187. de Pablo P, Chapple ILC, Buckley CD, Dietrich T. Periodontitis in systemic rheumatic diseases. Nature Reviews Rheumatology. 2009 Apr 1;5(4):218–24.

188. Nazir MA. Prevalence of periodontal disease, its association with systemic diseases and prevention. International journal of health sciences. 2017;11(2):72–80.

189. Kim J, Amar S. Periodontal disease and systemic conditions: a bidirectional relationship. Odontology. 2006 Sep;94(1):10–21.

190. Arimatsu K, Yamada H, Miyazawa H, Minagawa T, Nakajima M, Ryder MI, et al. Oral pathobiont induces systemic inflammation and metabolic changes associated with alteration of gut microbiota. Scientific reports. 2014 May 6;4:4828.

191. Tiisanoja A, Syrjälä A-M, Tertsonen M, Komulainen K, Pesonen P, Knuuttila M, et al. Oral diseases and inflammatory burden and Alzheimer's disease among subjects aged 75 years or older. Special Care in Dentistry. 2019 Mar 1;39(2):158–65.

192. Olsen I, Singhrao SK. Can oral infection be a risk factor for Alzheimer's disease? Vol. 7, Journal of Oral Microbiology. Co-Action Publishing; 2015. p. 29143.

193. Ding Y, Ren J, Yu H, Yu W, Zhou Y. Porphyromonas gingivalis, a periodontitis causing bacterium, induces memory impairment and age-dependent neuroinflammation in mice. Immunity & ageing : I & A. 2018 Jan 30;15:6.

194. Wang Y-X, Kang X-N, Cao Y, Zheng D-X, Lu Y-M, Pang C-F, et al. Porphyromonas gingivalis induces depression via downregulating p75NTR-mediated BDNF maturation in astrocytes. Brain, Behavior, and Immunity. 2019;81:523–34.

195. Poole S, Singhrao SK, Kesavalu L, Curtis MA, Crean S. Determining the presence of periodontopathic virulence factors in short-term postmortem Alzheimer's disease brain tissue. Journal of Alzheimer's Disease. 2013;36(4):665–77.

196. Adler DH, Wisse LEM, Ittyerah R, Pluta JB, Ding SL, Xie L, et al. Characterizing the human hippocampus in aging and Alzheimer's disease using a computational atlas derived from ex vivo MRI and histology. Proceedings of the National Academy of Sciences of the United States of America. 2018;115(16):4252–7.

197. Saavedra-López E, Casanova P V, Cribaro GP, Barcia C. Neuroinflammation in Movement Disorders. In: Steiner H, Tseng KYBT-H of BN, editors. Handbook of Basal Ganglia Structure and Function, Second Edition. Elsevier; 2016. p. 771–82.

198. Barres BA. The Mystery and Magic of Glia: A Perspective on Their Roles in Health and Disease. Vol. 60, Neuron. 2008. p. 430–40.

199. Allen NJ, Barres BA. Neuroscience: Glia - more than just brain glue. Vol. 457, Nature. 2009. p. 675–7.

200. Franceschi C, Capri M, Monti D, Giunta S, Olivieri F, Sevini F, et al. Inflammaging and anti-inflammaging: A systemic perspective on aging and longevity emerged from studies in humans. Mechanisms of Ageing and Development. 2007;128(1):92–105.

201. Noda M, Doi Y, Liang J, Kawanokuchi J, Sonobe Y, Takeuchi H, et al. Fractalkine attenuates excito-neurotoxicity via microglial clearance of damaged neurons and antioxidant enzyme heme oxygenase-1 expression. Journal of Biological Chemistry. 2011;

202. Cerbai F, Lana D, Nosi D, Petkova-Kirova P, Zecchi S, Brothers HM, et al. The Neuron-Astrocyte-Microglia Triad in Normal Brain Ageing and in a Model of Neuroinflammation in the Rat Hippocampus. PLoS ONE. 2012;7(9).

203. Colton CA, Mott RT, Sharpe H, Xu Q, Van Nostrand WE, Vitek MP. Expression profiles for macrophage alternative activation genes in AD and in mouse models of AD. Journal of Neuroinflammation. 2006;3.

204. Morgan D. Modulation of microglial activation state following passive immunization in amyloid depositing transgenic mice. Neurochemistry International. 2006;49(2):190–4.

205. Kashon ML, Ross GW, O'Callaghan JP, Miller DB, Petrovitch H, Burchfiel CM, et al. Associations of cortical astrogliosis with cognitive performance and dementia status. Journal of Alzheimer's Disease. 2004;6(6):595–604.

206. Rivera-Escalera F, Pinney JJ, Owlett L, Ahmed H, Thakar J, Olschowka JA, et al. IL-1β-driven amyloid plaque clearance is associated with an expansion of transcriptionally reprogrammed microglia. Journal of Neuroinflammation. 2019;16(1):261.

207. Baron R, Babcock AA, Nemirovsky A, Finsen B, Monsonego A. Accelerated microglial pathology is associated with Aβ plaques in mouse models of Alzheimer's disease. Aging Cell. 2014;13(4):584–95.

208. Seminotti B, Zanatta Â, Ribeiro RT, da Rosa MS, Wyse ATS, Leipnitz G, et al. Disruption of Brain Redox Homeostasis, Microglia Activation and Neuronal Damage Induced by Intracerebroventricular Administration of S-Adenosylmethionine to Developing Rats. Molecular Neurobiology. 2019;56(4):2760–73.

209. Wang L, Jiang Q, Chu J, Lin L, Li XG, Chai GS, et al. Expression of Tau40 Induces Activation of Cultured Rat Microglial Cells. PLoS ONE. 2013;8(10).

210. Das R, Balmik AA, Chinnathambi S. Phagocytosis of full-length Tau oligomers by Actin-remodeling of activated microglia. Journal of Neuroinflammation. 2020;17(1):10.

211. Wan Yaacob WMH, Long I, Zakaria R, Othman Z. Tualang honey and its methanolic fraction improve LPS-induced learning and memory impairment in male rats: Comparison with Memantine. Current Nutrition & Food Science. 2018;15:59.

212. Meo SA, Al-Asiri SA, Mahesar AL, Ansari MJ. Role of honey in modern medicine. Vol. 24, Saudi Journal of Biological Sciences. 2017. p. 975–8.

213. Pasupuleti VR, Sammugam L, Ramesh N, Gan SH. Honey, Propolis, and Royal Jelly: A Comprehensive Review of Their Biological Actions and Health Benefits. Vol. 2017, Oxidative Medicine and Cellular Longevity. 2017.

214. Rao PV, Krishnan KT, Salleh N, Gan SH. Biological and therapeutic effects of honey produced by honey bees and stingless bees: A comparative review. Vol. 26, Brazilian Journal of Pharmacognosy. Sociedade Brasileira de Farmacognosia; 2016. p. 657–64.

215. Tonks AJ, Cooper RA, Jones KP, Blair S, Parton J, Tonks A. Honey stimulates inflammatory cytokine production from monocytes. Cytokine. 2003;21(5):242–7.

216. Afrin S, Gasparrini M, Forbes-Hernández TY, Cianciosi D, Reboredo-Rodriguez P, Manna PP, et al. Protective effects of Manuka honey on LPS-treated RAW 264.7 macrophages. Part 1: Enhancement of cellular viability, regulation of cellular apoptosis and improvement of mitochondrial functionality. Food and Chemical Toxicology. 2018;121:203–13.

217. Ahmad RS, Hussain MB, Saeed F, Waheed M, Tufail T. Phytochemistry, metabolism, and ethnomedical scenario of honey: A concurrent review. Vol. 20, International Journal of Food Properties. 2017. p. S254–69.

218. Al-Rahbi B, Zakaria R, Othman Z, Hassan A, Mohd Ismail ZI, Muthuraju S. Tualang honey supplement improves memory performance and hippocampal morphology in stressed ovariectomized rats. Acta Histochemica. 2014;116(1):79–88.

219. Johnson M. MATER METHODS [Internet]. 2. 2012. p. 113. Available from: https://www.labome.com/method/Laboratory-Mice-and-Rats.html

220. Noldus Information Technology. Behavioral Research Blog [Internet]. [cited 2022 Feb 27]. Available from: https://www.noldus.com/blog/y-maze-learning-and-memory-testing

221. Mathiasen JR, DiCamillo A. Novel Object Recognition in the Rat: A Facile Assay for Cognitive Function. Current Protocols in Pharmacology. 2010 Jun 1;49(1):5.59.1-5.59.15.

222. Ennaceur A, Delacour J. A new one-trial test for neurobiological studies of memory in rats. 1: Behavioral data. Behavioural brain research. 1988;31(1):47–59.

223. Fields CT, Chassaing B, Castillo-Ruiz A, Osan R, Gewirtz AT, De Vries GJ. Effects of gut-derived endotoxin on anxiety-like and repetitive behaviors in male and female mice. Biology of Sex Differences. 2018;9(1):1–14.

224. Sotocina SG, Sorge RE, Zaloum A, Tuttle AH, Martin LJ, Wieskopf JS, et al. The Rat Grimace Scale: A Partially Automated Method for Quantifying Pain in the Laboratory Rat via Facial Expressions. Molecular Pain. 2011 Jan 1;7:1744–55.

225. Prieur E, Jadavji N. Assessing Spatial Working Memory Using the Spontaneous Alternation Y-maze Test in Aged Male Mice. BIO-PROTOCOL. 2019;9(3).

226. Nicole O, Hadzibegovic S, Gajda J, Bontempi B, Bem T, Meyrand P. Soluble amyloid beta oligomers block the learning-induced increase in hippocampal sharp wave-ripple rate and impair spatial memory formation. Scientific Reports. 2016;6(March).

227. Lueptow LM. Novel Object Recognition Test for the Investigation of Learning and Memory in Mice. Journal of visualized experiments : JoVE. 2017 Aug 30;(126):55718.

228. Orta-Salazar E, Vargas-Rodríguez I, Castro-Chavira SA, Feria-Velasco AI, Díaz-Cintra S. Alzheimer's Disease: From Animal Models to the Human Syndrome. In: Update on Dementia. InTech; 2016.

229. Zhao J, Bi W, Xiao S, Lan X, Cheng X, Zhang J, et al. Neuroinflammation induced by lipopolysaccharide causes cognitive impairment in mice. Scientific Reports.

2019;9(1):1–12.

230. Aging NI of. How Is Alzheimer's Disease Diagnosed? | National Institute on Aging [Internet]. National Institute on Aging. 2017. Available from: https://www.nia.nih.gov/health/how-alzheimers-disease-diagnosed

231. Hung A, Schneider M, Lopez MH, McClellan M. Preclinical Alzheimer Disease Drug Development: Early Considerations Based on Phase 3 Clinical Trials. Journal of Managed Care & Specialty Pharmacy. 2020 Jun 25;26(7):888–900.

232. Akanmu MA, Olowookere TA, Atunwa SA, Ibrahim BO, Lamidi OF, Adams PA, et al. Neuropharmacological effects of Nigerian honey in mice. African Journal of Traditional, Complementary and Alternative Medicines. 2011;8(3).

233. Marwitz SE, Woodie LN, Blythe SN. Western-style diet induces insulin insensitivity and hyperactivity in adolescent male rats. Physiology & behavior. 2015;151:147–54.

234. Torre ND La. CUNY Academic Works Cognitive Changes Caused by LPS-induced Neuroinflammation How does access to this work benefit you ? Let us know ! The City University of New York; 2021.

235. Czerniawski J, Miyashita T, Lewandowski G, Guzowski JF. Systemic lipopolysaccharide administration impairs retrieval of context-object discrimination, but not spatial, memory: Evidence for selective disruption of specific hippocampus-dependent memory functions during acute neuroinflammation. Brain, behavior, and immunity. 2015;44:159–66.

236. Bandeira F, Lent R, Herculano-Houzel S. Changing numbers of neuronal and non-neuronal cells underlie postnatal brain growth in the rat. Proceedings of the National Academy of Sciences. 2009;106(33):14108–13.

237. Downes N, Mullins P. The development of myelin in the brain of the juvenile rat. Toxicologic pathology. 2014;42(5):913–22.

238. Bassi GS, Kanashiro A, Santin FM, de Souza GEP, Nobre MJ, Coimbra NC. Lipopolysaccharide-Induced Sickness Behaviour Evaluated in Different Models of Anxiety and Innate Fear in Rats. Basic & Clinical Pharmacology & Toxicology. 2012

Apr 1;110(4):359–69.

239. Tanaka S, Young JW, Halberstadt AL, Masten VL, Geyer MA. Four factors underlying mouse behavior in an open field. Behavioural Brain Research. 2012;233(1):55–61.

240. Choi D-Y, Lee JW, Lin G, Lee YK, Lee YH, Choi IS, et al. Obovatol attenuates LPS-induced memory impairments in mice via inhibition of NF-κB signaling pathway. Neurochemistry international. 2012;60(1):68–77.

241. Shaw KN, Commins S, O'Mara SM. Lipopolysaccharide causes deficits in spatial learning in the watermaze but not in BDNF expression in the rat dentate gyrus. Behavioural brain research. 2001;124(1):47–54.

242. Maze-Engineers. General Guide To Behavioral Testing In Mice [Internet]. [cited 2022 Jan 20]. Available from: https://conductscience.com/maze/general-guide-behavioral-testing/

243. Zakaria R, Wan Yaacob WMH, Othman Z, Long I, Ahmad AH, Al-Rahbi B. Lipopolysaccharide-induced memory impairment in rats: A model of Alzheimer's disease. Physiological Research. 2017;66(4):553–65.

244. Hennigan A, Trotter C, Kelly ÁM. Lipopolysaccharide impairs long-term potentiation and recognition memory and increases p75NTR expression in the rat dentate gyrus. Brain research. 2007;1130:158–66.

245. Hauss-Wegrzyniak B, Vannucchi MG, Wenk GL. Behavioral and ultrastructural changes induced by chronic neuroinflammation in young rats. Brain research. 2000;859(1):157–66.

246. Shaw KN, Commins S, O'Mara SM. Cyclooxygenase inhibition attenuates endotoxin-induced spatial learning deficits, but not an endotoxin-induced blockade of long-term potentiation. Brain research. 2005;1038(2):231–7.

247. Vasconcelos AR, Yshii LM, Viel TA, Buck HS, Mattson MP, Scavone C, et al. Intermittent fasting attenuates lipopolysaccharide-induced neuroinflammation and memory impairment. Journal of neuroinflammation. 2014;11(1):1–14.

248. Kiefer R, Streit WJ, Toyka K V, Kreutzberg GW, Hartung H-P. Transforming growth

factor-β1: A lesion-associated cytokine of the nervous system. International Journal of Developmental Neuroscience. 1995 Jun 1;13(3–4):331–9.

249. Lambertsen KL, Clausen BH, Babcock AA, Gregersen R, Fenger C, Nielsen HH, et al. Microglia protect neurons against ischemia by synthesis of tumor necrosis factor. The Journal of neuroscience : the official journal of the Society for Neuroscience. 2009 Feb 4;29(5):1319–30.

250. Imai F, Suzuki H, Oda J, Ninomiya T, Ono K, Sano H, et al. Neuroprotective Effect of Exogenous Microglia in Global Brain Ischemia. Journal of Cerebral Blood Flow & Metabolism. 2006 Jul 5;27(3):488–500.

251. Miller DL, Papayannopoulos IA, Styles J, Bobin SA, Lin YY, Biemann K, et al. Peptide Compositions of the Cerebrovascular and Senile Plaque Core Amyloid Deposits of Alzheimer′s Disease. Archives of Biochemistry and Biophysics. 1993;301(1):41–52.

252. Tucker HM, Kihiko M, Caldwell JN, Wright S, Kawarabayashi T, Price D, et al. The plasmin system is induced by and degrades amyloid-β aggregates. Journal of Neuroscience. 2000;20(11):3937–46.

253. Martel CL, Mackic JB, Matsubara E, Governale S, Miguel C, Miao W, et al. Isoform-Specific Effects of Apolipoproteins E2, E3, and E4 on Cerebral Capillary Sequestration and Blood-Brain Barrier Transport of Circulating Alzheimer's Amyloid β. Journal of Neurochemistry. 2002;69(5):1995–2004.

254. Maness LM, Banks WA, Podlisny MB, Selkoe DJ, Kastin AJ. Passage of human amyloid β-protein 1-40 across the murine blood-brain barrier. Life Sciences. 1994;55(21):1643–50.

255. Ghersi-Egea J-F, Gorevic PD, Ghiso J, Frangione B, Patlak CS, Fenstermacher JD. Fate of Cerebrospinal Fluid-Borne Amyloid β-Peptide: Rapid Clearance into Blood and Appreciable Accumulation by Cerebral Arteries. Journal of Neurochemistry. 2002;67(2):880–3.

256. Hardy J, Selkoe DJ. The amyloid hypothesis of Alzheimer's disease: Progress and problems on the road to therapeutics. Vol. 297, Science. 2002. p. 353–6.

257. Sondag CM, Dhawan G, Combs CK. Beta amyloid oligomers and fibrils stimulate differential activation of primary microglia. Journal of Neuroinflammation. 2009;6(1).

258. Hayden EY, Teplow DB. Amyloid β-protein oligomers and Alzheimer's disease. Alzheimer's Research and Therapy. 2013;5(60).

259. Peng HB, de Lannoy IAM, Pang KS. Measuring Amyloid-β Peptide Concentrations in Murine Brain with Improved ELISA Assay. Current Protocols. 2021 Oct 1;1(10):e253.

260. Scientific T. Overview of ELISA [Internet]. [cited 2020 Jan 16]. Available from: https://www.thermofisher.com/za/en/home/life-science/protein-biology/protein-biology-learning-center/protein-biology-resource-library/pierce-protein-methods/overview-elisa.html%0D

261. Kumar A, Singh A, Ekavali. A review on Alzheimer's disease pathophysiology and its management: an update. Pharmacological Reports. 2015;67(2):195–203.

262. Lyman M, Lloyd DG, Ji X, Vizcaychipi MP, Ma D. Neuroinflammation: The role and consequences. Neuroscience Research. 2014;79:1–12.

263. Wang L-M, Wu Q, Kirk RA, Horn KP, Ebada Salem AH, Hoffman JM, et al. Lipopolysaccharide endotoxemia induces amyloid-β and p-tau formation in the rat brain. American journal of nuclear medicine and molecular imaging. 2018 Apr 25;8(2):86–99.

264. Tauber AI. Metchnikoff and the phagocytosis theory. Nature Reviews Molecular Cell Biology. 2003;4(11):897–901.

265. Mizobuchi H, Soma GI. Low-dose lipopolysaccharide as an immune regulator for homeostasis maintenance in the central nervous system through transformation to neuroprotective microglia. Neural Regeneration Research. 2021;16(10):1928–34.

266. Thygesen C, Ilkjær L, Kempf SJ, Hemdrup AL, von Linstow CU, Babcock AA, et al. Diverse Protein Profiles in CNS Myeloid Cells and CNS Tissue From Lipopolysaccharide- and Vehicle-Injected APPSWE/PS1ΔE9 Transgenic Mice Implicate Cathepsin Z in Alzheimer's Disease. Frontiers in Cellular Neuroscience. 2018;12.

267. Kobayashi Y, Inagawa H, Kohchi C, Kazumura K, Tsuchiya H, Miwa T, et al. Oral administration of Pantoea agglomerans-derived lipopolysaccharide prevents metabolic dysfunction and Alzheimer's disease-related memory loss in senescence-accelerated prone 8 (SAMP8) mice fed a high-fat diet. PloS one. 2018 Jun 1;13(6):e0198493–e0198493.

268. Jendresen C, Digre A, Cui H, Zhang X, Vlodavsky I, Li J-P, et al. Systemic LPS-induced Aβ-solubilization and clearance in AβPP-transgenic mice is diminished by heparanase overexpression. Scientific Reports. 2019;9(1):4600.

269. Neher JJ, Cunningham C. Priming Microglia for Innate Immune Memory in the Brain. Trends in Immunology. 2019 Apr 1;40(4):358–74.

270. Inagawa H, Saika T, Nisizawa T, Kohchi C, Uenobe M, Soma G-I. Dewaxed brown rice contains a significant amount of lipopolysaccharide pointing to macrophage activation via TLRs. Anticancer Research. 2016;36(7):3599–605.

271. Tamura Y, Inagawa H, Nakata Y, Kohchi C, Soma G-I. Effects of the subaleurone layer of rice on macrophage activation and protection of pollen allergy in a murine model. Anticancer Research. 2015;35(8):4467–72.

272. Taniguchi Y, Yoshioka N, Nishizawa T, Inagawa H, Kohchi C, Soma G-I. Utility and safety of LPS-based fermented flour extract as a macrophage activator. Anticancer research. 2009;29(3):859–64.

273. Duraiyan J, Govindarajan R, Kaliyappan K, Palanisamy M. Applications of immunohistochemistry. Journal of pharmacy & bioallied sciences. 2012 Aug;4(Suppl 2):S307–9.

274. Qi Z, Min Z, Wang G, Feng Y, Guo H, Li Y, et al. Comparison of immunofluorescence and immunohistochemical staining with anti-insulin antibodies on formalin-fixed paraffin-embedded human pancreatic tissue microarray sections. International Journal of Clinical and Experimental Pathology. 2017;10(3):3671–6.

275. MacLachlan NJ, Dubovi EJBT-FVV (Fifth E, editors. Chapter 5 - Laboratory Diagnosis of Viral Infections. In: Fenner's Veterinary Virology. Boston: Academic Press; 2017. p. 105–29.

276. Robertson D, Savage K, Reis-Filho JS, Isacke CM. Multiple immunofluorescence labelling of formalin-fixed paraffin-embedded (FFPE) tissue. BMC Cell Biology. 2008;9:1–10.

277. Immunofluorescence Options for IHC Detection-ThermoFisher Scientific [Internet]. [cited 2022 Feb 28]. Available from: https://www.thermofisher.com/za/en/home/life-science/protein-biology/protein-biology-learning-center/protein-biology-resource-library/pierce-protein-methods/immunofluorescence-method-ihc-detection.html#2

278. Abu-Rumeileh S, Steinacker P, Polischi B, Mammana A, Bartoletti-Stella A, Oeckl P, et al. CSF biomarkers of neuroinflammation in distinct forms and subtypes of neurodegenerative dementia. Alzheimer's Research & Therapy. 2019;12(1):2.

279. Utans U, Arceci RJ, Yamashita Y, Russell ME. Cloning and characterization of allograft inflammatory factor-1: a novel macrophage factor identified in rat cardiac allografts with chronic rejection. The Journal of clinical investigation. 1995;95(6):2954–62.

280. Jacque CM, Vinner C, Kujas M, Raoul M, Racadot J, Baumann NA. Determination of glial fibrillary acidic protein (GFAP) in human brain tumors. Journal of the neurological sciences. 1978;35(1):147–55.

281. Kang J-B, Park D-J, Shah M-A, Kim M-O, Koh P-O. Lipopolysaccharide induces neuroglia activation and NF-κB activation in cerebral cortex of adult mice. Laboratory Animal Research. 2019;35(1):19.

282. Belfiore R, Rodin A, Ferreira E, Velazquez R, Branca C, Caccamo A, et al. Temporal and regional progression of Alzheimer's disease-like pathology in 3xTg-AD mice. Aging Cell. 2019;18(1):1–13.

283. Radenovic L, Nenadic M, Ułamek-Kozioł M, Januszewski S, Czuczwar SJ, Andjus PR, et al. Heterogeneity in brain distribution of activated microglia and astrocytes in a rat ischemic model of Alzheimer's disease after 2 years of survival. Aging (Albany NY). 2020;12(12):12251.

284. Mohammed Ali A. So, Antidepressant Drugs have Serious Adverse Effects, but what are the Alternatives? Novel Approaches in Drug Designing & Development. 2018;4(3).

285. Martin-Subero M, Anderson G, Kanchanatawan B, Berk M, Maes M. Comorbidity between depression and inflammatory bowel disease explained by immune-inflammatory, oxidative, and nitrosative stress; tryptophan catabolite; and gut–brain pathways. CNS spectrums. 2016;21(2):184–98.

286. Ali AM, Kunugi H. Bee honey protects astrocytes against oxidative stress: A preliminary in vitro investigation. Neuropsychopharmacology reports. 2019/09/17. 2019 Dec;39(4):312–4.

287. Mohr KM, Pallesen LT, Richner M, Vaegter CB. Discrepancy in the Usage of GFAP as a Marker of Satellite Glial Cell Reactivity. Vol. 9, Biomedicines . 2021.

288. Chen F, Yang D, Cheng X-Y, Yang H, Yang X-H, Liu H-T, et al. Astragaloside IV Ameliorates Cognitive Impairment and Neuroinflammation in an Oligomeric Aβ Induced Alzheimer's Disease Mouse Model *via* Inhibition of Microglial Activation and NADPH Oxidase Expression. Biological and Pharmaceutical Bulletin. 2021;44(11):1688–96.

289. Yahaya MAF, Bakar ARA, Stanslas J, Nordin N, Zainol M, Mehat MZ. Insights from molecular docking and molecular dynamics on the potential of vitexin as an antagonist candidate against lipopolysaccharide (LPS) for microglial activation in neuroinflammation. BMC biotechnology. 2021 Jun 5;21(1):38.

290. Zhao Y, Jiang Y, Chai J, Huang F, Zhang Z, Liu Q, et al. Neuroprotective nanoscavenger induces coaggregation of β-amyloid and facilitates its clearance in alzheimer's disease brain. CCS Chemistry. 2021;3(8):2316–30.

291. Wyss-Coray T, Rogers J. Inflammation in Alzheimer disease—a brief review of the basic science and clinical literature. Cold Spring Harbor perspectives in medicine. 2012;2(1):a006346.

292. Leng F, Edison P. Neuroinflammation and microglial activation in Alzheimer disease: where do we go from here? Nature Reviews Neurology. 2021;17(3):157–72.

293. Hoogland ICM, Houbolt C, van Westerloo DJ, van Gool WA, van de Beek D. Systemic inflammation and microglial activation: systematic review of animal experiments. Journal of neuroinflammation. 2015 Jun 6;12:114.

294. Norden DM, Trojanowski PJ, Villanueva E, Navarro E, Godbout JP. Sequential activation of microglia and astrocyte cytokine expression precedes increased iba-1 or GFAP immunoreactivity following systemic immune challenge. Glia. 2016 Feb 1;64(2):300–16.

295. Candiracci M, Piatti E, Dominguez-Barragán M, García-Antrás D, Morgado B, Ruano D, et al. Anti-inflammatory Activity of a Honey Flavonoid Extract on Lipopolysaccharide-Activated N13 Microglial Cells. Journal of Agricultural and Food Chemistry. 2012 Dec 19;60(50):12304–11.

296. Zotova E, Holmes C, Johnston D, Neal JW, Nicoll JAR, Boche D. Microglial alterations in human Alzheimer's disease following Aβ42 immunization. Neuropathology and Applied Neurobiology. 2011 Aug 1;37(5):513–24.

297. Hendrickx DAE, van Eden CG, Schuurman KG, Hamann J, Huitinga I. Staining of HLA-DR, Iba1 and CD68 in human microglia reveals partially overlapping expression depending on cellular morphology and pathology. Journal of Neuroimmunology. 2017 Aug 15;309:12–22.

298. Frost GR, Li Y-M. The role of astrocytes in amyloid production and Alzheimer's disease. Open biology. 2017;7(12):170228.

299. Bassendine MF, Taylor-Robinson SD, Fertleman M, Khan M, Neely D. Is Alzheimer's disease a liver disease of the brain? Journal of Alzheimer's Disease. 2020;75(1):1–14.

300. Rodrigue KM, Kennedy KM, Devous MD, Rieck JR, Hebrank AC, Diaz-Arrastia R, et al. β-Amyloid burden in healthy aging: regional distribution and cognitive consequences. Neurology. 2012;78(6):387–95.

301. Wan Yaacob WMH, Long I, Zakaria R, Othman Z. Tualang honey and its methanolic fraction ameliorate lipopolysaccharide-induced oxidative stress, amyloid deposition and neuronal loss of the rat hippocampus. Advances in Traditional Medicine. 2021;21(1):121–9.

302. Preman P, Alfonso-Triguero M, Alberdi E, Verkhratsky A, Arranz AM. Astrocytes in alzheimer's disease: Pathological significance and molecular pathways. Cells. 2021;10(3):1–19.

303. Hansen D V, Hanson JE, Sheng M. Microglia in Alzheimer's disease. Journal of Cell Biology. 2018;217(2):459–72.

304. Więckowska-Gacek A, Mietelska-Porowska A, Chutorański D, Wydrych M, Długosz J, Wojda U. Western Diet Induces Impairment of Liver-Brain Axis Accelerating Neuroinflammation and Amyloid Pathology in Alzheimer's Disease. Frontiers in Aging Neuroscience. 2021;13(April):1–27.

305. Lecours C, Bordeleau M, Cantin L, Parent M, Paolo T Di, Tremblay M-È. Microglial implication in Parkinson's disease: loss of beneficial physiological roles or gain of inflammatory functions? Frontiers in Cellular Neuroscience. 2018;282.

306. Qu W, Johnson A, Kim JH, Lukowicz A, Svedberg D, Cvetanovic M. Inhibition of colony-stimulating factor 1 receptor early in disease ameliorates motor deficits in SCA1 mice. Journal of neuroinflammation. 2017;14(1):1–11.

307. Biber K, Block ML. Neuroprotection versus neurotoxicity. In: Microglia in Health and Disease. Springer; 2014. p. 145–72.

308. Ma L, Yang S, Ma Y, Chen Y, Wang Z, James TD, et al. Benzothiazolium Derivative-Capped Silica Nanocomposites for β-Amyloid ImagingIn Vivo. Analytical Chemistry. 2021;93(37):12617–27.

309. Ziaunys M, Sneideris T, Smirnovas V. Formation of distinct prion protein amyloid fibrils under identical experimental conditions. Scientific reports. 2020;10(1):1–7.

310. Sakalauskas A, Ziaunys M, Smirnovas V. Concentration-dependent polymorphism of insulin amyloid fibrils. PeerJ. 2019;7:e8208.

311. Sidhu A, Vaneyck J, Blum C, Segers-Nolten I, Subramaniam V. Polymorph-specific distribution of binding sites determines thioflavin-T fluorescence intensity in α-synuclein fibrils. Amyloid. 2018;25(3):189–96.

312. Buell AK, Dobson CM, Knowles TPJ, Welland ME. Interactions between amyloidophilic dyes and their relevance to studies of amyloid inhibitors. Biophysical journal. 2010;99(10):3492–7.

313. Ziaunys M, Mikalauskaite K, Smirnovas V. Amyloidophilic molecule interactions on the

surface of insulin fibrils: cooperative binding and fluorescence quenching. Scientific reports. 2019;9(1):1–10.

314. Halabelian L, Relini A, Barbiroli A, Penco A, Bolognesi M, Ricagno S. A covalent homodimer probing early oligomers along amyloid aggregation. Scientific reports. 2015;5(1):1–12.

315. Kuznetsova IM, Sulatskaya AI, Uversky VN, Turoverov KK. Analyzing thioflavin T binding to amyloid fibrils by an equilibrium microdialysis-based technique. PloS one. 2012;7(2):e30724.

316. Gasparrini M, Afrin S, Forbes-Hernández TY, Cianciosi D, Reboredo-Rodriguez P, Amici A, et al. Protective effects of Manuka honey on LPS-treated RAW 264.7 macrophages. Part 2: Control of oxidative stress induced damage, increase of antioxidant enzyme activities and attenuation of inflammation. Food and Chemical Toxicology. 2018;120:578–87.

317. Wang X-H, Andrae L, Engeseth NJ. Antimutagenic Effect of Various Honeys and Sugars against Trp-p-1. Journal of Agricultural and Food Chemistry. 2002 Nov 1;50(23):6923–8.

318. Othman NH. Honey and cancer: sustainable inverse relationship particularly for developing nations-a review. Evidence-based complementary and alternative medicine : eCAM. 2012/06/17. 2012;2012:410406.

319. Chen L, Mehta A, Berenbaum M, Zangerl AR, Engeseth NJ. Honeys from Different Floral Sources as Inhibitors of Enzymatic Browning in Fruit and Vegetable Homogenates. Journal of Agricultural and Food Chemistry. 2000 Oct 1;48(10):4997–5000.

320. Emmertz A. Mineral composition of New Zealand monofloral honeys. 2010;

321. Gulinello M, Mitchell HA, Chang Q, Timothy O'Brien W, Zhou Z, Abel T, et al. Rigor and reproducibility in rodent behavioral research. Neurobiology of Learning and Memory. 2019;165(November 2017):0–1.

322. Batista CRA, Gomes GF, Candelario-Jalil E, Fiebich BL, de Oliveira ACP.

Lipopolysaccharide-Induced Neuroinflammation as a Bridge to Understand Neurodegeneration. International journal of molecular sciences. 2019 May 9;20(9):2293.

323. Ransohoff RM, El Khoury J. Microglia in health and disease. Cold Spring Harbor perspectives in biology. 2016;8(1):a020560.

324. Vandenbark AA, Offner H, Matejuk S, Matejuk A. Microglia and astrocyte involvement in neurodegeneration and brain cancer. Journal of Neuroinflammation. 2021;18(1):298.

325. Liddelow SA, Guttenplan KA, Clarke LE, Bennett FC, Bohlen CJ, Schirmer L, et al. Neurotoxic reactive astrocytes are induced by activated microglia. Nature. 2017;541(7638):481–7.

Addendum 1: Animal ethics committee approval-181/2020

[illegible]

[illegible]

[illegible]

Approval Certificate
Date of Renewal
([illegible])

AEC Reference No :	[illegible]
Title:	The effects of [illegible] induced by systemic lipopolysaccharide on the development of Sprague-Dawley rats
Researcher:	Ellen N. Chikwati
Student's Supervisor:	[redacted]

Dear Miss Ellen Chikwati,

This Annual Renewal as requested by [illegible] received between [illegible] and [illegible] for your research, was approved by the Animal Ethics Committee on its quarterly meeting of [illegible].

Please note the following about your ethics approval:

1. The use of specimens approved:

Species and Strain/s	Number Available
Male Sprague-Dawley	55

2. Ethics Approval is valid for 1 year and needs to be renewed annually by [illegible].
3. Please remember to use your protocol number (181/2020) on any documents or correspondence with the AEC regarding your research.
4. Please note that the AEC may ask further questions, seek additional information, require further modification, monitor the conduct of your research, or suspend or withdraw ethics approval.
5. All incidents must be reported by the PI by email to the Veterinary Ethics Officer (AEC Coordinator) within 5 days, and must be subsequently submitted electronically on the application system within 14 days.
6. The committee also requests that you record no personal information during your study for non-publishing, using any available digital recording system that captures in adequate quality, as it may be required if the committee needs to evaluate a complaint. However, if the committee has considered the information sensitively or it is generally not be considered critical, such recording will not be required.

Others required to adhere to the following:

4. The ethics approval is conditional on the research being conducted as stipulated by the details of all documents submitted to the Committee. In the event that a further novel scientific change after the investigations are, the methods or any other relevant such changes must be submitted as an amendment for approval by the Committee.

[illegible]

We wish you the best in all your endeavors.

Yours sincerely

Prof [illegible]

Chairperson: Educational Ethics Committee

Addendum 2: Animal Research Ethics Committee-2019/07/44/C

UNIVERSITY OF THE WITWATERSRAND, JOHANNESBURG

STRICTLY CONFIDENTIAL

ANIMAL RESEARCH ETHICS COMMITTEE (AREC)

CLEARANCE CERTIFICATE NO. 2019/07/44/C

APPLICANT: Prof W Daniels

SCHOOL/ DEPARTMENT/ LOCATION: Physiology

PROJECT TITLE: [redacted]

Summary and Details

[redacted]

Approval was given for the use of animals for the project described above at an AREC meeting held on [redacted]. This approval remains valid until [redacted].

[redacted]

An annual progress report must be provided

The use of these animals is subject to AREC guidelines for the use and care of animals, is limited to the procedures described in the application form and is subject to any additional conditions listed below:

Signed: _____ (CHAIRPERSON: AREC) Date: 1st October 2019

I am satisfied that the persons listed in this application are competent to perform the procedures therein, in terms of Section 23 (1) (b) of the Veterinary and Para-Veterinary Professions Act (19 of 1982)

Signed: _____ (REGISTERED VETERINARIAN) Date: 18 October 2019

cc: Supervisor(s)
Director: GAS

Web [redacted]

Addendum 3: MSc committee approval

MSc Committee
School of Medicine
Faculty of Health Sciences

MSc Committee
16 July 2018

Dr J Hofer
Department of Physiology
Faculty of Health Sciences

Dear Dr,

Mr N Dlamini, Student no 14161129

Please receive the following comments with reference to the MSc Committee submission of the above-mentioned student:

Student name	Mr Nontulukelo Dlamini	Student number	14161129
Name of study leader	Dr Janette Hofer		
Department	Physiology		
Title of MSc	The effects of neurotoxin-induced by synthetic lipopolysaccharide on the hippocampal of aged Sprague-Dawley rats		
Date of first submission	June 2018		
Comments to study leader June 2018	• Please indicate the names of the students that also will be part of the study. • Scientific genus names need to be defined before abbreviating in the protocol. Please correct. Please set the baseline names in italics. • Please remove the Mr before the objectives. • Please include the details of the instruments and reagents to be used. • Please define the references list. Journal names should be written in a consistent manner. • Please delete the word rodents from the aim. This also needs to be added to the title. • Please correct spelling and typographical errors. • Define how the neuroinflammation induced relates to Alzheimer's disease as Alzheimer's is not the main focus of the study. Please revise. This will improve of the study might assist in the understanding of the disease. • Please revise the title to "The effects of neuroinflammation induced by synthetic lipopolysaccharide on the Hippocampal of aged Sprague-Dawley rats".		
July 2018	• Thank you for submitting the revised protocol and MSc form.		

School of Medicine
Faculty of Health Sciences
University of Pretoria
Pretoria
South Africa
Private Bag X323, Gezina, 0031
Tel: +27 (0) 12 319 2323
Fax: +27 (0) 12 319 2324

Decision	This proposal has been provisionally approved. Please submit the revised proposal to ethics, and supply the MGC committee with proof of ethics clearance. The internal and external examiners can be nominated and submitted to the MGC Committee six months prior to submission of the dissertation. Please ensure that the CV of the examiners includes supervision, examination and publication records.

Yours sincerely

Prof Marlien Kock
Chair: MGC Committee

Addendum 4: Letter of statistical support

BIOSTATISTICS UNIT

LETTER OF STATISTICAL SUPPORT

18 July 2019

This letter is to confirm that student Nonkululeko Dhlamini **Faculty of Health Sciences**; University of Pretoria discussed the Project with the title **"The effects of neuroinflammation induced by systemic lipopolysaccharide on the hippocampi of aged Sprague-Dawley rats".** We therefore confirm that we are aware of the project and undertake to assist with the statistical analysis of the data generated from the project.

Data Analysis

The aim of this study is to investigate if systemic induced lipopolysaccharide (LPS) from Escherichia coli 055:B5 at a volume of 0.1 ml per kg of rat for 10 days induces neuroinflammation in aged Sprague-Dawley rats. Descriptive statistics like mean, median, standard deviation and range will be given for continuous data. Independent samples t-test will be undertaken to assess the effect of systemic induced LPS on the spatial memory between the control, vehicle and experimental aged Sprague-Dawley rats. Data will be captured into Excel and all statistics will be evaluated at 5% level and will be undertaken using STATA 15.

Sample size

To achieve the objectives of this study a sample of 18 aged Sprague-Dawley rats will be used.

Name: Tshifhiwa M Nkwenika
Biostatistics Unit
tshifhiwa.nkwenika@mrc.ac.za
012 339 8519

MEDICAL RESEARCH COUNCIL
Biostatistics Unit
Private Bag X385
Pretoria
0001
Tel: 012 339 8523 / Fax: 012 339 8582

THE SOUTH AFRICAN MEDICAL RESEARCH COUNCIL
1 Soutpansberg Road, Pretoria, 0002 | Private Bag X385, Pretoria 0001, South Africa
Tel +27 (0)12 339 8519 | Fax +27 (0)12 339 8582 | Web www.samrc.ac.za

Addendum 5: Study log-Welfare monitoring form

Central Animal Service

Farms and Rodents # FR SLWM005:Group
STUDY LOG: WELFARE MONITORING
Category C Group

UNIVERSITY OF THE WITWATERSRAND, JOHANNESBURG

PI NAME:	AREA:	
PROCEDURE/ INTERVENTION	DATE:	

	Day: AM	PM	DR:	Day: AM	PM	DR:	Day: AM	PM	DR:
UNDISTURBED OBSERVATION	[illegible]								
Eating and drinking: Yes, No									
[illegible]									
[illegible]									
[illegible]									
[illegible]									
[illegible]									
[illegible]									
[illegible]									
[illegible]	[illegible]								
[illegible]									
[illegible]									
[illegible]									
[illegible]									
[illegible]									
[illegible]									
[illegible]									
[illegible]									
[illegible]									
[illegible]									
OTHER OBSERVATIONS/ COMMENTS									

Observations: [illegible] Record normal [illegible] recording of observations by [illegible]

Scores: 0 Normal; 1 Mild; 2 Moderate; 3 Severe
Action to take: 1 Normal

Page 1

2 Record, REPORT and observe more often

3 Record, REPORT and evaluate for humane termination

Page 2

Developed by: M Castle, G [illegible]

Checked by: [illegible] 2014/12/19 Review in 6M

SRC Approval: [illegible]

Addendum 6: List of materials and reagents

Material / Reagent	Vendor
1 mm glass slide	Labocare®
24-well plates	Sigma-Aldrich®
Coverslips	Lasec®
Amyloid-β_{42} staining kit (E-EL-R1402)	Elabscience®
Anti-GFAP antibody (ab33922)	Abcam®
Anti-Iba-1 antibody (ab5076)	Abcam®
CD68 antibody (ab31630)	Abcam®
Thioflavin T dye (T3516)	Sigma-Aldrich®
Fluoromount™ mounting medium	Sigma-Aldrich®
Formaldehyde	Merck
Manuka honey	Ample Resources South Africa
Sodium phosphate monobasic (S0751)	Sigma-Aldrich®
Sodium phosphate dibasic (S0876)	Sigma-Aldrich®
Sucrose (S-8501)	Sigma-Aldrich®
Glycerine (G31-500)	ThermoFisher Scientific™
Ethylene Glycol (BP230-1)	ThermoFisher Scientific™
Bovine serum albumin	Sigma-Aldrich®
Triton X-100	Sigma-Aldrich®
Sodium chloride (S-9888)	Sigma-Aldrich®
Trizma base (T-1503)	Sigma-Aldrich®
Trizma hydrochloride (T-3253)	Sigma-Aldrich®
Sodium azide (S2002)	Sigma-Aldrich®
Isfor®	Safeline Pharmaceuticals
Lipopolysaccharide 055:B5 (L2880)	Sigma-Aldrich®
EzLys™ tissue protein extraction reagent	Biocom Africa
DNAse 1 protease inhibitor cocktail	Sigma-Aldrich®